Table of contents

1. Synthesis

1.1. Equipment and characterizations

The starting compounds **3f**, **3g** and **8a–h**, solvents and reagents were purchased from TCI, Aldrich, Apollo, Fluka or Penta and were used as obtained without further purification. Starting DAMN (**5**) was purchased from Aldrich but was recrystallized from EtOH prior to use. The Jacomex PureMod nitrogen-filled glovebox was used for working under strictly inert condition. The solvents were evaporated on a Heidolph Laborota 4000 and 4001. The entire reaction sequence for the preparation of derivative **1a** was conducted in a glovebox. The other 1*H*-imidazoles were prepared in a fume hood in air or in a Schlenk flask under an inert atmosphere of argon. Thin-layer chromatography was performed on aluminium plates coated with SiO_2 60 F254 silica gel (Merck) and visualized under UV lamp (254 or 360 nm). Melting points were determined in open capillaries on a Büchi B-540 instrument. The ^{1}H-, ^{13}C-, ^{19}F- and ^{7}Li-NMR spectra were measured in DMSO-d_6, THF-d_8, CD_3OD or acetone-d_6 at 25 °C on a Bruker Ascend^{TM} instrument at 500/194/125/470 MHz. The ^{1}H- and ^{13}C-NMR chemical shifts are given in ppm relative to the Me_4Si signal. The residual solvent signal was used as an internal standard (DMSO-d_6: 2.50 and 39.52, acetone-d_6: 2.05 and 206.68 (29.92), CD_3OD: 3.31 and 49.00 and THF-d_8 1.72/3.58 and 25.31/67.21 ppm. 1M LiCl in D_2O and C_6F_6 were used as external standards for ^{7}Li- and ^{19}F-NMR spectra. Interaction constants (*J*) are given in Hz. The observed signals are described as *bs* (broad singlet), *d* (doublet), and *m* (multiplet). The mass spectra were measured on a GC/EI-MS configuration consisting of an Agilent 7890B Series GC Custom gas chromatograph. High resolution mass spectra were measured by the dried droplet method using a MALDI mass spectrometer LTQ Orbitrap XL (Thermo Fisher Scientific) equipped with a nitrogen UV laser (337 nm, 60 Hz). Spectra were measured in the negative mode in normal mass range with a resolution of 100 000 at *m/z* = 400. 9-AA was used as matrix.

Thirteen 1*H*-imidazoles (**3a–e**, **4a–h**) were prepared, all previously reported. In contrast, 11 of the corresponding lithium imidazolides are new, only salts **1c**[15], **2c**[16], and **LiTDI** (**1a**)[14] are known from the literature.

1.2. 2-Trifluoromethyl-1*H*-imidazole-4,5-dicarbonitrile[1] (3a)

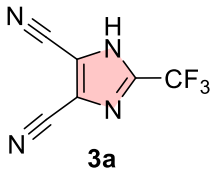

3a

TFAA (1.05 mmol, 221 mg) was added dropwise to a stirred solution of diaminomaleonitrile **5** (1.0 mmol, 108 mg) in 1,4-dioxane (5 ml) placed in a Schlenk flask. The reaction was stirred at 80 °C for 5 h, the orange solution was concentrated under reduced pressure, Et_2O (5 ml) and charcoal (50 mg) were added, the suspension was filtered, the solvent was evaporated under reduced pressure and the residue was suspended in water (10 ml). The precipitate obtained was filtered off and washed with water (10 ml). The product **3a** was obtained as a white solid in 37 % yield (69 mg). M.p. = 67–68 °C (lit.[1] 86–88 °C), R_f = 0.44 (SiO_2; EtOAc:CyHex 1:1). ^{1}H-NMR (500 MHz, 25 °C, THF-d_8): δ = 6.80 (s, 1H, NH) ppm. ^{13}C-NMR (125 MHz, 25 °C, THF-d_8): δ = 110.56; 118.25; 118.54 (m); 141.259 (m). ^{19}F-NMR (470 MHz, 25 °C. THF-d_8): δ = –63.49 ppm. HR-FT-MALDI-MS (9-AA) *m/z*: calculated for $C_6F_3N_4^-$ ([M-H]$^-$) 185.00805; found 185.00799

1.3. 2-Methyl-1*H*-imidazole-4,5-dicarbonitrile[2] (3b)

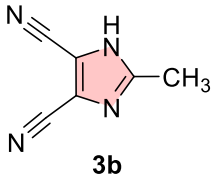

3b

In a round bottom flask, triethylorthoacetate (1.1 mmol, 178 mg) and **5** (1 mmol, 108 mg) were dissolved in ACN (4 ml) and the reaction mixture was heated to 85 °C for 24 h. The reaction mixture was concentrated under reduced pressure, xylene (4 ml) was added, and the mixture was heated to 150 °C for 24 h. The solvent was removed under reduce pressure, ethanol (5 ml) and activated charcoal (60 mg) were added and the suspension was heated to 75 °C for 4 h. After filtration and evaporation of the solvent, the solid product was filtered off and washed with ice-cold dichloromethane (DCM) (2×4 ml). The product **3b** was obtained as an off-white solid in 68 % yield (90 mg). M.p. = 227–228 °C (lit.[2] 228 °C). R_f = 0.8 (SiO_2; EtOAc:hexane 2:1). ^{1}H-NMR (500 MHz, 25 °C, CD_3OD): δ = 2.44 (s, 3H, CH_3), 5.18 (br s, 1H, NH) ppm. ^{13}C-NMR (125 MHz, 25 °C, CD_3OD): δ = 13.89; 111.35; 152.48 ppm. HR-FT-MALDI-MS (9-AA) *m/z*: calculated for $C_6H_3N_4^-$ ([M-H]$^-$) 131.03632; found 131.03618.

---

[1] R.W. Begland, D. R. Hartter, W. A. Sheppard, O. W. Webster, *J. Org. Chem.*, **1974**, *39*(16), 2341–2350.
[2] J. Li, H. Liu, H. Zhu, W. Yao, D. Wang, *ChemCatChem,* **2021**, *13*, 4751.

1.4. 1*H*-Imidazole-2,4,5-tricarbonitrile[3] (3c)

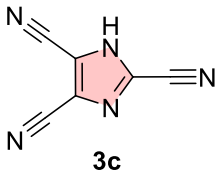

3c

1*H*-Imidazole **3g** (1 mmol, 133 mg) was charged into a narrow-necked flask with a stirrer together with conc. HCl (12 mmol, 1 ml) and water (3 ml). The reaction mixture was cooled to 0 °C in an ice bath. $NaNO_2$ (1.4 mmol, 97 mg) in water (4 ml) was added with a vigorous stirring and the resulting diazonium salt was filtered off after 20 minutes and directly transferred into a flask charged with NaCN (2 mmol, 98 mg), CuCN (1.05 mmol, 94 mg) and water (6 ml). The reaction mixture was stirred at 25 °C for 2 h, TMAI (3 mmol, 603 mg) was added and, after 2 h, the resulting black suspension was filtered off using a steel cannula with a filter baffle. The filtrate obtained was extracted with EtOAc (3×10 ml), the combined organic fractions were dried (Na_2SO_4), the solvent was evaporated in vacuo and residue was acid-hydrolysed by adding HCl (10%, 50 ml) to pH = 1. The aqueous solution was extracted with Et_2O (3×15 ml), the combined extracts were dried (Na_2SO_4) and the solvent was evaporated in vacuo affording **3c** as an off-white solid in 25 % yield (36 mg). M.p. = 163–166 °C (lit.[3] 161–163 °C). R_f = 0.7 (SiO_2; acetone:DCM 1:1). ^{1}H-NMR (500 MHz, 25 °C, DMSO-d_6): δ = 6.02 (br s, 1H, NH) ppm. ^{13}C-NMR (125 MHz, 25 °C, DMSO-d_6): δ = 114.44; 115.68; 119.87; 132.00 ppm. HR-FT-MALDI-MS (9-AA) *m/z*: calculated for $C_6N_5^-$ ([M-H]$^-$) 142.01592; found 142.01580.

1.5. 2-Bromo-1*H*-imidazole-4,5-dicarbonitrile[4] (3d)

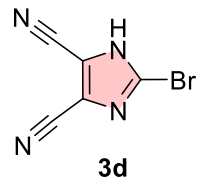

3d

1*H*-Imidazole-4,5-dicarbonitrile **3f** (1 mmol, 118 mg) and aq. NaOH (0.1M, 0.25 mmol, 2.5 ml) were charged into a narrow-necked flask. After 30 minutes, Br_2 (3.5 mmol, 559 mg) was gradually added, the reaction was stirred at 25 °C for 12 h and diluted with 0.5M HCl (5 ml) to adjust pH = 4. The resulting suspension was stirred at 25 °C for 6 h, the solid was filtered off and recrystallized from water. The resulting product was washed with water (15 ml) and DCM (10 ml) during filtration and upon drying, the product **3d** was obtained as a white solid in 68% yield (134 mg). M.p. = 150 °C (lit.[4] 148–149 °C). R_f = 0.6 (SiO_2; EtOAc:MeOH 4:1). ^{1}H-NMR (500 MHz, 25 °C, acetone-d_6): δ = 13.04 (br s, 1H, NH) ppm. ^{13}C-NMR (125 MHz, 25 °C, acetone-d_6): δ = 110.298; 118.42;

[3] P. G. Rasmussen, P. G. Apen, *Heterocycles*, **1989**, *29(7),* 1325.
[4] O. W. Webster, U. S. Patent 3793339A, 1972.

124.06 ppm. HR-FT-MALDI-MS (9-AA) *m/z*: calculated for $C_5BrN_4^-$ ($[M-H]^-$) 194.93118; found 194.93108.

1.6. 2-Nitro-1*H*-imidazole-4,5-dicarbonitrile[5] (3e)

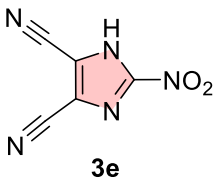

3e

A mixture of **3g** (1 mmol, 133 mg), water (4 ml) and conc. HCl (8.5 mmol, 0.75 ml) was cooled in an ice bath to 0 °C, whereupon $NaNO_2$ (2.5 mmol, 172 mg) dissolved in water (3 ml) was slowly added. After 15 min, the reaction was heated to 25 °C and stirred for 15 h. The reaction mixture was extracted with EtOAc (3×10 ml), the combined extracts were dried (Na_2SO_4) and the solvent was removed in vacuo affording **3e** as an orange solid in 76 % yield (124 mg). M.p. = 148 °C (explosive decomposition). R_f = 0.75 (SiO_2; EtOAc). ^{1}H-NMR (500 MHz, 25 °C, acetone-d_6): δ = 2.95 (s, 1H, NH) ppm. ^{13}C-NMR (125 MHz, 25 °C, acetone-d_6): δ = 112.15; 125.39; 126.89 ppm. HR-FT-MALDI-MS (9-AA) *m/z*: calculated for $C_5HN_4^-$ ($[M-NO_2]^-$) 117.02067; found 117.02030.

1.7. General method for the preparation of a series of 2-phenyl-1*H*-imidazole-4,5-dicarbonitrile 4a–h

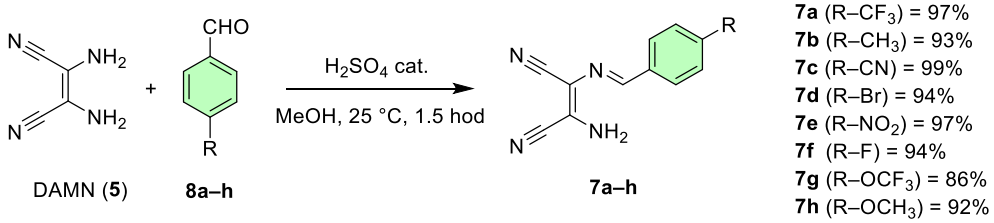

Figure S1. The first reaction step towards **4**, preparation of intermediates **7**.

DAMN **5** (1.05 mmol, 114 mg) and MeOH (5 ml) were added to a 25 ml round bottom flask followed by a gradual addition of 4-substituted benzaldehyde **8a**–**h** (1 mmol). The reaction was stirred at 25 °C for 5 min, H_2SO_4 (conc., 3 drops) was added accompanied by an immediate formation of the corresponding imine **7a–h**. After 90 min, the suspension was filtered affording the first batch of **7a–h**, which was dried using evaporator. The filtrate was further concentrated in vacuo and, after cooling, afforded the second batch of **7a–h**. Both batches were combined to afford **7a–h** in the yields as indicated in Figure S1.

[5] Lu, Y., Just, G., *Tetrahedron* **2001**, *57*, 1677–1687.

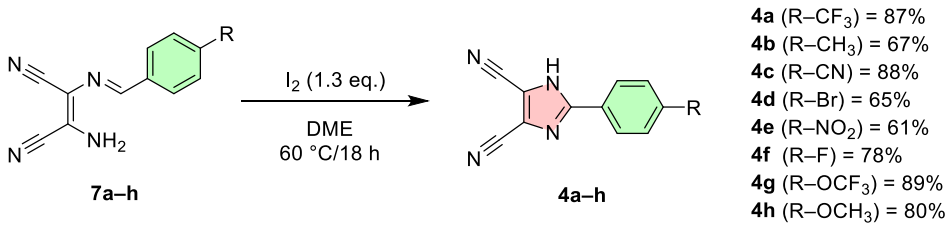

Figure S2. The second step towards **4a–h**.

Imine **7a–h** was dissolved in DME (10 ml), iodine (1.3 mmol, 330 mg) was added, and the reaction was stirred at 60 °C for 12 h. The reaction mixture was concentrated in vacuo and EtOAc (10 ml) and aq. sat. $Na_2S_2O_3$ (10 ml) were added. The organic layer was further extracted with EtOAc (3×5 ml), the combined organic fractions were dried (Na_2SO_4), the solvent was evaporated, and methanol (10 ml) and charcoal (60 mg) were added. The suspension was boiled under reflux for 30 min, filtered off, the solvent was evaporated, and the residue was taken in $CHCl_3$ (5 ml). After 15 minutes, the suspension was filtered, and the product was washed with $CHCl_3$ (2×2 ml) and dried in a vacuum desiccator to afford **4a–h** in the yields as indicated in Figure S2.

1.8. 2-(4-Trifluoromethylphenyl)-1*H*-imidazole-4,5-dicarbonitrile[6] (4a)

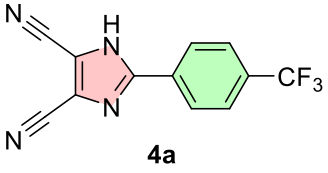

4a

The title compound **4a** was synthesized from 4-(trifluoromethyl)benzaldehyde **8a** (174 mg) following the General method. The product **4a** was obtained as a white solid in 84 % yield (220 mg). M.p. = 242–244 °C (lit.[6] 251–252 °C). R_f = 0.21 (SiO_2; EtOAc:hexane 1:2). ^{1}H-NMR (500 MHz, 25 °C, acetone-d_6): δ = 7.89 (d, J = 8.3 Hz, 2H), 8.23 (d, J = 8.3 Hz, 2H), 12.48 (br s, 1H, NH), ppm. ^{13}C-NMR (125 MHz, 25 °C, acetone-d_6): δ = 111.17; 117.7; 124.79 (q, J = 271.6 Hz); 127.03 (q, J = 3.67 Hz); 127.94; 131.86; 132.66 (q, J = 32.67 Hz); 150.25 ppm. ^{19}F-NMR (470 MHz, 25 °C, acetone-d_6): δ = –60.95 ppm. HR-FT-MALDI-MS (9-AA) *m/z*: calculated for $C_{12}H_4F_3N_4^-$ ([M-H]$^-$) 261.03935; found 261.03911.

[6] R.W. Begland, D. R. Hartter, W. A. Sheppard, O. W. Webster, *J. Org. Chem.*, **1974**, *39*, 2341–2350.

1.9. 2-(4-Methylphenyl)-1*H*-imidazole-4,5-dicarbonitrile[7] (4b)

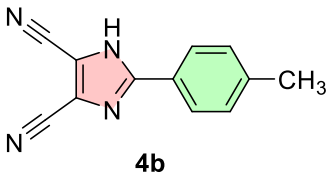

4b

The compound **4b** was synthesized from 4-methyl-benzaldehyde **8b** (120 mg) following the General method. The product **4b** was obtained as an off-white solid in 62 % yield (129 mg). M.p. = 261–263 °C (lit.[7] 143–145 °C). R_f = 0.3 (SiO_2; EtOAc:hexane 1:2). ^{1}H-NMR (500 MHz, 25 °C, acetone-d_6): δ = 2.38 (s, 3H, CH_3), 7.33 (d, J = 8.1 Hz, 2H), 7.87 (d, J = 8.2 Hz, 2H), 12.50 (s, 1H, NH) ppm. ^{13}C-NMR (125 MHz, 25 °C, acetone-d_6): δ = 21.38; 111.41; 125.48; 127.08; 130.57; 142.33; 151.92 ppm. HR-FT-MALDI-MS (9-AA) *m/z*: calculated for $C_{12}H_7N_4$ ([M-H]$^-$) 207.06762; found 207.06762.

1.10. 2-(4-Cyanophenyl)-1*H*-imidazole-4,5-dicarbonitrile[8] (4c)

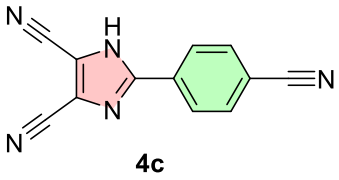

4c

Derivative **4c** was prepared from 4-formylbenzonitrile **8c** (131 mg) via a modified General method. A mixture of DCM:hexane (1:1) was used to wash the imine **7c** during the filtration to improve its crystallinity. Due to its high solubility in $CHCl_3$, the resulting product **4c** was purified by column chromatography (SiO_2; EtOAc:hexane 2:3). The product **4c** was prepared as a yellow solid in 87 % yield (191 mg). M.p. = 289–291 °C. R_f = 0.1 (SiO_2; EtOAc:hexane 2:3). ^{1}H-NMR (500 MHz, 25 °C, CD_3OD): δ = 7.72 (d, J = 8.4 Hz, 2H), 8.10 (d, J = 8.5 Hz, 2H) ppm. ^{13}C-NMR (125 MHz, 25 °C, CD_3OD): δ = 111.83; 115.85; 119.88; 120.85; 127.53; 133.47; 139.39; 157.35 ppm. HR-FT-MALDI-MS (9-AA) *m/z*: calculated for $C_{12}H_4N_5^-$ ([M-H]$^-$) 218.04722; found 218.04699.

1.11. 2-(4-Bromophenyl)-1*H*-imidazole-4,5-dicarbonitrile[9] (4d)

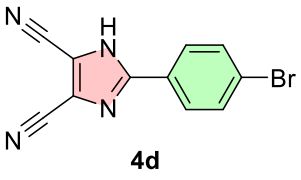

4d

The compound **4d** was synthesized from 4-bromobenzaldehyde **8d** (185 mg) following the General method. The product **4d** was obtained as a white solid in 61 % yield (167 mg). M.p. 313–315 °C (lit.[9] 316–321 °C). R_f = 0.5 (SiO_2; EtOAc:hexane 1:2). ^{1}H-NMR (500 MHz, 25 °C, acetone-d_6): δ = 7.33 (1H, NH), 7.54 (d, J = 8.7 Hz, 2H), 7.94 (d, J = 8.7 Hz, 2H) ppm. ^{13}C-NMR (125 MHz, 25 °C,

[7] O. Ravi, A. Shaikh, A. Upare, S. R. Bathula, *J. Org. Chem.*, **2017**, *82*, 4422–4428.
[8] G. Schmidt, WO Pat., 2013182768A1, 2013
[9] M. Kalhor, Z. Seyedzade, *Res. Chem. Intermed.*, **2017**, *43*, 3349–3360

acetone-d_6): δ = 113.92; 118.70; 123.43; 128.69; 131.37; 132.47; 154.43 ppm. HR-FT-MALDI-MS (9-AA) *m/z*: calculated for $C_{11}H_5BrN_4^-$ ([M-H]$^-$) [^{79}Br] 270.96248; found 270.96281.

1.12. 2-(4-Nitrophenyl)-1*H*-imidazole-4,5-dicarbonitrile[10] (4e)

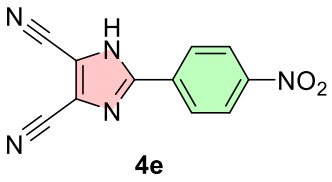

4e

The compound **4e** was prepared from 4-nitrobenzaldehyde **8e** (151 mg) via a modified General method**.** The oxidation of **7e** was carried out at 100 °C under a reflux condenser for 2 d. The product **4e** was additionally purified by column chromatography (SiO_2; EtOAc:hexane 1:1) to afford **4e** as a yellow solid in 59 % yield (141 mg). M.p. = 214–217 °C (lit.[10] 252–254 °C). R_f = 0.1 (SiO_2; EtOAc:hexane 1:1). ^{1}H-NMR (500 MHz, 25 °C, CD_3OD): δ = 4.91 (s, 1H, NH), 8.14 (d, *J* = 8.9 Hz, 2H), 8.29 (d, *J* = 9 Hz, 2H) ppm. ^{13}C-NMR (125 MHz, 25 °C, CD_3OD): δ = 113.73; 119.83; 125.07; 128.04; 138.12; 149.34; 153.94 ppm. HR-FT-MALDI-MS (9-AA) *m/z*: calculated for $C_{11}H_4N_5O_2^-$ ([M-H]$^-$) 238.03705; found 238.03694.

1.13. 2-(4-Fluorophenyl)-1*H*-imidazole-4,5-dicarbonitrile[11] (4f)

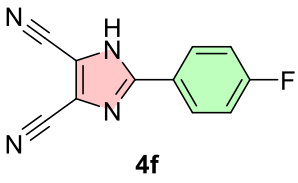

4f

The compound **4f** was synthesized from 4-fluorobenzaldehyde **8f** (124 mg) following the General method. The product **4f** was obtained as an off-white solid in 73 % yield (155 mg). M.p. 211–213 °C (lit.[11] 220–221 °C). R_f = 0.4 (SiO_2; EtOAc:hexane 1:2). ^{1}H-NMR (500 MHz, 25 °C, acetone-d_6): δ = 7.23–7.27 (m, 2H), 8.07–8.09 (m, 2H) 8.26 (br s, 1H, NH) ppm. ^{13}C-NMR (125 MHz, 25 °C, acetone-d_6): δ = 112.68; 116.77 (d, *J* = 22,6 Hz); 117.98; 126.92 (d, *J* = 2,8 Hz); 129.54 (d, *J* = 8,2 Hz); 152.84; 163.62; 165.59 ppm. ^{19}F-NMR (470 MHz, 25 °C, acetone-d_6): δ = –109.23 ppm. HR-FT-MALDI-MS (9-AA) *m/z*: calculated for $C_{11}H_5FN_4^-$ ([M-H]$^-$) 211.04255; found 211.04250.

1.14. 2-(4-Trifluoromethoxyphenyl)-1*H*-imidazole-4,5-dicarbonitrile[12] (4g)

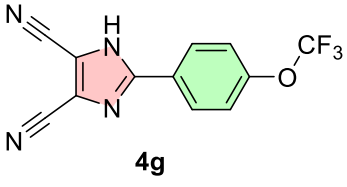

4g

The compound **4g** was synthesized from 4-trifluoromethoxybenzaldehyde **8g** (190 mg) following the General method. The product **4g** was obtained as a white solid in 77 % yield (214 mg). M.p. >410 °C (lit.[12] 182–183 °C). R_f = 0.4 (SiO_2; EtOAc:hexane 1:2). ^{1}H-NMR (500 MHz, 25 °C, acetone-d_6):

[10] M. Kalhor, Z. Seyedzade, *Res. Chem. Intermed.*, **2017**, *43*, 3349–3360
[11] R.W. Begland, D. R. Hartter, W. A. Sheppard, O. W. Webster, *J. Org. Chem.*, **1974**, *39*, 2341–2350.
[12] G.A. Feldwick, L.R. Hatton, R.H. Hewett, B.L. Pedgrift, European Patent: *0269238A1*, 1988.

δ = 5.41 (br s, 1H, NH), 7.26 (d, *J* = 8 Hz, 2H), 8.18 (d, *J* = 8.16 Hz, 2H) ppm. ^{13}C-NMR (125 MHz, 25 °C, acetone-d_6): δ = 117.10; 120.16; 121.40 (q, *J* = 255.1 Hz); 121.43; 127.96; 135.71; 148.77; 157.29 ppm. ^{19}F-NMR (470 MHz, 25 °C, acetone-d_6): δ = –55.92 ppm. HR-FT-MALDI-MS (9-AA) *m/z*: calculated for $C_{12}H_4F_3N_4O^-$ ([M-H]$^-$) 277.03427; found 277.03449.

1.15. 2-(4-Methoxyphenyl)-1*H*-imidazole-4,5-dicarbonitrile[13] (4h)

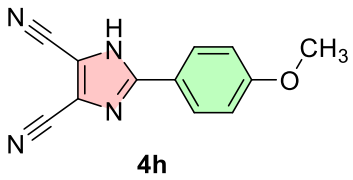

4h

The compound **4h** was synthesized from 4-methoxybenzaldehyde **8h** (136 mg) following the General method. The product **4h** was obtained as a white solid in 74 % yield (166 mg). M.p. 232–235 °C (lit.[13] 230–232 °C). R_f = 0.3 (SiO_2; EtOAc:hexane 1:2). ^{1}H-NMR (500 MHz, 25 °C, acetone-d_6): δ = 3.85 (s, 3H, CH_3), 7.03 (d, *J* = 8.9 Hz, 2H), 7.94 (d, *J* = 8.9 Hz, 2H), 12.40 (s, 1H, NH) ppm. ^{13}C-NMR (125 MHz, 25 °C, acetone-d_6): δ = 55.75; 112.04; 115.19; 117.18; 121.57; 128.78; 152.83; 162.48 ppm. HR-FT-MALDI-MS (9-AA) *m/z*: calculated for $C_{12}H_7N_4O^-$ ([M-H]$^-$) 223.06253; found 223.06265.

1.16. General method for lithiation of 1*H*-imidazoles 3 and 4

In nitrogen-filled glovebox, 1*H*-imidazole **3b**–**f** or **4a–h** (1 mmol) was dissolved in DMC (5 ml, for **3b–f**) or DME (5 ml, for **3a** and **4a–h**) and lithium hydride (1.2 mmol, 9.5 mg) was added slowly accompanied by a hydrogen evolution. The suspension was stirred at 25 °C for 2 h, the solvent was evaporated under reduced pressure and the solid residue was suspended in dichloromethane (DCM, 5 ml). The product was filtered off, washed with DCM (5 ml) and dried under vacuum (100 °C/15 Torr).

1.17. Lithium 2-trifluoromethyl-4,5-dicyanoimidazol-1-ide[14] (LiTDI, 1a)

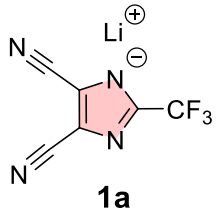

1a

LiTDI derivative **1a** was prepared via a modified one-pot method. In a nitrogen-filled glovebox, TFAA (1.05 mmol, 146 µl) was added dropwise to a stirred solution of **5** (1 mmol, 108 mg) in 1,4-dioxane (5 ml) and the reaction was stirred at 80 °C for 5 h. The solvent and volatile by-products were distilled off by vacuum distillation (70 °C/50 Torr) and the residue was dissolved in 1,2-dimethoxyethane (5 ml). Lithium hydride **6** (1.3 mmol, 10.3 mg) was gradually added with vigorous stirring. After 3 h,

[13] M. Kalhor, Z. Seyedzade, *Res. Chem. Intermed.*, **2017**, *43*, 3349–3360.
[14] L. Niedzicki, G. Z. Żukowska, *Electrochim. Acta,* **2010**, *55*, 1450–1454.

the suspension was filtered off and the clear red solution was concentrated to dryness by vacuum distillation in a nitrogen glovebox (60 °C/5 Torr). The crude product was suspended in DCM (5 ml), filtered and dried under high vacuum (60 °C/5 Torr). **LiTDI** was obtained as a white solid in 87 % yield (167 mg). M.p. = >274 °C (dec.). R_f = 0.2 (SiO_2; EtOAc). ^{7}Li-NMR (194 MHz, 25 °C, acetone-d_6): δ = 2.60 ppm. ^{13}C-NMR (125 MHz, 25 °C, acetone-d_6): δ = 115.71; 120.19; 121.20 (q, J = 267.0 Hz); 148.46 (q, J = 36.6 Hz); ppm. ^{19}F-NMR (470 MHz, 25 °C, acetone-d_6): δ = –61.41 ppm. HR-FT-MALDI-MS (9-AA) *m/z*: calculated for $C_6F_3N_4^-$ ([M]$^-$) 185.00805; found 185.00826.

1.18. Lithium 2-methyl-4,5-dicyanoimidazol-1-ide (1b)

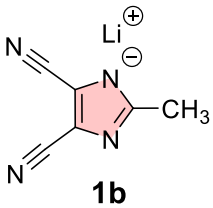

1b

The compound **1b** was synthesized from **3b** (132 mg) following the General method. The product **1b** was obtained as a white solid in 98 % yield (135 mg). M.p. >410 °C. ^{1}H-NMR (500 MHz, 25 °C, acetone-d_6): δ = 2.61 (s, 3H, CH_3) ppm. ^{7}Li-NMR (194 MHz, 25 °C, acetone-d_6): δ = 2.61 ppm. ^{13}C-NMR (125 MHz, 25 °C, acetone-d_6): δ = 14.19; 111.48; 116.24; 151.83 ppm. HR-FT-MALDI-MS (9-AA) *m/z*: calculated for $C_6H_3N_4^-$ ([M]$^-$) 131.03632; found 131.03626.

1.19. Lithium 2,4,5-tricyanoimidazol-1-ide (1c)[15]

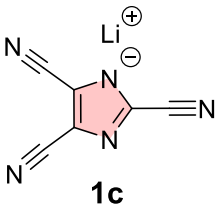

1c

The compound **1c** was synthesized from **3c** (143 mg) following the General method. The product **1c** was obtained as a white solid in 84 % yield (125 mg). M.p. >410 °C. ^{7}Li-NMR (194 MHz, 25 °C, acetone-d_6): δ = 2.67 ppm. ^{13}C-NMR (125 MHz, 25 °C, acetone-d_6): δ = 115.30; 116.61; 121.00; 133.47 ppm. HR-FT-MALDI-MS (9-AA) *m/z*: calculated for $C_6N_5^-$ ([M]$^-$) 142.01592; found 142.01585.

1.20. Lithium 2-bromo-4,5-dicyanoimidazol-1-ide (1d)

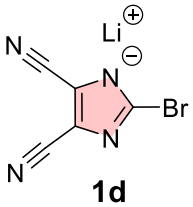

1d

The compound **1d** was synthesized from **3d** (197 mg) following the General method. The product **1d** was obtained as a white solid in 83 % yield (168 mg). M.p. > 294 °C (dec.). ^{7}Li-NMR (194 MHz, 25 °C, aceton-d_6): δ = 2.59 ppm. ^{13}C-NMR (125 MHz, 25 °C, aceton-d_6): δ = 114.73; 120.36; 131.11 ppm. HR-FT-MALDI-MS (9-AA) *m/z*: calculated for $C_5BrN_4^-$ ([M]$^-$) 194.93118; found 194.93116 Da.

[15] T. L. Dzwiniel, K. Z. Pupek, US Pat., 20230406828A1, 2023.

1.21. Lithium 2-nitro-4,5-dicyanoimidazol-1-ide (1e)

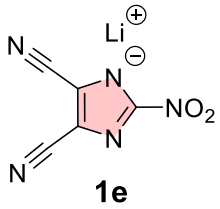

1e

The compound **1e** was synthesized from **3e** (163 mg) following the General method. The product **1e** was obtained as an orange solid in 77 % yield (130 mg). M.p. = >410 °C. ^{7}Li-NMR (194 MHz, 25 °C, acetone-d_6): δ = 2.57 ppm. ^{13}C-NMR (125 MHz, 25 °C, acetone-d_6): δ = 116.18; 118.91; 148.76 ppm. HR-FT-MALDI-MS (9-AA) *m/z*: calculated for $C_5N_4^-$ ([M-NO_2]$^-$) 116.01284; found 116.01286 Da.

1.22. Lithium 4,5-dicyanoimidazol-1-ide (1f)

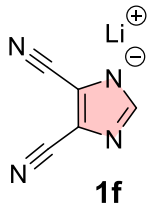

1f

The compound **1f** was synthesized from **3f** (118 mg) following the General method. The product **1f** was obtained as a white solid in 98 % yield (122 mg). M.p. = >410 °C. ^{1}H-NMR (500 MHz, 25 °C, acetone-d_6): δ = 7.57 (s, 1H, CH) ppm. ^{7}Li-NMR (194 MHz, 25 °C, acetone-d_6): δ = 2.95 ppm. ^{13}C-NMR (125 MHz, 25 °C, acetone-d_6): δ = 115.12; 118.67; 148.09 ppm. HR-FT-MALDI-MS (9-AA) *m/z*: calculated for $C_5HN_4^-$ ([M]$^-$) 117.02067; found 117.02076 Da.

1.23. Lithium 4,5-dicyano-2-(4-trifluoromethylphenyl)-imidazol-1-ide (2a)

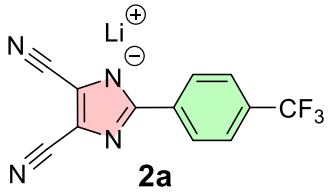

2a

The compound **2a** was synthesized from **4a** (262 mg) following the General method. The product **2a** was obtained as a white solid in 89 % yield (239 mg). M.p. = 332–335 °C (dec.). ^{1}H-NMR (500 MHz, 25 °C, acetone-d_6): δ = 7.63 (d, J = 8 Hz, 2H), 8.27 (d, J = 8.5 Hz, 2H) ppm. ^{7}Li-NMR (194 MHz, 25 °C, acetone-d_6): δ = 2.49 ppm. ^{13}C-NMR (125 MHz, 25 °C, acetone-d_6): δ = 116.96; 120.61; 125.60 (q, J = 269.4 Hz); 125.73 (q, J = 3.8 Hz); 126.86; 128.63 (q, J = 31.4 Hz); 130.16; 140.15; 157.35 ppm. ^{19}F-NMR (470 MHz, 25 °C, acetone-d_6): δ = –60.06 ppm. HR-FT-MALDI-MS (9-AA) *m/z*: calculated for $C_{12}H_4F_3N_4^-$ ([M]$^-$) 261.03935; found 261.03930 Da.

1.24. Lithium 4,5-dicyano-2-(4-methylphenyl)-imidazol-1-ide (2b)

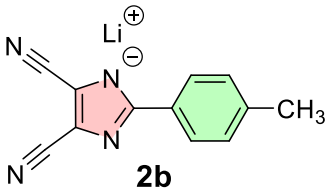

2b

The compound **2b** was synthesized from **4b** (208 mg) following the General method. The product **2b** was obtained as an off-white solid in 88 % yield (188 mg). M.p. >410 °C. ^{1}H-NMR (500 MHz, 25 °C, acetone-d_6): δ = 2.30 (s, 3H, CH_3), 7.12 (d, J = 8 Hz, 2H), 7.91 (d, J = 7.5 Hz, 2H) ppm. ^{7}Li-NMR (194 MHz, 25 °C, acetone-d_6): δ = 2.34 ppm. ^{13}C-NMR (125 MHz, 25 °C, acetone-d_6): δ = 21.07; 117.06; 119.98; 126.93; 129.25; 133.57; 137.22; 159.42 ppm. HR-FT-MALDI-MS (9-AA) *m/z*: calculated for $C_{12}H_7N_4^-$ ([M]$^-$) 207.06762; found 207.06770 Da.

1.25. Lithium 4,5-dicyano-2-(4-cyanophenyl)-imidazol-1-ide[16] (2c)

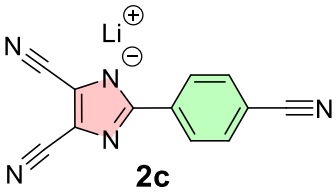

2c

The compound **2c** was synthesized from **4c** (219 mg) following the General method. The product **2c** was obtained as a white solid in 75 % yield (169 mg). M.p. >410 °C. ^{1}H-NMR (500 MHz, 25 °C, acetone-d_6): 7.69 (d, J = 8.5 Hz, 2H), 8.25 (d, J = 8.5 Hz, 2H) ppm. ^{7}Li-NMR (194 MHz, 25 °C, acetone-d_6): δ = 2.10 ppm. ^{13}C-NMR (125 MHz, 25 °C, acetone-d_6): δ = 110.20; 117.06; 119.87; 120.83; 126.81; 132.77; 140.88; 157.02 ppm. HR-FT-MALDI-MS (9-AA) *m/z*: calculated for $C_{12}H_4N_5^-$ ([M]$^-$) 218.04722; found 218.04708 Da.

1.26. Lithium 4,5-dicyano-2-(4-bromophenyl)-imidazol-1-ide (2d)

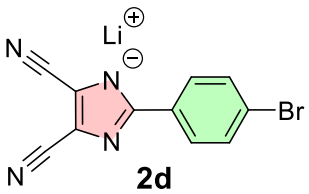

2d

The compound **2d** was synthesized from **4d** (273 mg) following the General method. The product **2d** was obtained as a white solid in 68 % yield (190 mg). M.p. >410 °C. ^{1}H-NMR (500 MHz, 25 °C, acetone-d_6): δ = 7.47 (d, J = 8.5 Hz, 2H), 8.01 (d, J = 8.5 Hz, 2H) ppm. ^{7}Li-NMR (194 MHz, 25 °C, acetone-d_6): δ = 2.67 ppm ^{13}C-NMR (125 MHz, 25 °C, acetone-d_6): δ = 117.33; 120.28; 120.76; 128.38; 131.73; 136.04; 157.80 ppm. HR-FT-MALDI-MS (9-AA) *m/z*: calculated for $C_{11}H_4BrN_4^-$ ([M]$^-$) [^{79}Br] 270.96248; found 270.96301 Da.

[16] G. Schmidt, WO Pat., 2013182768A1, 2013

1.27. Lithium 4,5-dicyano-2-(4-nitrophenyl)-imidazol-1-ide (2e)

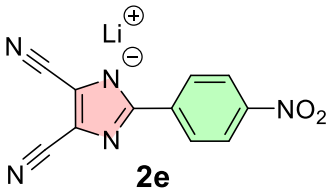

2e

The compound **2e** was synthesized from **4e** (239 mg) following the General method. The product **2e** was obtained as a yellow solid in 78 % yield (191 mg). M.p. >410 °C. ^{1}H-NMR (500 MHz, 25 °C, acetone-d_6): δ = 8.19 (d, J = 9 Hz, 2H), 8.28 (d, J = 9 Hz, 2H) ppm. ^{7}Li-NMR (194 MHz, 25 °C, acetone-d_6): δ = 2.34 ppm. ^{13}C-NMR (125 MHz, 25 °C, acetone-d_6): δ = 116.94; 121.17; 124.27; 126.79; 142.78; 147.13; 156.81 ppm. HR-FT-MALDI-MS (9-AA) *m/z*: calculated for $C_{11}H_4N_5O_2^-$ ([M]$^-$) 238.03705; was found 238.03708 Da.

1.28. Lithium 4,5-dicyano-2-(4-fluorophenyl)-imidazol-1-ide (2f)

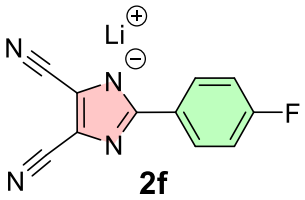

2f

The compound **2f** was synthesized from **4f** (212 mg) following the General method. The product **2f** was obtained as a beige solid in 94 % yield (205 mg). M.p. >410 °C. ^{1}H-NMR (500 MHz, 25 °C, acetone-d_6): δ = 7.03–7.06 (m, 2H), 8.08–8.11 (m, 2H) ppm. ^{7}Li-NMR (194 MHz, 25 °C, acetone-d_6): δ = 2.47 ppm. ^{13}C-NMR (125 MHz, 25 °C, acetone-d_6): δ = 115.24 (d, J = 21.5 Hz); 117.60; 120.05; 128.17 (d, J = 7.9 Hz); 133.49 (d, J = 2.8 Hz); 158.06; 161.81; 163.74 ppm. ^{19}F-NMR (470 MHz, 25 °C, acetone-d_6): δ = –115.3 ppm. HR-FT-MALDI-MS (9-AA) *m/z*: calculated for $C_{11}H_5FN_4^-$ ([M]$^-$) 211.04255; found 211.04246 Da.

1.29. Lithium 4,5-dicyano-2-(4-trifluoromethoxyphenyl)-imidazol-1-ide (2g)

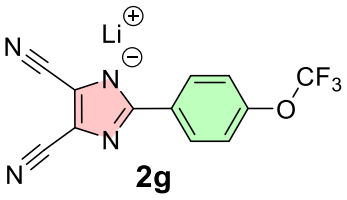

2g

The compound **2g** was synthesized from **4g** (278 mg) following the General method. The product **2g** was obtained as a white solid in 93 % yield (264 mg). M.p. >410 °C. ^{1}H-NMR (500 MHz, 25 °C, acetone-d_6): δ = 7.26 (d, J = 7.9 Hz, 2H), 8.16 (d, J = 8 Hz, 2H) ppm. ^{7}Li-NMR (194 MHz, 25 °C, acetone-d_6): δ = 2.36 ppm. ^{13}C-NMR (125 MHz, 25 °C, acetone-d_6): δ = 117.18; 120.37; 121.38; 121.39 (q, J = 253 Hz); 128.08; 135.90; 148.71; 157.71 ppm. ^{19}F-NMR (470 MHz, 25 °C, acetone-d_6): δ = –55.88 ppm. HR-FT-MALDI-MS (9-AA) *m/z*: calculated for $C_{12}H_4F_3N_4O^-$ ([M]$^-$) 277.03427; found 277.03441 Da.

1.30. Lithium 4,5-dicyano-2-(4-methoxyphenyl)-imidazol-1-ide (2h)

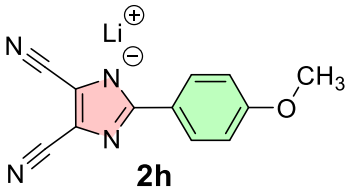

2h

The compound **2h** was synthesized from **4h** (224 mg) following the General method. The product **2h** was obtained as a white solid in 86 % yield (198 mg). M.p. = 348–352 °C. ^{1}H-NMR (500 MHz, 25 °C, acetone-d_6): δ = 3.78 (s, 3H, CH_3), 6.86 (d, J = 9 Hz, 2H), 7.96 (d, J = 9 Hz, 2H) ppm ^{7}Li-NMR (194 MHz, 25 °C, acetone-d_6): δ = 2.47 ppm, ^{13}C-NMR (125 MHz, 25 °C, acetone-d_6): δ = 55.40; 114.00; 117.35; 119.88; 128.12; 129.43; 159.23; 159.86 ppm. HR-FT-MALDI-MS (9-AA) *m/z*: calculated for $C_{12}H_7N_4O^-$ ([M]$^-$) 223.06253; found 223.06252 Da.

2. Dissociation constants and substituent effects

The dissociation constants of 1*H*-imidazoles **3** and **4** were quantified by potentiometric titration in a non-aqueous environment on a RADIOMETER TITRALAB 3 set-up consisting of an ABU93 automatic burette, a TIM90 control panel and a SAM90 stirrer. The measured potential difference was based on the setup of an indicating glass electrode G 2040 B (RADIOMETER) and a reference calomel electrode K 4040 (RADIOMETER). Benzoic acid in MeOH and ACN at the concentration of 5×10^{-3} M was used as model substance and standard. The titration reagent was a methanolic solution of tetrabutylammonium hydroxide (FLUKA AG) with a working concentration of 0.1M. Solutions of the determined 1*H*-imidazole were prepared in 10 ml volumetric flasks in the chosen solvent at a concentration of 5×10^{-3} M. The potentiometric measurement was repeated 3–5 times for each 1*H*-imidazole. The average of the two E_0 potential values of the standard, immediately after the measurement of the sample, was used to calculate the pK_{HA} of a particular sample. The dissociation constants were measured at 25 °C with dried solvents (MeOH and ACN).

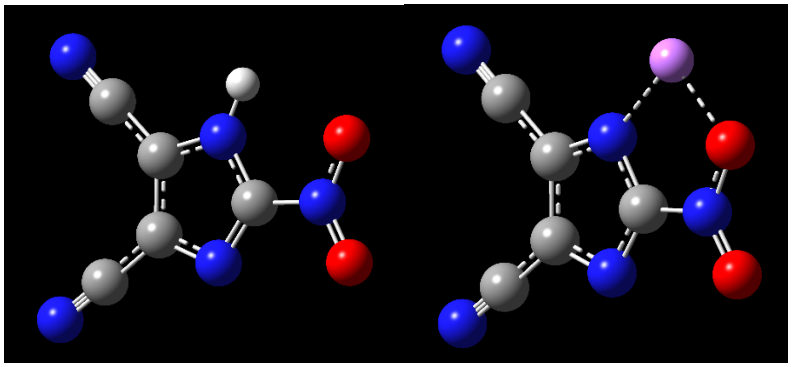

Figure S3. DFT-optimized structures of **3e** and **1e**.

Table S1. ^{13}C-NMR chemical shifts of the C2-imidazole carbon atom (125 MHz, acetone-d_6, 25 °C) and the corresponding Hammett constants σ_p.

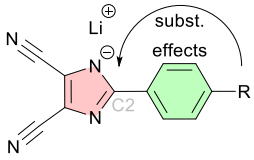

Imidazolide	**2a**	**2b**	**2c**	**2d**	**2e**	**2f**	**2g**	**2h**
Substitution (R)	CF_3	CH_3	CN	Br	NO_2	F	OCF_3	OCH_3
δ (^{13}C-C2) [ppm]	157.35	159.42	157.02	157.80	156.81	158.06	157.71	159.23
σ_p (lit.[17])	+0.53	–0.14	+0.71	+0.22	+0.81	+0.06	+0.32	–0.28

[17] O. Exner: Correlation Analysis of Chemical Data. Plenum, New York **1988**, p. 61-2, ISBN 0-306-41559-3.

3. Thermal characteristics

Thermal properties of selected Li salts were determined by differential scanning calorimetry DSC with a Mettler-Toledo STARe System DSC 2/700 equipped with FRS 6 ceramic sensor and cooling system HUBER TC100-MT RC 23. Thermal behavior was measured in aluminous crucibles sealed with a holed lid under N_2 inert atmosphere. DSC curves were recorded with a scan rate of 5 °C/min within the range 25-450 °C.

Based on the measured DSC curves (Figure S4), inorganic **$LiPF_6$** does not melt but instead undergoes direct thermal decomposition upon heating. This degradation is endothermic and begins at 180 °C. **LiTDI** also decomposes directly; however, its thermal degradation appears as a consecutive exothermic process starting above 240 °C, indicating greater thermal robustness compared to **$LiPF_6$**. The extended lithium imidazoles **2a** and **2g** exhibit an endothermic melting process, which is immediately followed by gradual decomposition, reflecting the instability of these salts in the liquid phase. The decomposition is typically exothermic for **2a**, whereas the trifluoromethoxy analogue **2g** displays an unusual gradual endothermic degradation and shows lower thermal stability as well. Overall, the thermal stability of **$LiPF_6$** and **2g** is comparable, with both decomposing at temperatures below 200 °C. In contrast, the thermal robustness of **1a** and **2a** is enhanced by about +50 °C.

Table S2. Thermal characterization of the investigated Li salts.

Der.	T_m [°C][a]	T_d [°C][b]
$LiPF_6$	-	180
1a (**LiTDI**)	-	240
2a	240	260
2g	173	190

[a] T_m = melting point (the point of intersection of a baseline and a tangent of thermal effect = onset). [b] T_d = temperature of endothermic/exothermic decomposition under inert atmosphere.

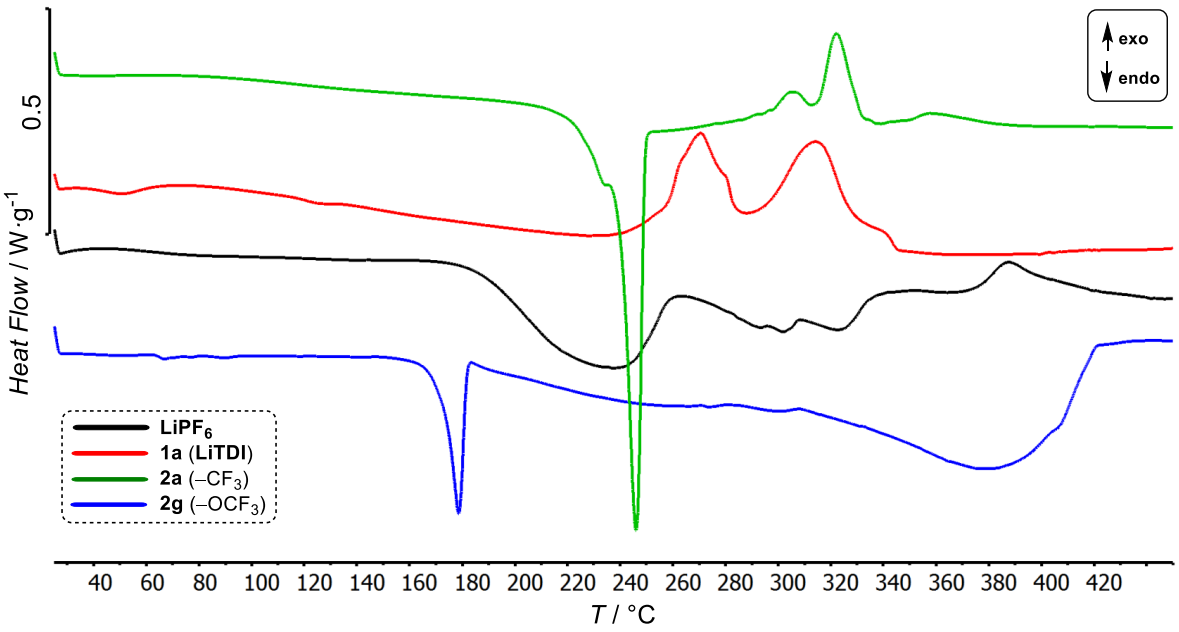

Figure S4. DSC thermograms of the selected Li salts determined with a scan rate of 5 °C/min within the range 25–450 °C.

4. Optical properties and aggregation

Ultraviolet-visible spectra were measured on a fluorescence and absorption spectrometer Horiba Duetta at the concentration of the samples 1×10^{-5}M and 5×10^{-2} M in DME/DMC 1:1 (v/v).

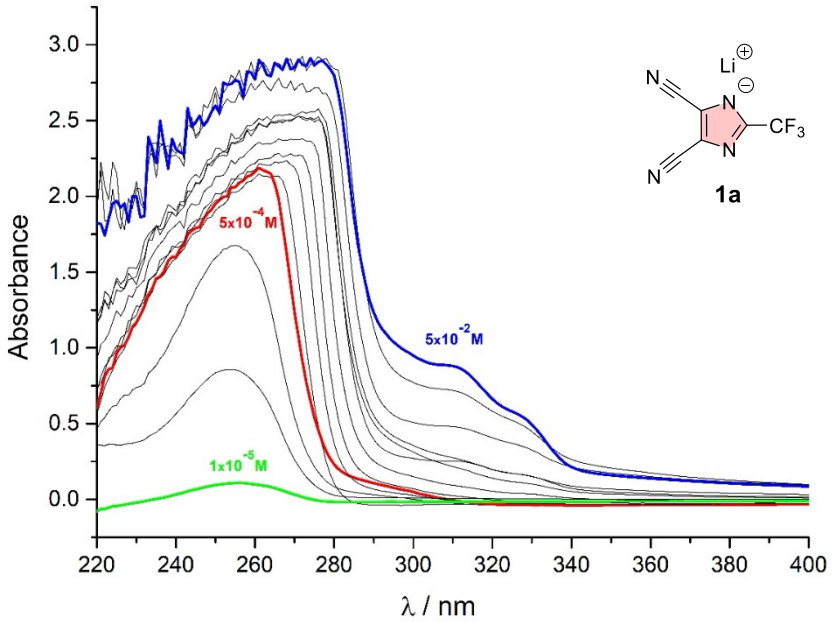

Figure S5. UV-Vis spectra of **1a** (**LiTDI**) measured within the concentration range of 1×10^{-5} (green) to 5×10^{-2} M (blue) in DME/DMC (1:1). The spectrum used to determine the first aggregation is shown in red.

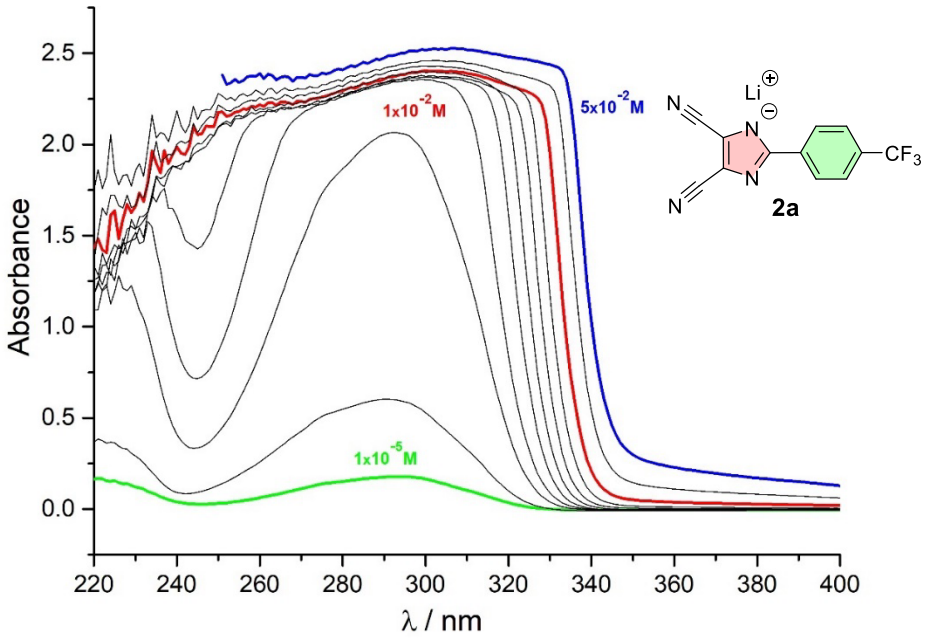

Figure S6. UV-Vis spectra of **2a** measured within the concentration range of 1×10^{-5} (green) to 5×10^{-2} M (blue) in DME/DMC (1:1). The spectrum used to determine the first aggregation is shown in red.

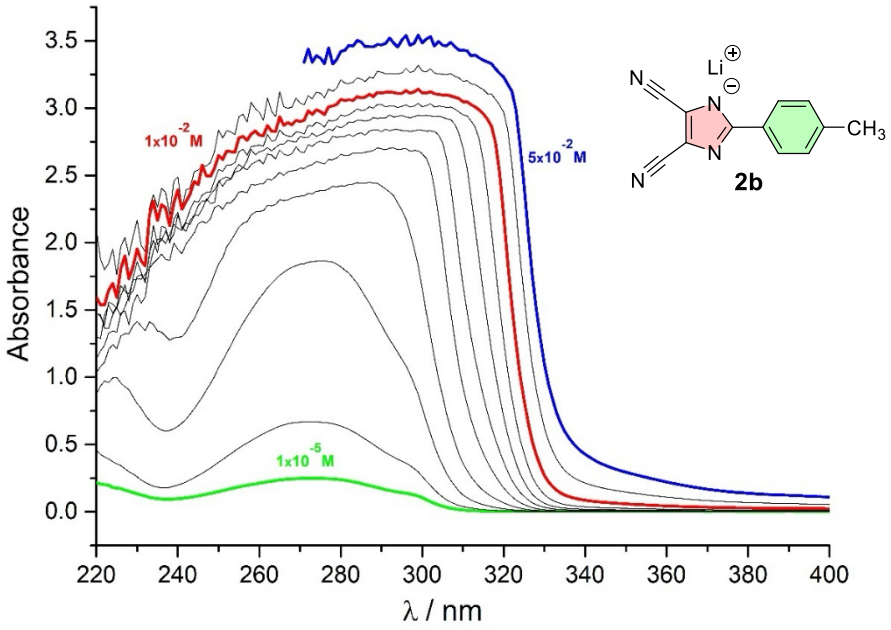

Figure S7. UV-Vis spectra of **2b** measured within the concentration range of 1×10^{-5} (green) to 5×10^{-2} M (blue) in DME/DMC (1:1). The spectrum used to determine the first aggregation is shown in red.

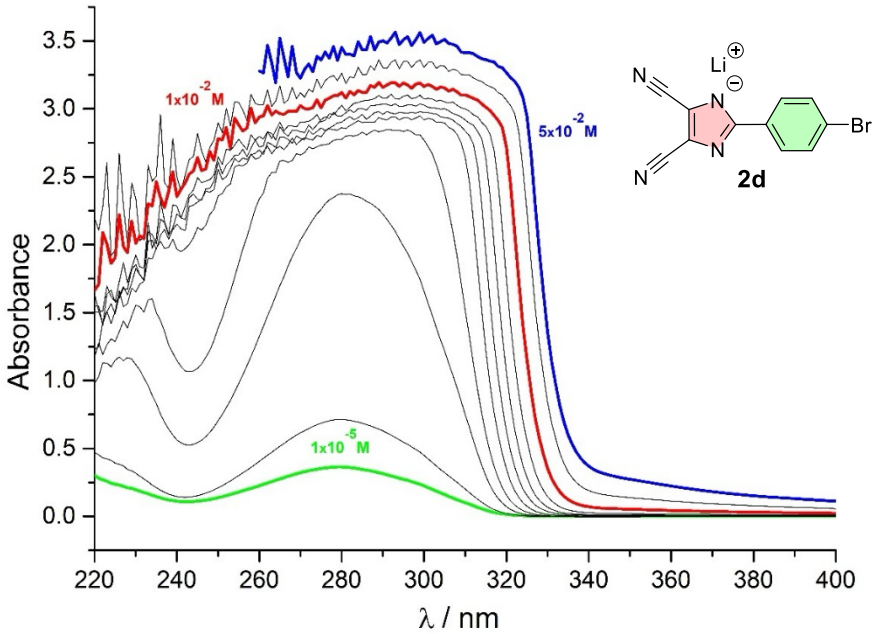

Figure S8. UV-Vis spectra of **2d** measured within the concentration range of 1×10^{-5} (green) to 5×10^{-2} M (blue) in DME/DMC (1:1). The spectrum used to determine the first aggregation is shown in red.

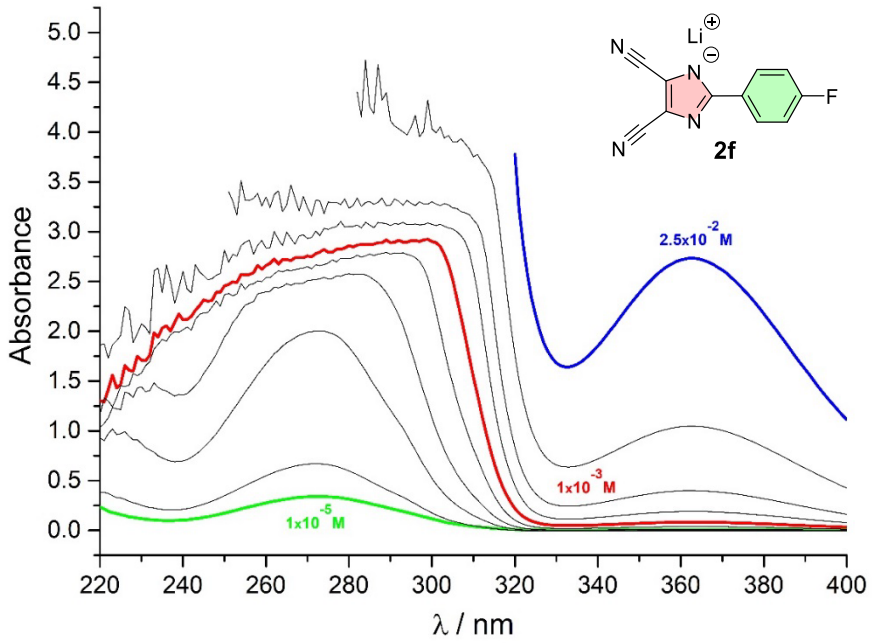

Figure S9. UV-Vis spectra of **2f** measured within the concentration range of 1×10^{-5} (green) to 5×10^{-2} M (blue) in DME/DMC (1:1). The spectrum used to determine the first aggregation is shown in red.

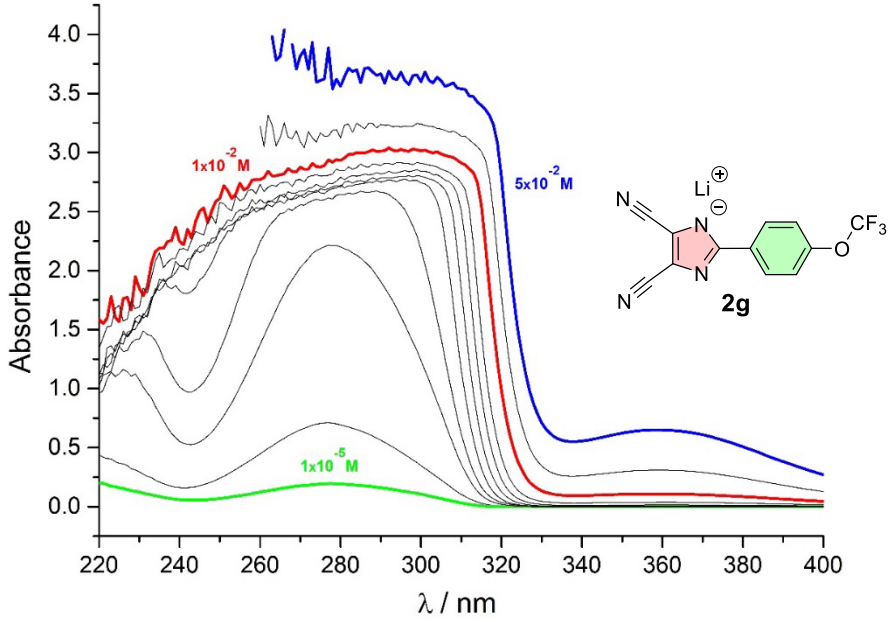

Figure S10. UV-Vis spectra of **2g** measured within the concentration range of 1×10^{-5} (green) to 5×10^{-2} M (blue) in DME/DMC (1:1). The spectrum used to determine the first aggregation is shown in red.

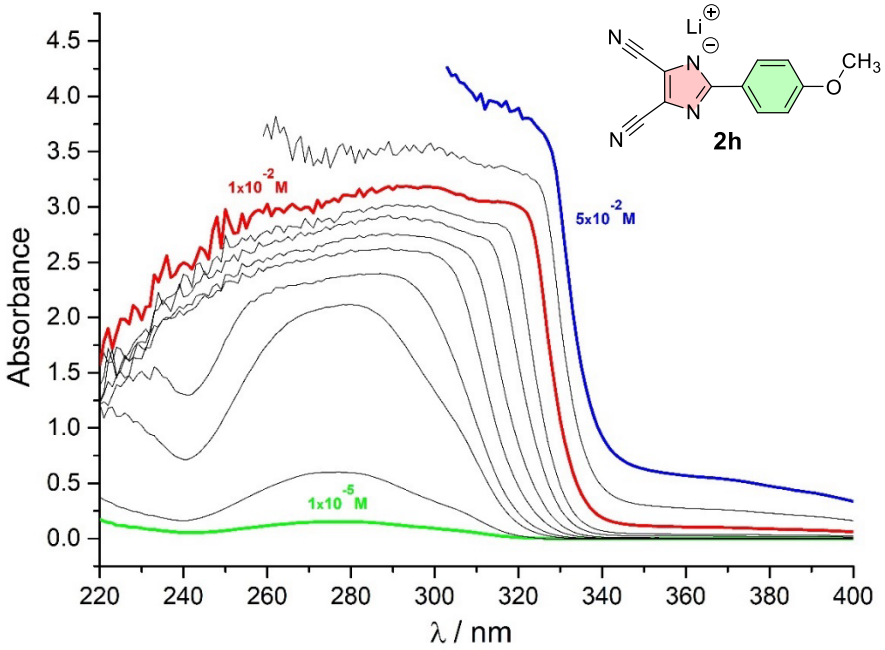

Figure S11. UV-Vis spectra of **2h** measured within the concentration range of 1×10^{-5} (green) to 5×10^{-2} M (blue) in DME/DMC (1:1). The spectrum used to determine the first aggregation is shown in red.

5. Viscosity and density

The dynamic viscosity and density of the prepared electrolytes were measured using an Anton Paar SVM 3001 viscometer based on modified Couette flow at temperatures ranging from 10 to 60 °C and an Anton Paar MCR 702e rotational rheometer at temperatures of –10 and 0 °C. For the SVM 3001 viscometer measurements, a volume of 1 ml of the sample was introduced into the measuring cell. Subsequently, the cell underwent flushing with acetone after each measurement to mitigate the risk of cross-contamination between samples. The assessment using the rotational rheometer was performed with the aid of liquid nitrogen, and a measuring assembly consisting of a spindle and cup fabricated from Inconel was employed. In this instance, a sample volume of 7 ml was utilized, and a shear rate of 60 s^{-1} was applied to determine the dynamic viscosity. The kinematic viscosity was subsequently derived from the measured values of dynamic viscosity and density.

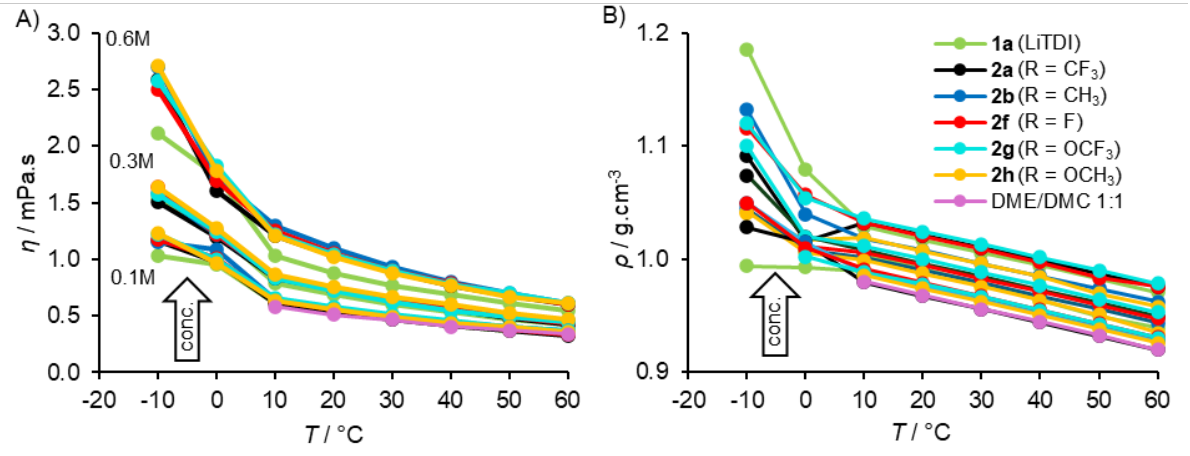

Figure S12. Relationship between the dynamic viscosity (A) and density (B) at different temperatures with increased concentration from 0.1 to 0.6 M in DME:DMC (1:1).

5.1. Arrhenius analysis

The dynamic viscosity η was fitted using the Arrhenius equation:

$$\ln \eta = \ln \eta_0 + \frac{E_\eta}{R} \cdot \frac{1}{T}$$

where η is the viscosity, η_0 is the pre-exponential factor, E_η is the activation energy of viscous flow, R is the universal gas constant and T is the absolute temperature.

Table S3. The activation energies of viscous flow (E_η) and their differences.

	E_η [kJ·mol^{-1}]			ΔE_η [kJ·mol^{-1}][a]	ΔE[b]		
der./conc.	0.1M	0.3M	0.6M		0.1M	0.3M	0.6M
1a (**LiTDI**)	11.33	13.35	14.10	2.77	0	0	0
2a	13.24	12.87	14.21	0.97	1.91	–0.48	0.11
2b	12.57	12.89	14.47	1.90	1.24	–0.45	0.38
2f	12.34	13.45	14.07	1.73	1.01	0.10	–0.03
2g	13.13	13.00	14.34	1.21	1.80	–0.34	0.25
2h	12.49	12.79	14.85	2.36	1.16	–0.56	0.75

[a] ΔE_η is a difference between the E_η values at 0.1 and 0.6 M solutions of the particular derivative. [b] $\Delta E = E_\eta - E_{LiTDI}$, a difference in the activation energy of viscous flow of the particular derivative compared to the benchmark derivative **1a**.

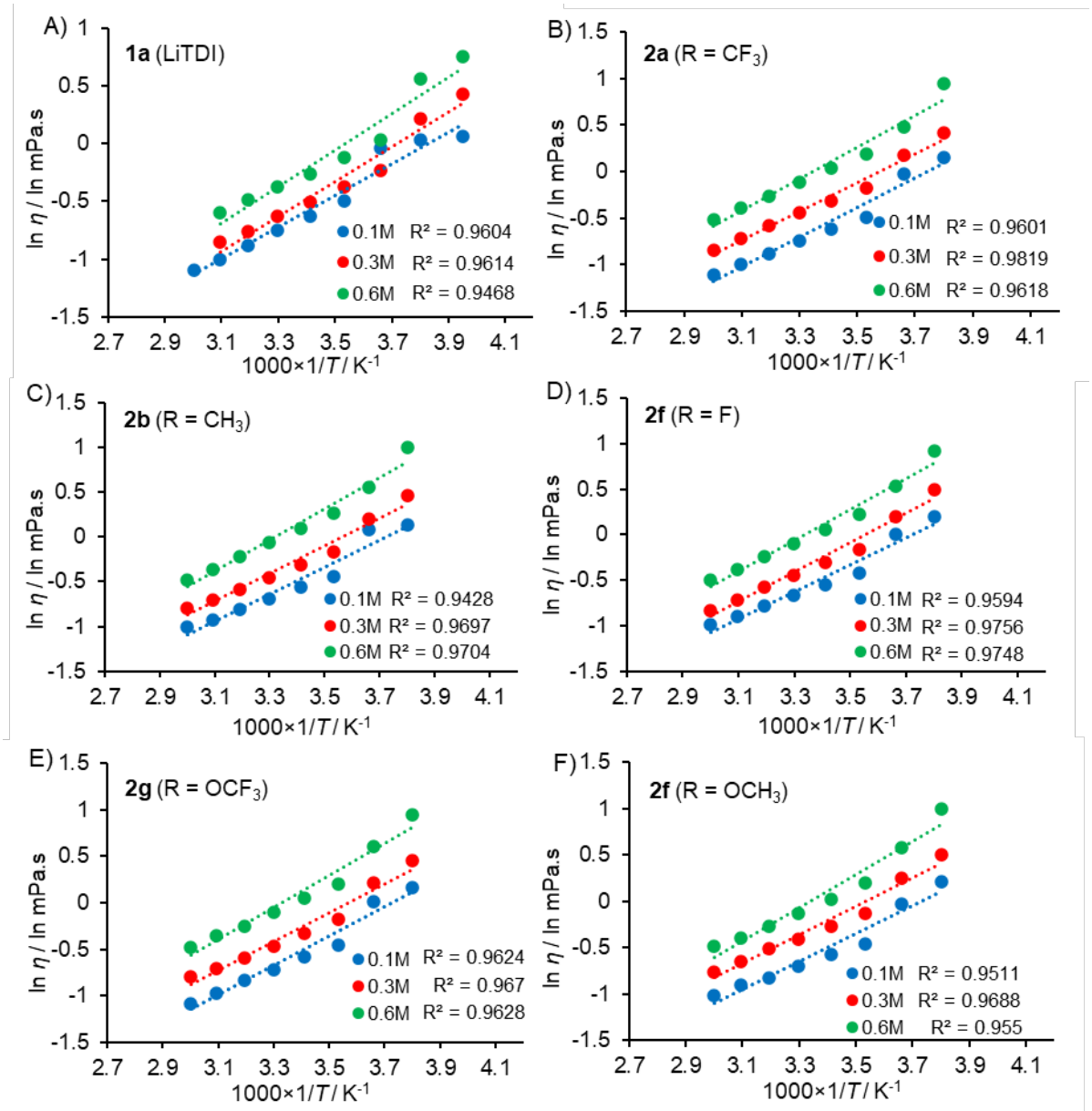

Figure S13. The dynamic viscosity ln η as a function of 1/T for 0.1, 0.3 and 0.6 M solutions of **1a** (A), **2a** (B), **2b** (C), **2f** (D), **2g** (E) and **2h** (F) in DME/DMC (1:1).

5.2. Eyring analysis

The Gibbs energy of activation ($\Delta G^{\ddagger}$) was evaluated using Eyring's equation[18]:

$$\Delta G^{\ddagger} = RT \cdot \ln\left(\frac{\eta \cdot k_B T \lambda}{h}\right)$$

where, η is the dynamic viscosity, λ the molecular jump distance (estimated as the cube root of the molar volume V_m) and is also interpreted as the diameter of the diffusing species, T the absolute temperature, and k_B, h, and R are physical constants. Linear plots of $\ln(\eta\lambda/T)$ versus $1/T$ were constructed to extract the activation enthalpy ($\Delta H^{\ddagger}$) and entropy ($\Delta S^{\ddagger}$) via the linearized form of the Eyring equation:

$$\ln\left(\frac{\eta\lambda}{T}\right) = \frac{\Delta H^{\ddagger}}{RT} - \frac{\Delta S^{\ddagger}}{R} + \ln\frac{h}{k_B}$$

Table S4. The Gibbs energy of activation calculated using Eyring equation.

	$\Delta G^{\ddagger}$ [kJ·mol^{-1}], 20 °C			$\Delta G^{\ddagger}$ [kJ·mol^{-1}], 40 °C			$\Delta G^{\ddagger}$ [kJ·mol^{-1}], 60 °C		
der./conc.	0.1M	0.3M	0.6M	0.1M	0.3M	0.6M	0.1M	0.3M	0.6M
1a	1.98	2.58	3.17	1.37	1.98	2.58	0.87	1.47	2.06
2a	2.28	3.00	3.83	1.65	2.37	3.12	1.12	1.73	2.52
2b	2.22	2.81	3.79	1.63	2.18	3.05	1.18	1.69	2.43
2f	2.27	2.85	3.71	1.71	2.20	3.00	1.24	1.59	2.39
2g	2.39	3.01	3.89	1.79	2.36	3.20	1.22	1.90	2.65
2h	2.23	2.97	3.68	1.84	2.58	3.16	1.38	2.00	2.64

Table S5. The enthalpy and entropy of activation calculated using linearized Eyring equation.

	$\Delta H^{\ddagger}$ [kJ·mol^{-1}]			$\Delta S^{\ddagger}$ [J·mol^{-1}·K^{-1}]		
der./conc.	0.1M	0.3M	0.6M	0.1M	0.3M	0.6M
1a	14.47	16.24	15.96	136.49	140.11	137.16
2a	15.31	13.95	15.27	138.22	133.06	134.77
2b	14.63	15.03	16.46	136.06	135.51	137.18
2f	12.76[a]	16.04	16.11	129.85[a]	138.79	136.22
2g	15.21	15.05	16.40	137.49	134.89	136.36
2h	14.15	14.91	17.04	133.80	133.95	138.58

[a] Considered as outliers.

[18] a) L. J. dos Santos, L. A. Espinoza-Velasquez, J. A. P. Countinho, S. Monteiro, *Fluid Phase Equilib.*, **2020**, *522*, 112774. b) S. P. Mousavi, S. Atashrouz, M. N. Amar, A. Hemmati-Sarapardeh, A. Mohaddespour, A. Mosavi, *Molecules,* **2021**, *26*, 156.

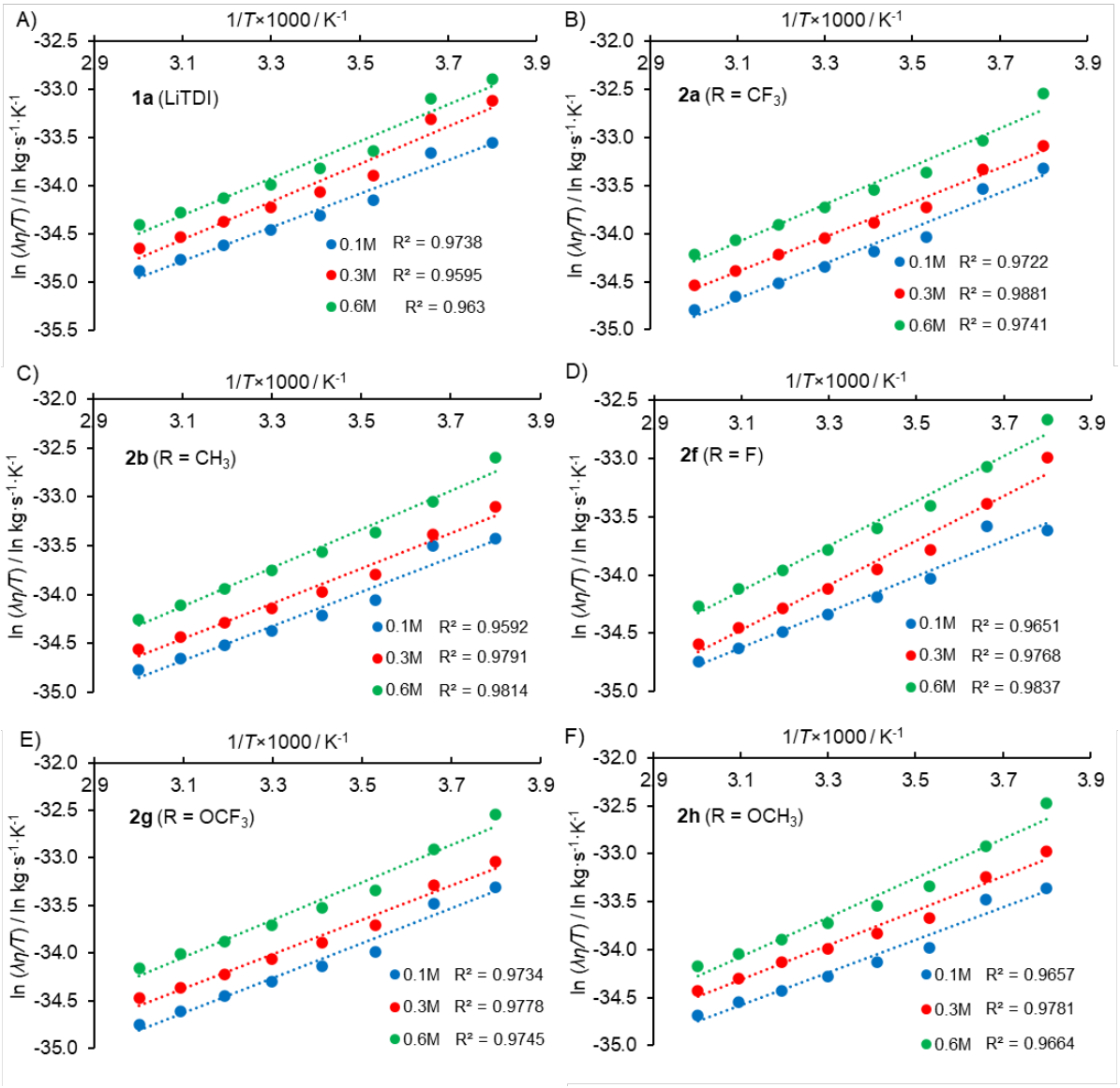

Figure S14. The term ln ($\eta\lambda/T$) vs. 1/T (Eyring equation) for 0.1, 0.3 and 0.6 M solutions of **1a** (A), **2a** (B), **2b** (C), **2f** (D), **2g** (E) and **2h** (F) in DME/DMC (1:1).

5.3. JDK analysis

The Jones–Dole–Kaminski (JDK) equation was used to determine B and D coefficients from the measured dynamic viscosity of the electrolytes with varied concentration:

$$\eta_r = 1 + A\sqrt{c} + Bc + Dc^2$$

where $\eta_r = \eta/\eta_0$ is the relative viscosity, c the salt concentration and the constants A, B and D describe long-range ionic interactions, volume effects and short-range structural effects. At low concentrations (< 0.1 mol/l), the $A\sqrt{c}$ and Bc terms dominate, while the Dc^2 contribution is diminished. However, at higher concentrations, the Dc^2 term

becomes increasingly important and the $A\sqrt{c}$ suppressed. From the fitted B coefficient, the effective solute radius r_s was calculated using the following equation:

$$r_s = \sqrt[3]{\left(\frac{3}{10\pi N_A B}\right)}$$

Table S6. The B and D parameters along with the effective solute radii for **1a**, **2a**–**b** and **2f**–**g** at 20 °C.

der./par.	B [mol^{-1}·l]	D (mol^{-2}·l^{-2}]	r_s [nm]
1a	1.040	0.346	0.548
2a	1.093	1.098	0.557
2b	0.927	1.611	0.528
2f	1.153	1.025	0.568
2g	0.953	1.328	0.533
2h	1.482	0.367	0.617

Table S7. The B and D parameters along with the effective solute radii for **1a** and **2a** as a function of temperature.

der./temp. [°C]		10	20	30	40	50	60
1a	B [mol^{-1}·l]	1.065	1.040	0.827	0.828	0.566	0.626
	D (mol^{-2}·l^{-2}]	0.427	0.346	0.496	0.634	0.944	0.789
	r_s [nm]	0.553	0.548	0.508	0.508	0.448	0.463
2a	B [mol^{-1}·l]	1.085	1.093	0.918	0.959	0.605	0.421
	D (mol^{-2}·l^{-2}]	1.293	1.098	1.104	0.990	1.350	1.496
	r_s [nm]	0.556	0.557	0.526	0.534	0.458	0.406

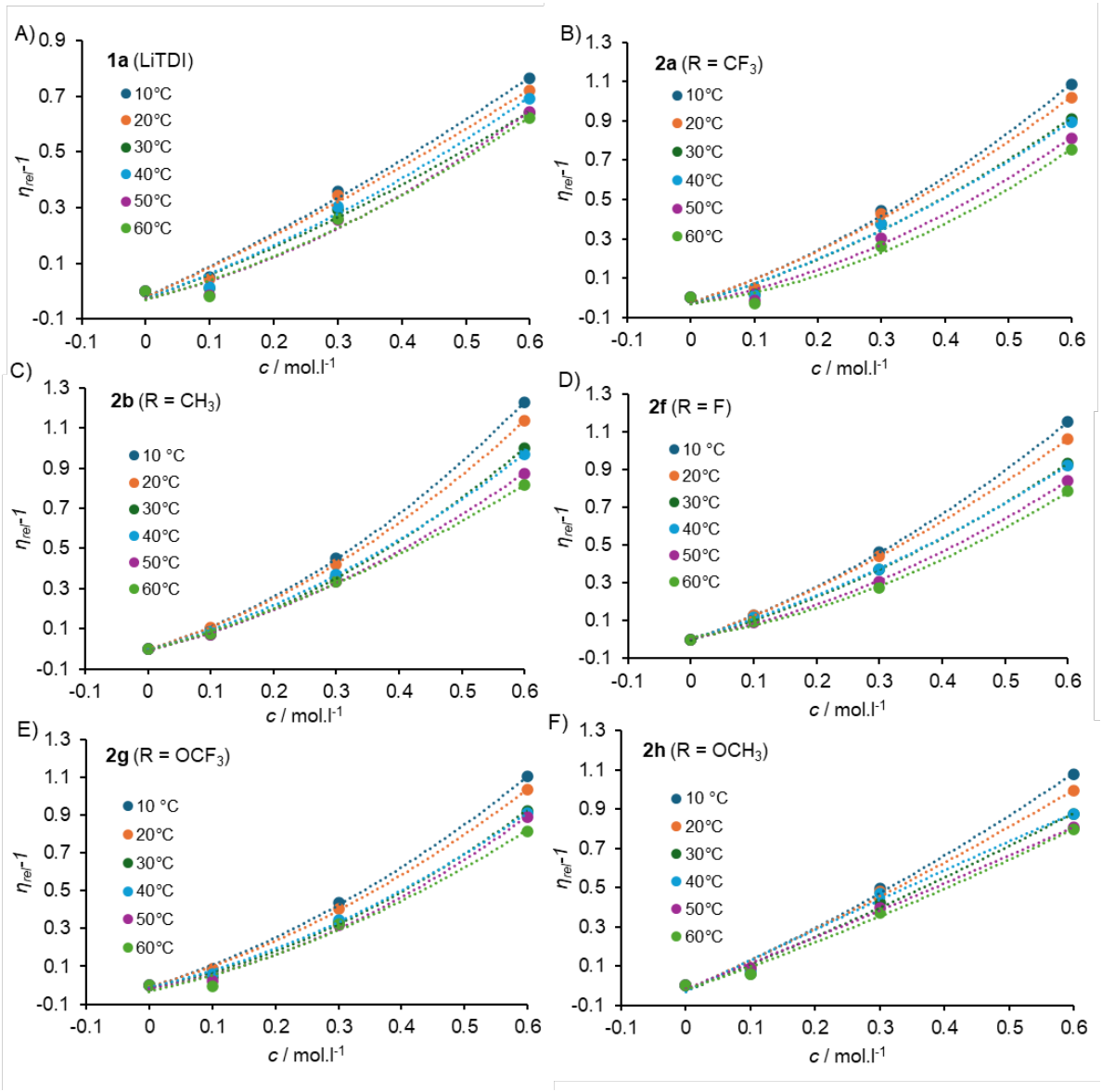

Figure S15. The relative dynamic viscosity (η_{rel}-1) of **1a** (A), **2a** (B), **2b** (C), **2f** (D), **2g** (E) and **2h** (F) in DME/DMC (1:1) as a function of the concentration at different temperatures.

5.4. Einstein analysis

The effective hydrodynamic radius r_{eff} was evaluated through a viscosity-based formulation derived from Einstein's theory of dilute suspensions. In this model, the increase in the solution viscosity due to the presence of solute particles is related to their volume fraction, yielding the following expression for spherical solutes:

$$r_{\text{eff}} = \sqrt[3]{\left(\frac{3}{4\pi} \cdot \frac{1}{N_A} \cdot \frac{\frac{\eta}{\eta_0} - 1}{2.5 \cdot c}\right)}$$

where η/η_0 is the relative dynamic viscosity, N_A is Avogadro's number, c is the salt concentration in mol/m^3 and the prefactor 2.5 corresponds to the intrinsic viscosity of hard spheres in dilute solution.

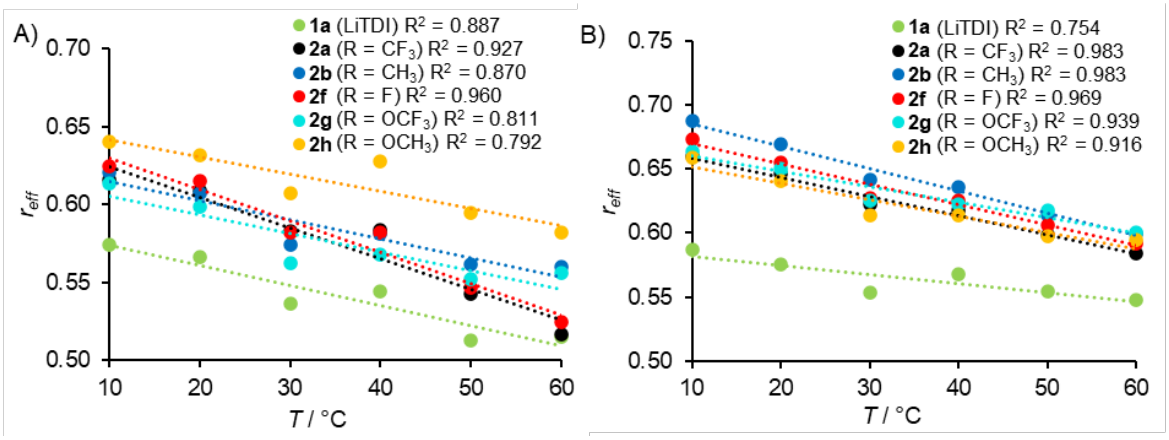

Figure S16. Effective hydrodynamic radius r_{eff} calculated using the modified Einstein-Stokes equation as a function of temperature for 0.3 (A) and 0.6 M (B) solutions of **1a**, **2a**–**b** and **2f**–**h** in DME/DMC (1:1).

5.5. Self-diffusion coefficient

The self-diffusion coefficient D can be estimated using the Stokes–Einstein equation:

$$D = \frac{k_B T}{6\pi\eta r_{eff}}$$

where k_B is the Boltzmann constant, T is the absolute temperature, η is the dynamic viscosity of the solvent, and r_{eff} is the hydrodynamic radius of the solvated ion from the Einstein viscosity-based approach.

Table S8. Self-diffusion coefficient D of **1a**, **2a**–**b** and **2f**–**g** at 20 ° and varied concentration.

	D [×10^{-10} m^2·s^{-1}]		
der./conc.	0.1M	0.3M	0.6M
1a	9.763	5.502	4.222
2a	9.288	4.818	3.205
2b	6.807	4.842	2.925
2f	6.326	4.725	3.092
2g	7.512	4.973	3.154
2h	7.377	4.479	3.274

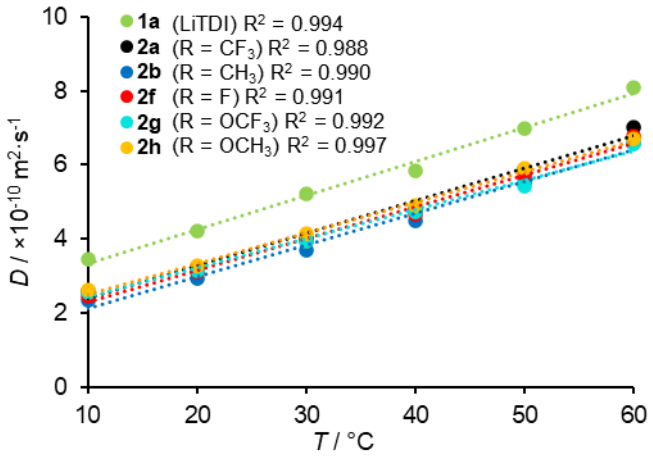

Figure S17. Self-diffusion coefficient *D* of **1a**, **2a**–**b** and **2f**–**h** in DME/DMC (1:1) as a function of temperature.

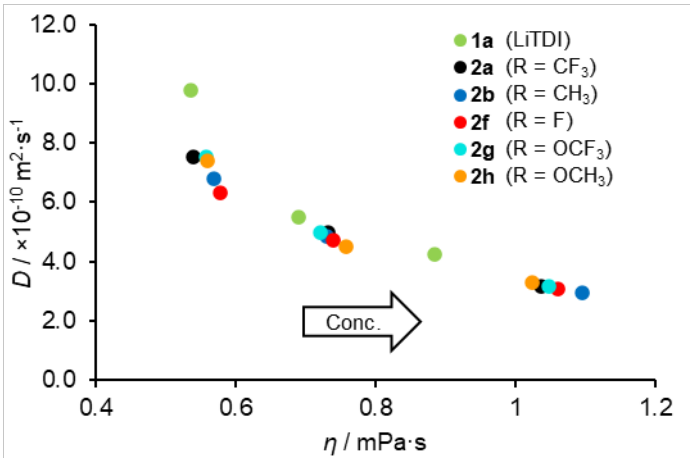

Figure S18. Self-diffusion coefficient *D* of **1a**, **2a**–**b** and **2f**–**h** in DME/DMC (1:1) as a function of the dynamic viscosity/concentration.

6. Electrochemical measurements

6.1. Conductometry

Conductometry was used to determine the conductivity of the electrolyte. The conductivity measurements were carried out using a calibrated Mettler Toledo SevenDirect SD30 equipped with a Conductivity cell InLab® 710, and a cell constant verified using a certified conductivity standard solution 1413 µS/cm. The measurements were performed at a controlled temperature of 20 °C. Calibration was checked before and after the series to confirm stability. Conductivity for reference 1M $LiPF_6$ in DME:DMC 1:1 electrolyte was estimated to be 13.26 $mS \cdot cm^{-1}$, resp. 7.866 $mS \cdot cm^{-1}$ for 0.6 M $LiPF_6$ in DME:DMC 1:1.

Table S9. Conductometric data estimated for various concentration in DME:DMC (1:1).

Electrolyte	κ [$mS \cdot cm^{-1}$]
0,6 M $LiPF_6$	7.866
1.0 M $LiPF_6$	13.257
0.1 M **LiTDI**	0.490
0.3 M **LiTDI**	2.613
0.6 M **LiTDI**	6.334
1.0 M **LiTDI**	9.049

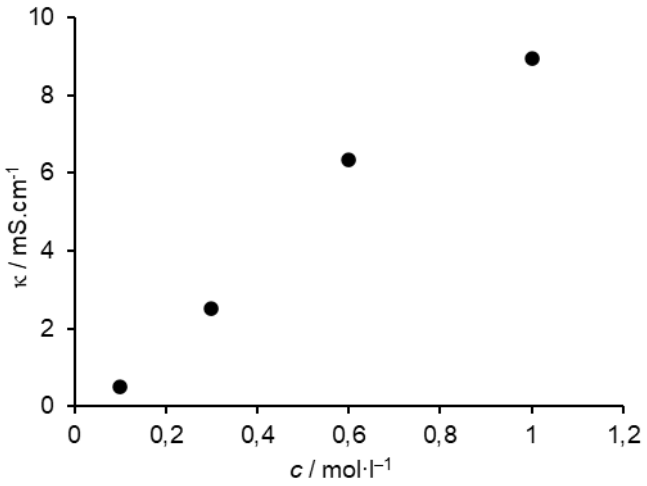

Figure S19. The conductivity of **LiTDI** (**1a**) as a function of the concentration (0.1–1.0 M solutions in DME/DMC 1:1).

6.2. Walden plot analysis

Table S10. Deviation from the ideal KCl conductivity line at 20 °C for the studied imidazolides in DME:DMC (1:1) and the calculated ionicity values.

Salt (conc.)	$\log(\Lambda)_{ideal}$ ($\log(S\cdot cm^2\cdot mol^{-1})$)	$\log(\Lambda)_{real}$ ($\log(S\cdot cm^2\cdot mol^{-1})$)	ΔW	ionicity
1a (0.6M)	2.054	1.023	–1.030	0.0933
1a (0.3M)	2.161	0.925	–1.237	0.0580
1a (0.1M)	2.271	0.691	–1.580	0.0263
2a (0.6M)	1.984	1.014	–0.970	0.1071
2b (0.6M)	1.960	0.798	–1.162	0.0688
2f (0.6M)	1.975	0.995	–0.980	0.1048
2g (0.6M)	1.980	1.016	–0.964	0.1087
2h (0.6M)	1.990	0.705	–1.285	0.0519
$LiPF_6$ (0.6M)	1.917	1.118	–0.799	0.1588

6.3. Electrochemical impedance spectroscopy (EIS)

The EIS measurements were performed using a PalmSense Sensit BT. The frequency range was set from 50 Hz to 200 kHz, with an AC amplitude of 10 mV applied at the open-circuit potential. All measurements were conducted at a controlled temperature of 20 °C under argon atmosphere (in Glovebox Jacomex). Data were collected using PSTouch and fitted to an equivalent circuit model using PSTrace5.

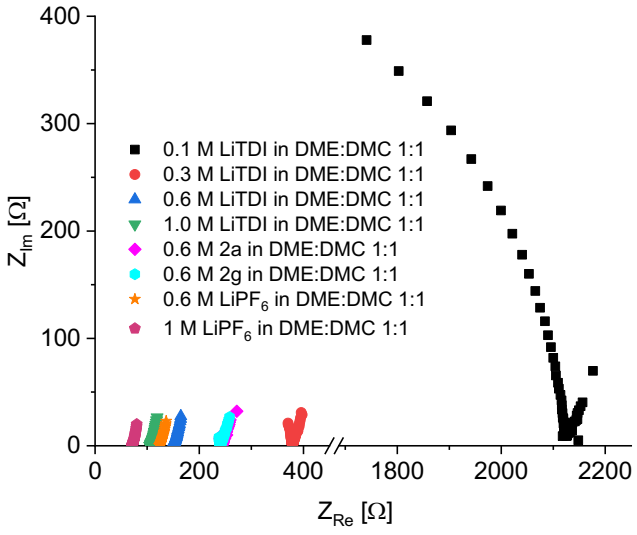

Figure S20. Nyquist plots obtained from the EIS measurements for **LiTDI** (*c* = 0.1 to 1.0 M), **2a**, **2g** (*c* = 0.6 M) in DME:DMC (1:1) and for **$LiPF_6$** (*c* = 0.6 and 1 M).

6.4. Linear sweep voltammetry (LSV)

LSV measurements were realised in a two-electrode configuration, where both the working and counter electrodes consisted of stainless-steel discs. The electrolyte under investigation was placed between the stainless-steel disc electrodes separated by GF (glassy fibre) separator. Coin cell with two stainless steel discs were assembled and crimped under inert argon atmosphere in Glovebox Jacomex. LSV measurements were performed using a Biologic BCS-805 device. The potential window was swept from 0 V to the final potential 5 V at a scan rate of 10 $mV \cdot s^{-1}$. The current values were normalized to the geometric surface area of the electrode to obtain current density ($mA \cdot cm^{-2}$), which was plotted against the applied potential. All measurements were performed at 20 °C.

7. ^{1}H and ^{13}C-NMR Spectra o imidazolides 1 and 2

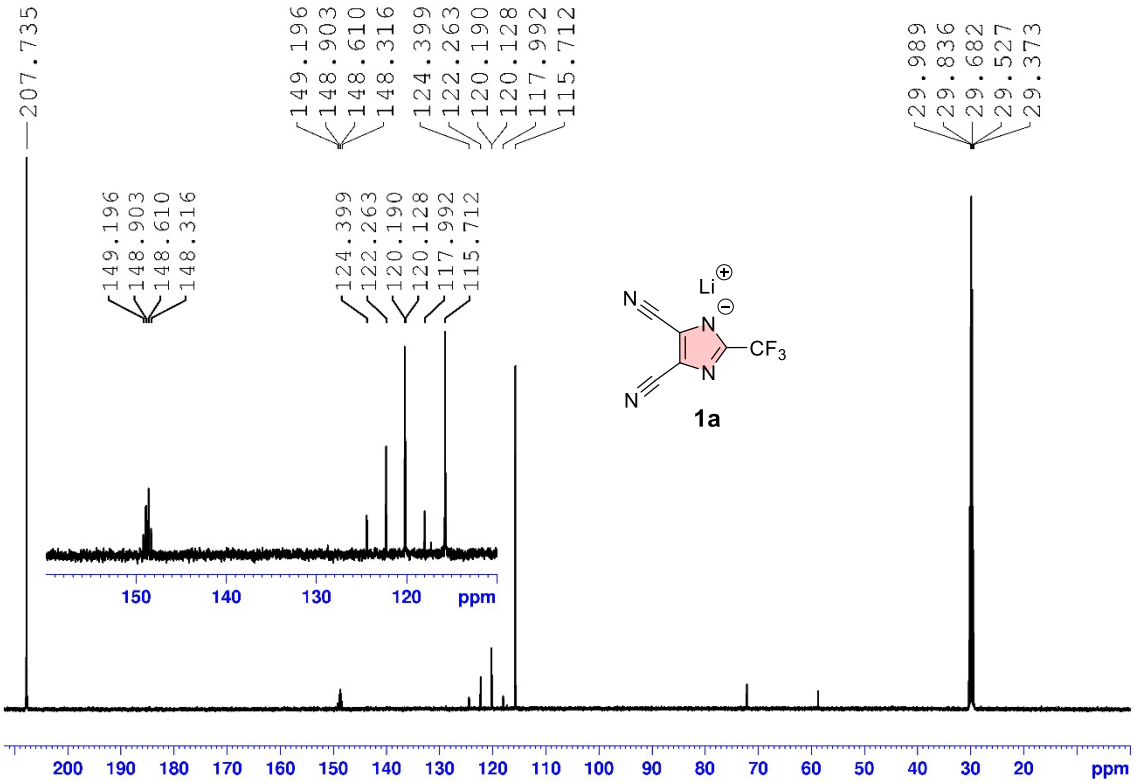

Figure S21. ^{13}C-NMR (125 MHz, acetone-d_6, 25 °C) spectrum of compound **1a**.

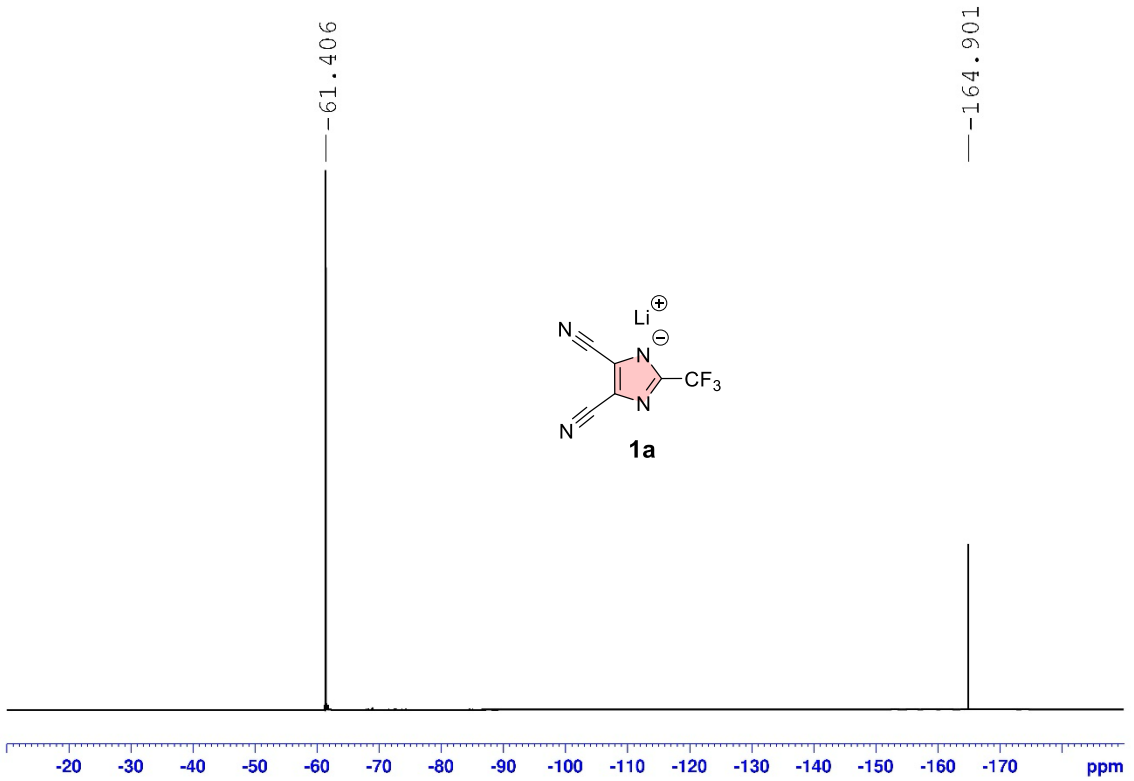

Figure S22. ^{19}F-NMR (470 MHz, acetone-d_6, 25 °C) spectrum of compound **1a**.

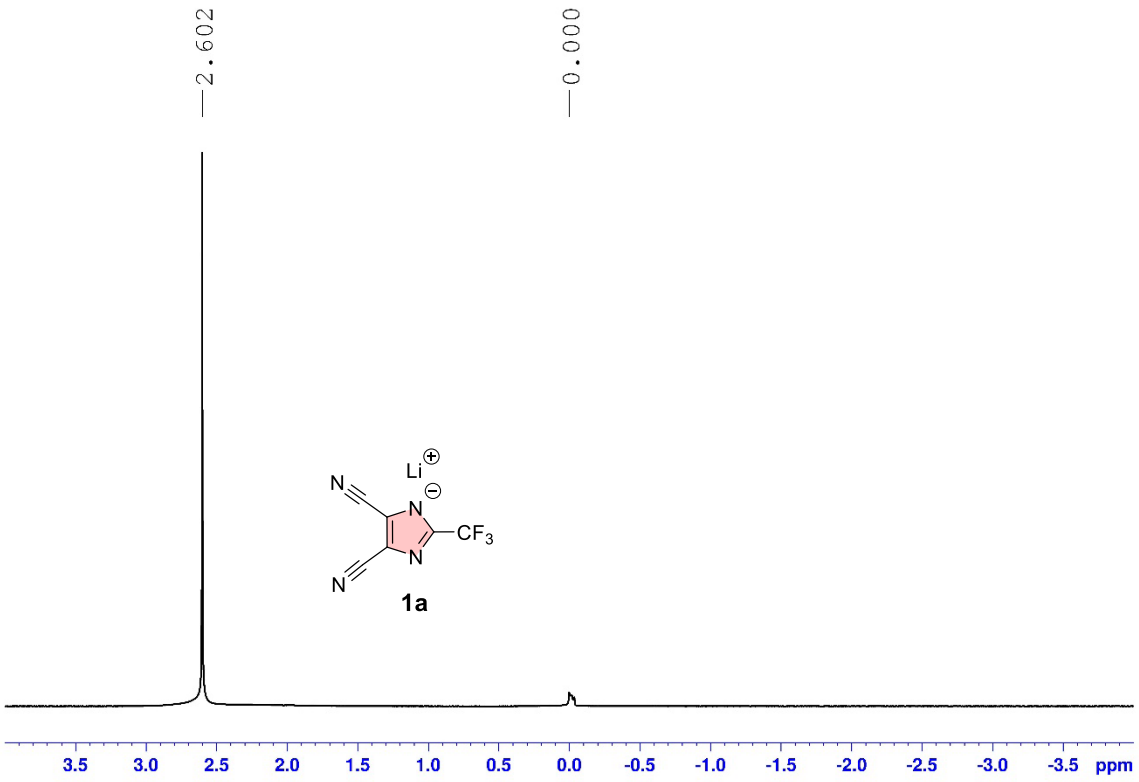

Figure S23. ^{7}Li-NMR (194 MHz, acetone-d_6, 25 °C) spectrum of compound **1a**.

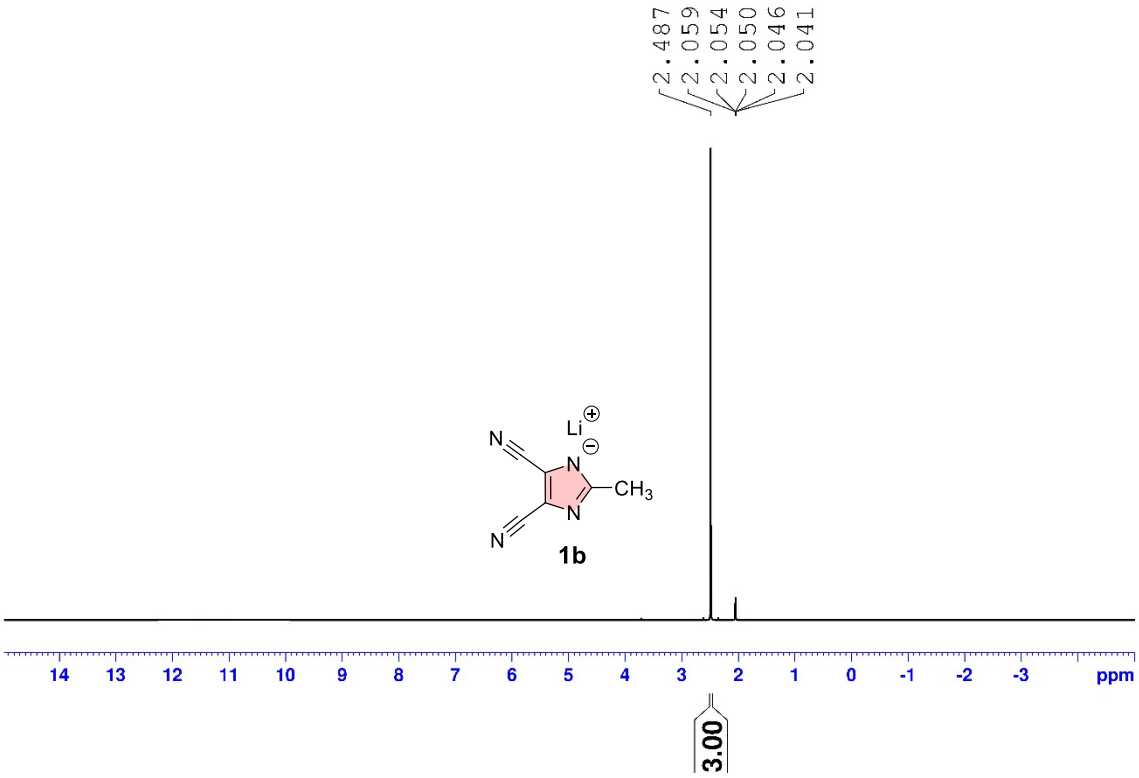

Figure S24. ^{1}H-NMR (500 MHz, acetone-d_6, 25 °C) spectrum of compound **1b**.

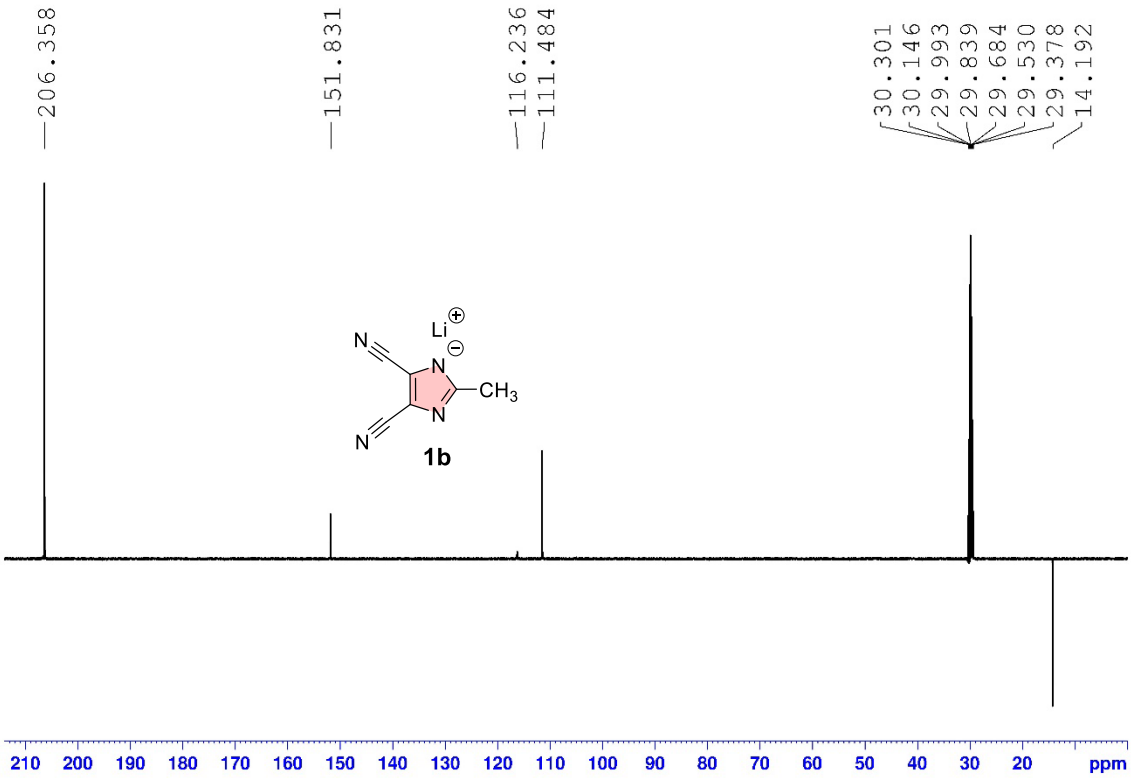

Figure S25. ^{13}C-NMR (125 MHz, acetone-d_6, 25 °C) spectrum of compound **1b**.

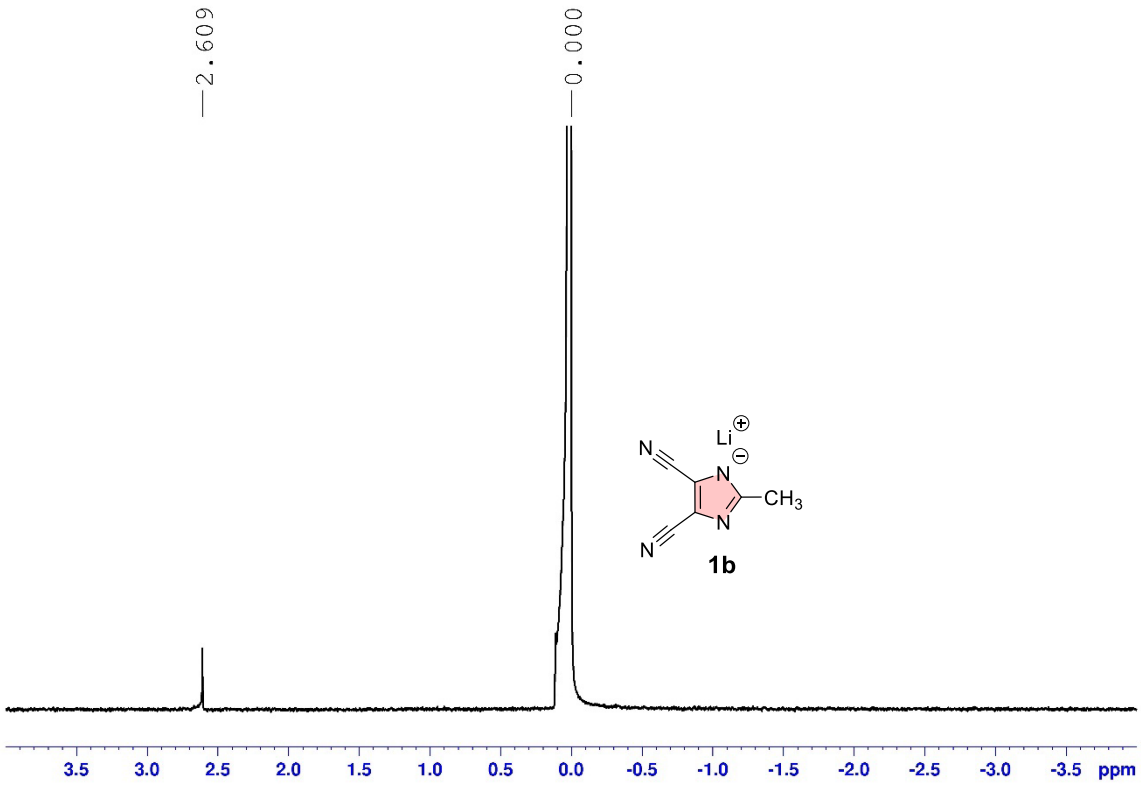

Figure S26. ^{7}Li-NMR (194 MHz, acetone-d_6, 25 °C) spectrum of compound **1b**.

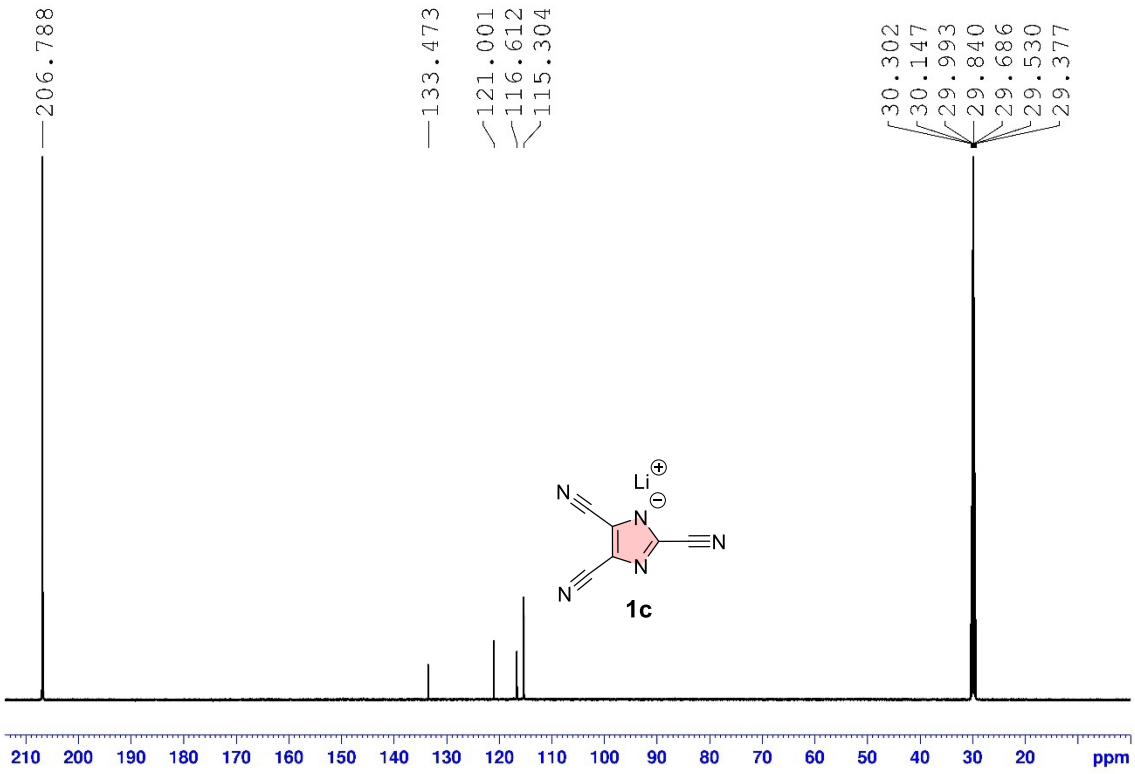

Figure S27. ^{13}C-NMR (125 MHz, acetone-d_6, 25 °C) spectrum of compound **1c**.

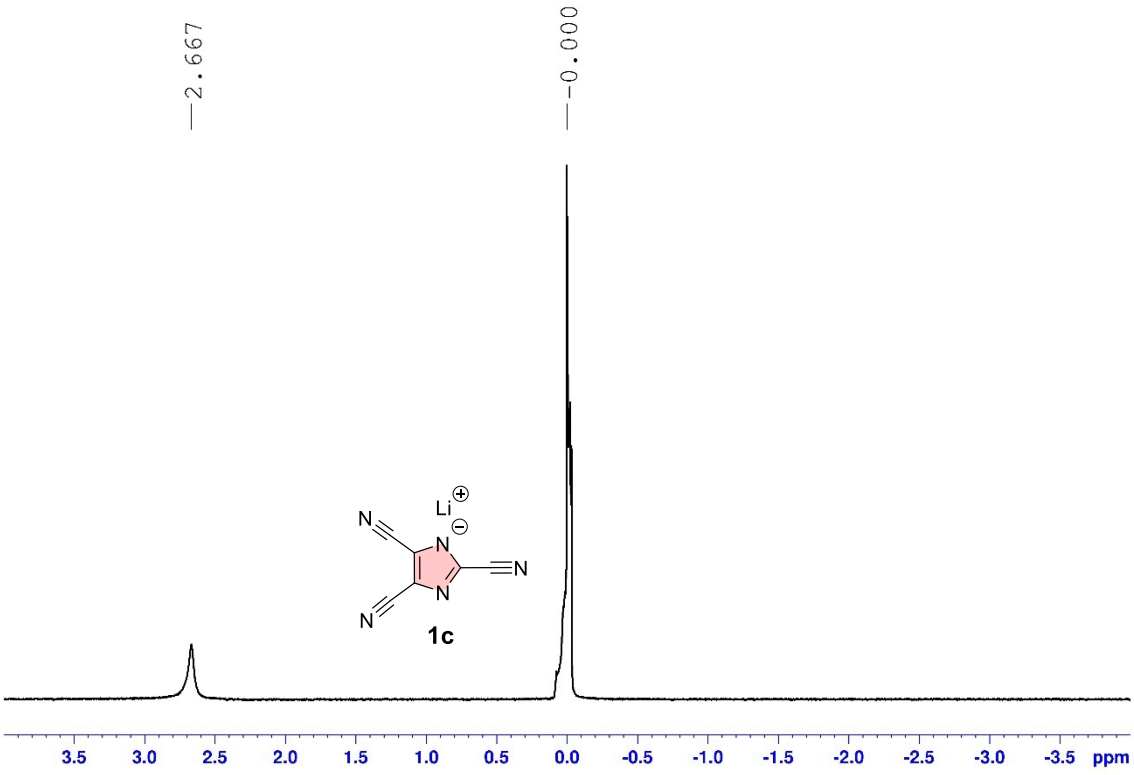

Figure S28. ^{7}Li-NMR (194 MHz, acetone-d_6, 25 °C) spectrum of compound **1c**.

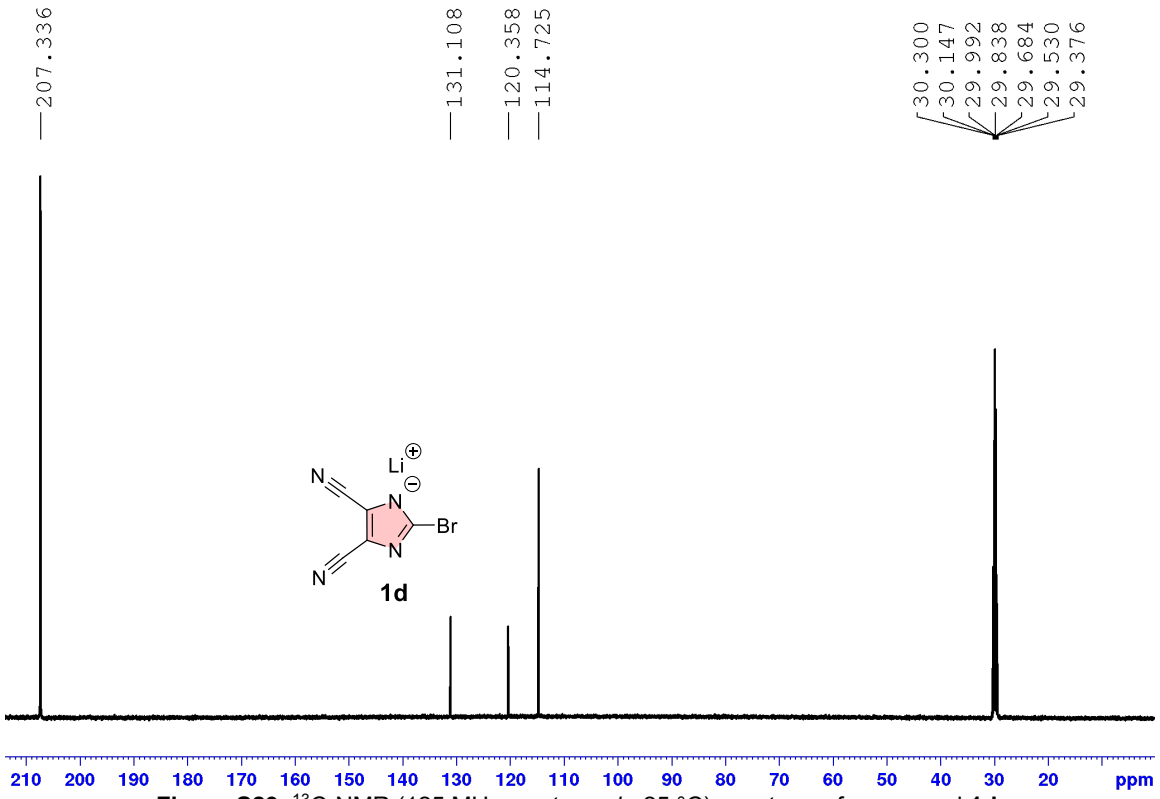

Figure S29. ^{13}C-NMR (125 MHz, acetone-d_6, 25 °C) spectrum of compound **1d**.

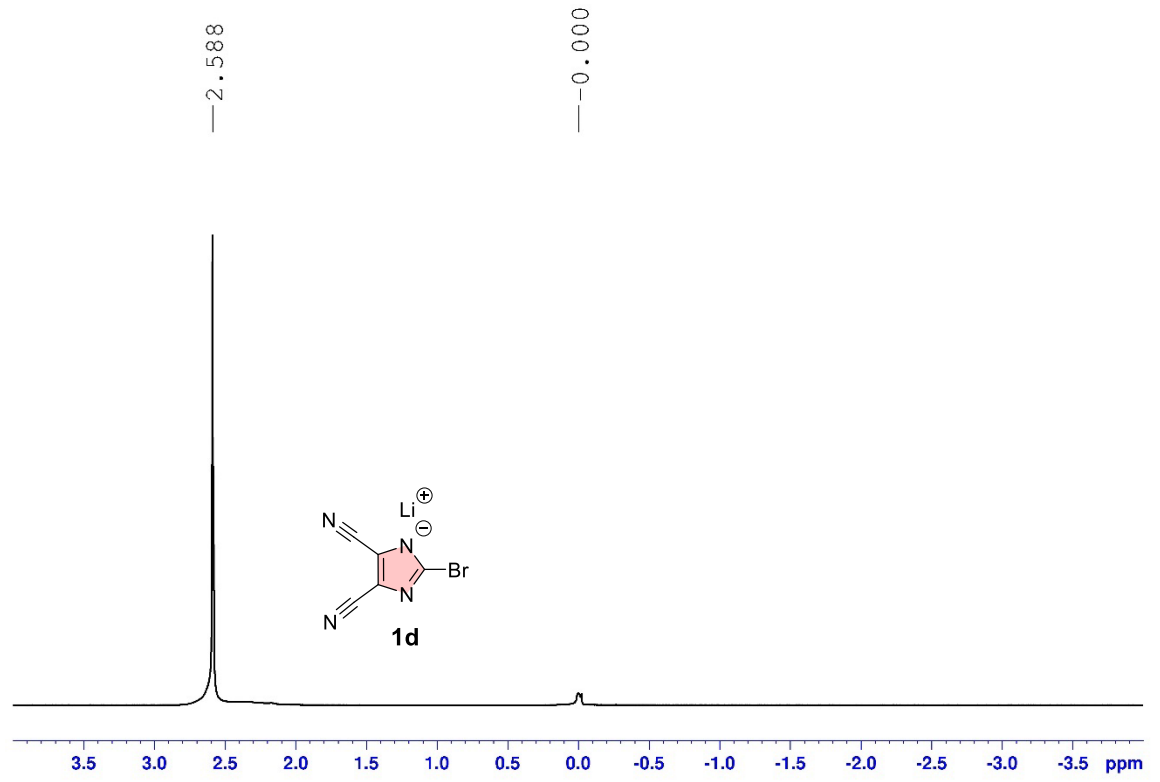

Figure S30. ^{7}Li-NMR (194 MHz, acetone-d_6, 25 °C) spectrum of compound **1d**.

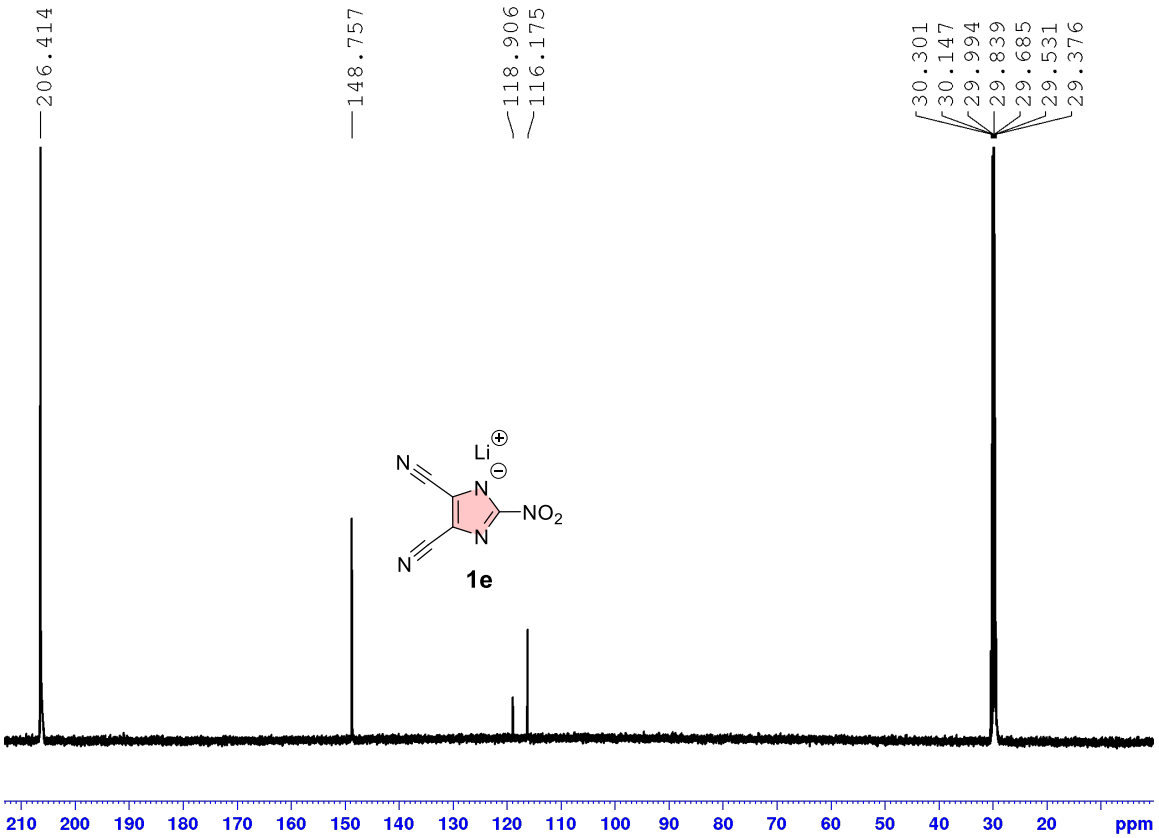

Figure S31. ^{13}C-NMR (125 MHz, acetone-d_6, 25 °C) spectrum of compound **1e**.

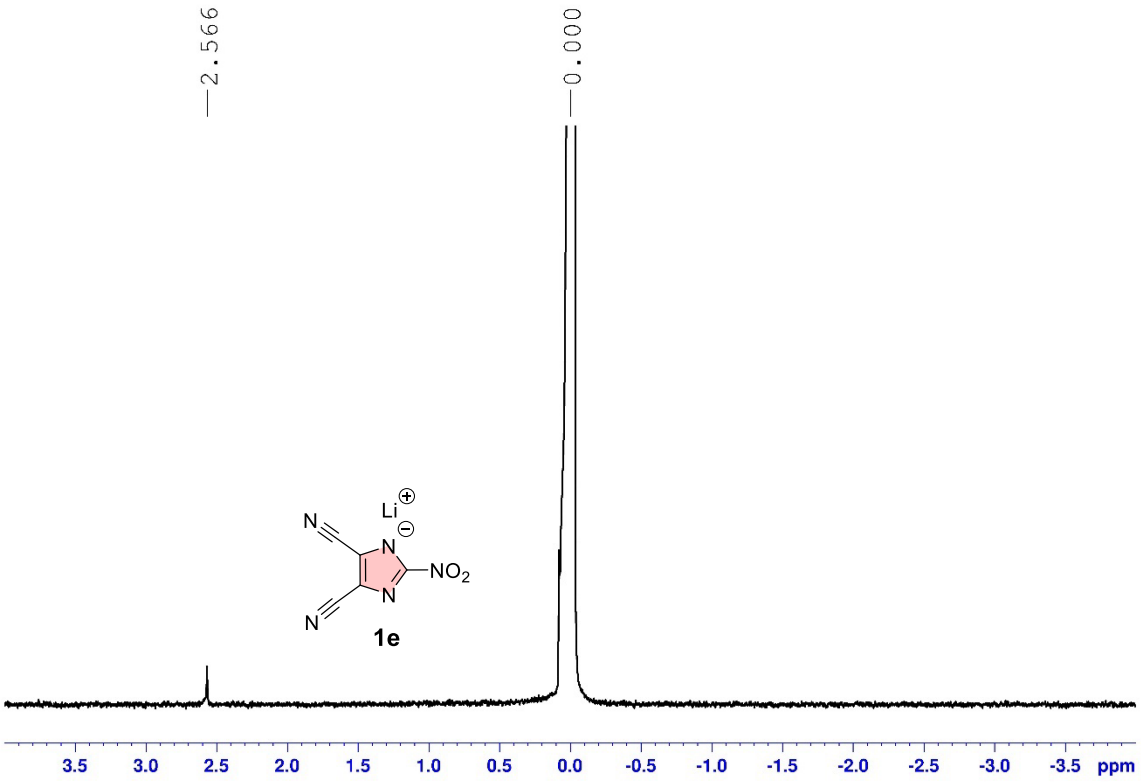

Figure S32. ^{7}Li-NMR (194 MHz, acetone-d_6, 25 °C) spectrum of compound **1e**.

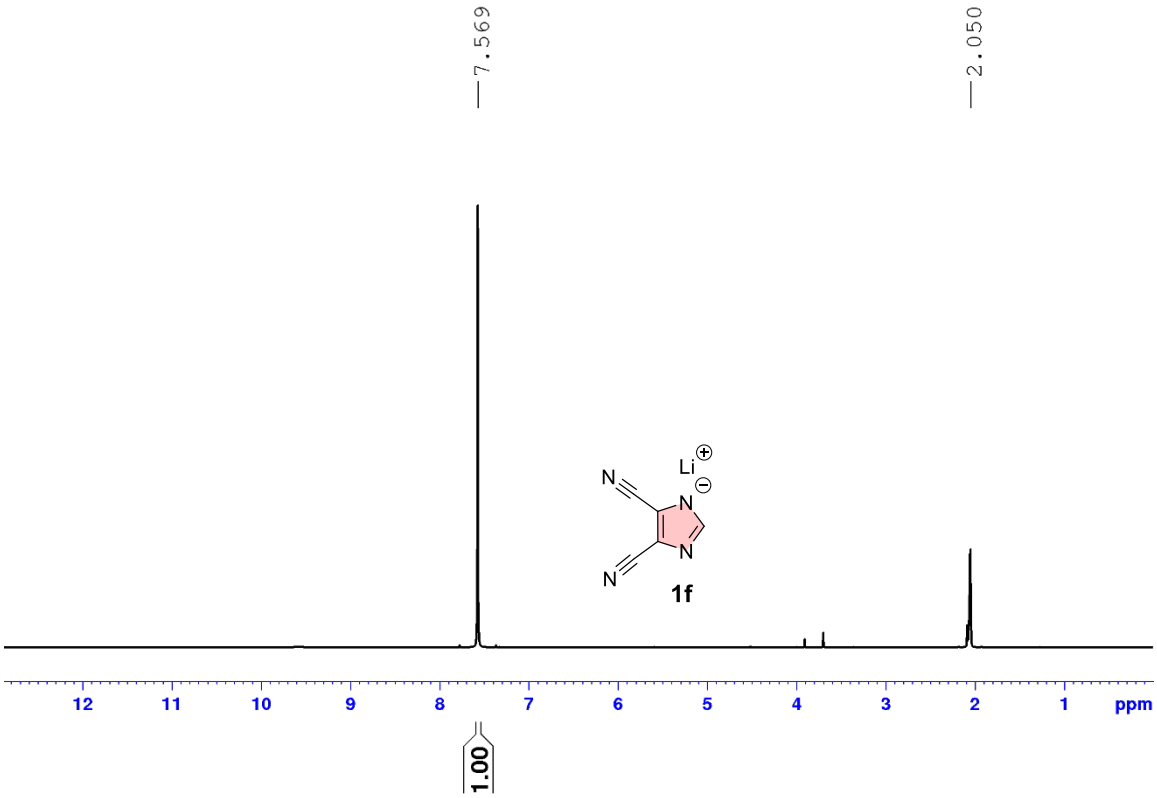

Figure S33. ^{1}H-NMR (500 MHz, acetone-d_6, 25 °C) spectrum of compound **1f**.

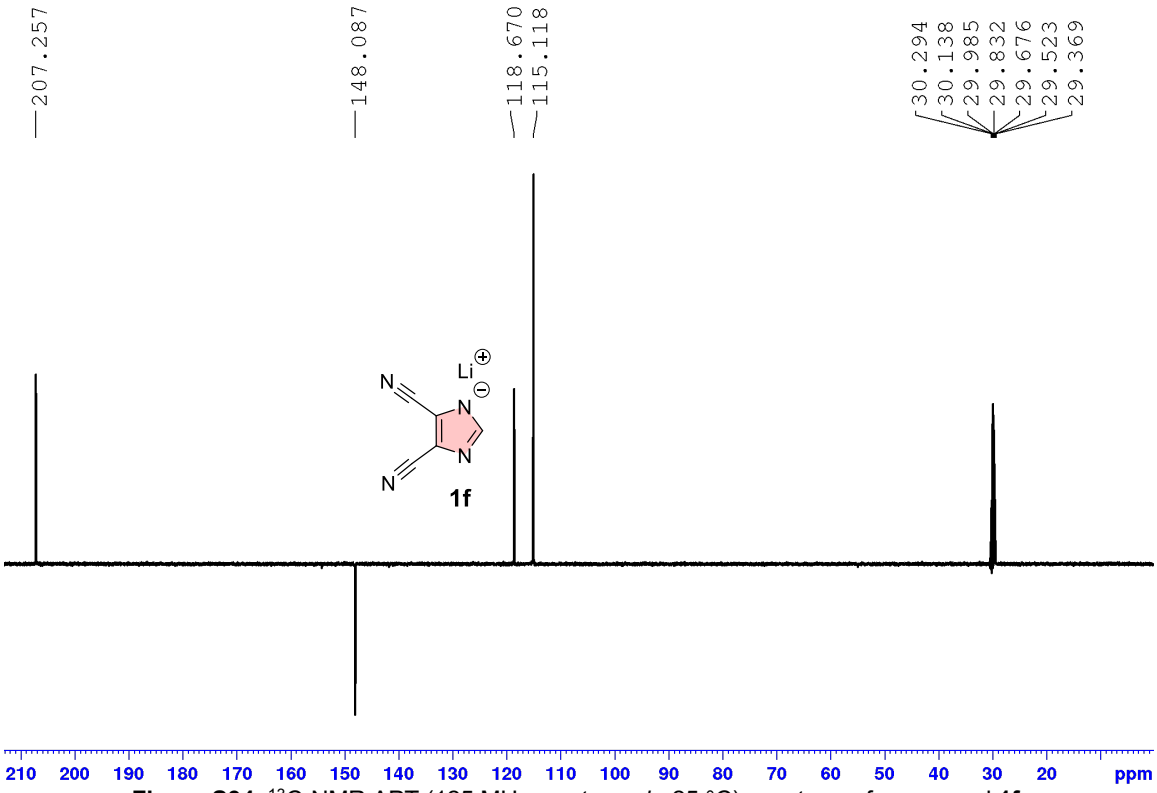

Figure S34. ^{13}C-NMR APT (125 MHz, acetone-d_6, 25 °C) spectrum of compound **1f**.

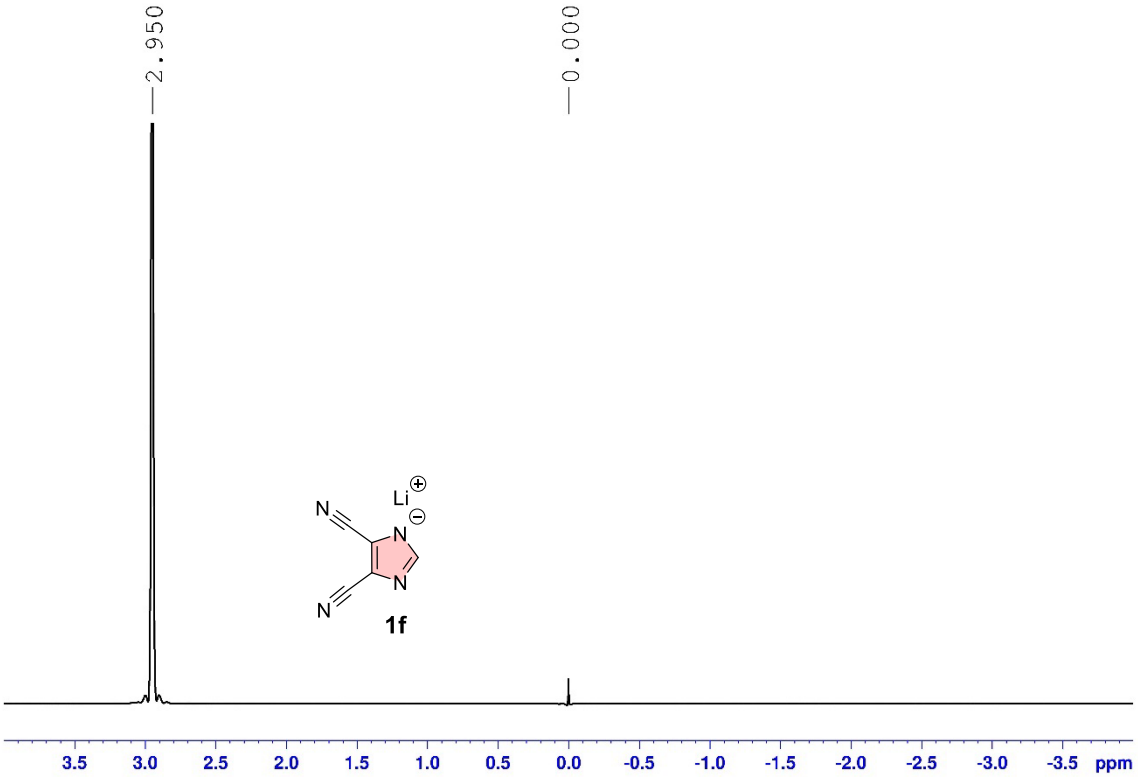

Figure S35. ^{7}Li-NMR (194 MHz, acetone-d_6, 25 °C) spectrum of compound **1f**.

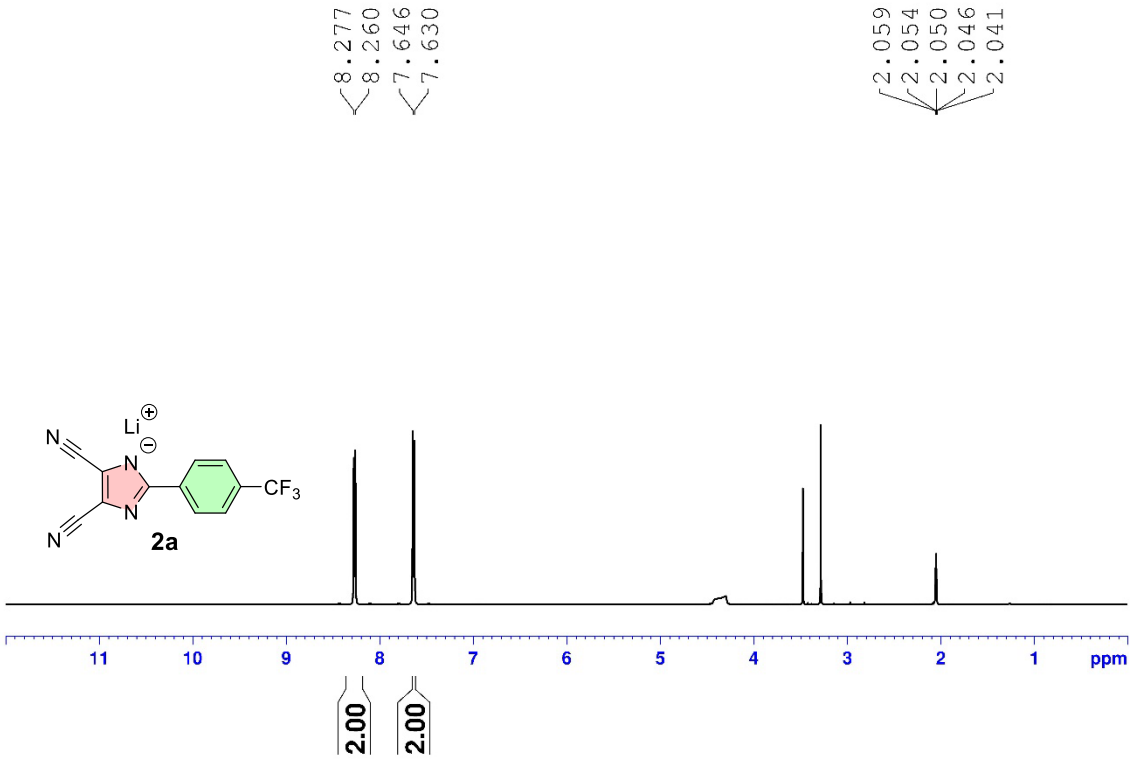

Figure S36. ^{1}H-NMR (500 MHz, acetone-d_6, 25 °C) spectrum of compound **2a**.

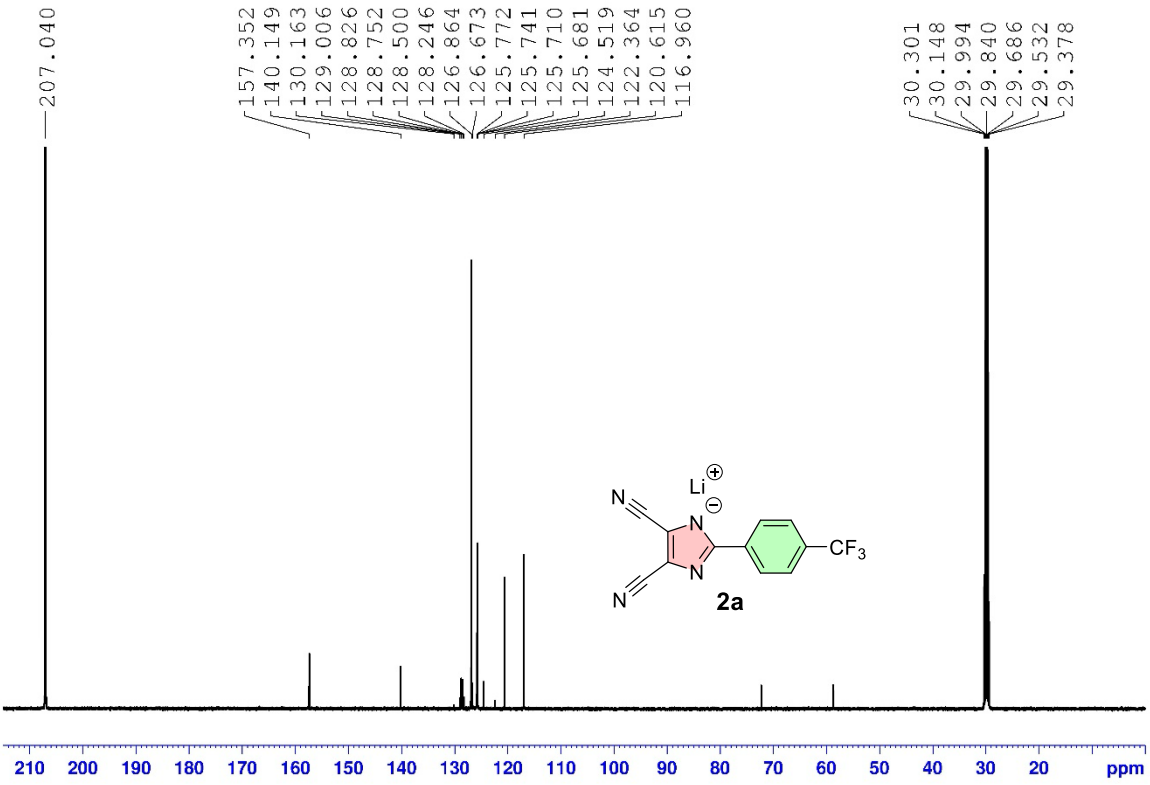

Figure S37. ^{13}C-NMR (125 MHz, acetone-d_6, 25 °C) spectrum of compound **2a**.

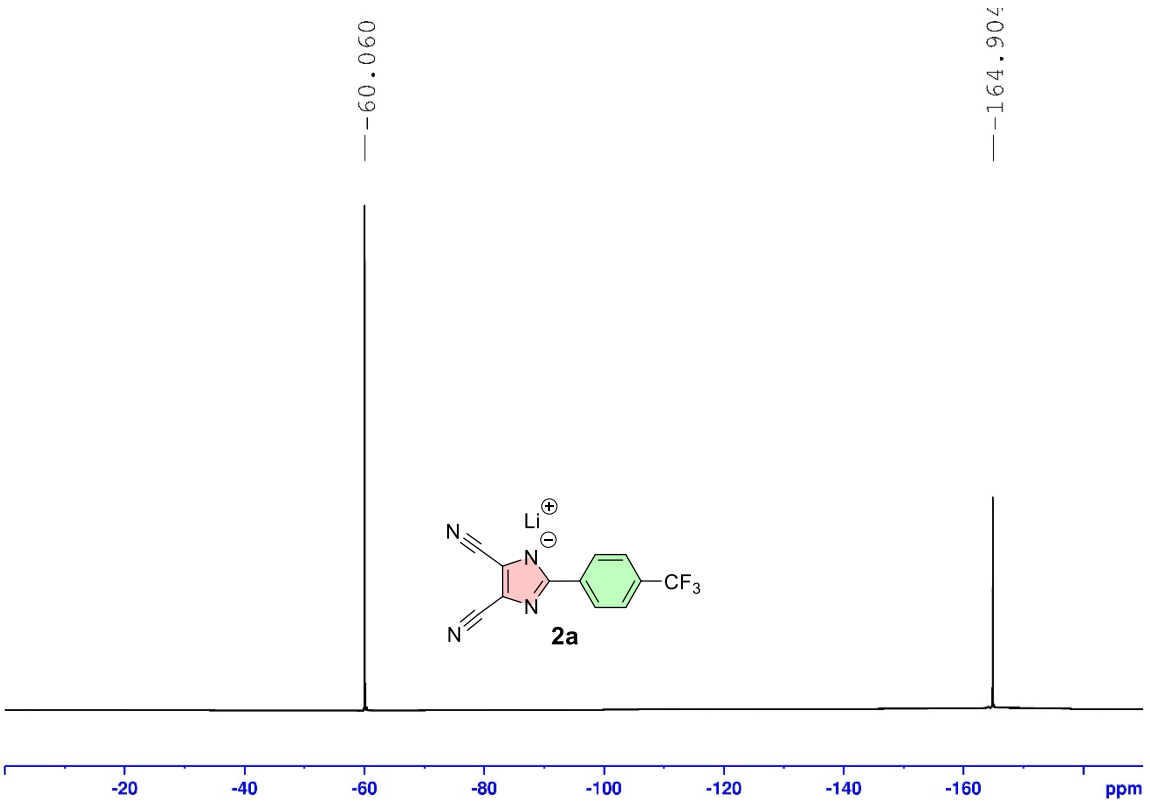

Figure S38. ^{19}F-NMR (470 MHz, acetone-d_6, 25 °C) spectrum of compound **2a**.

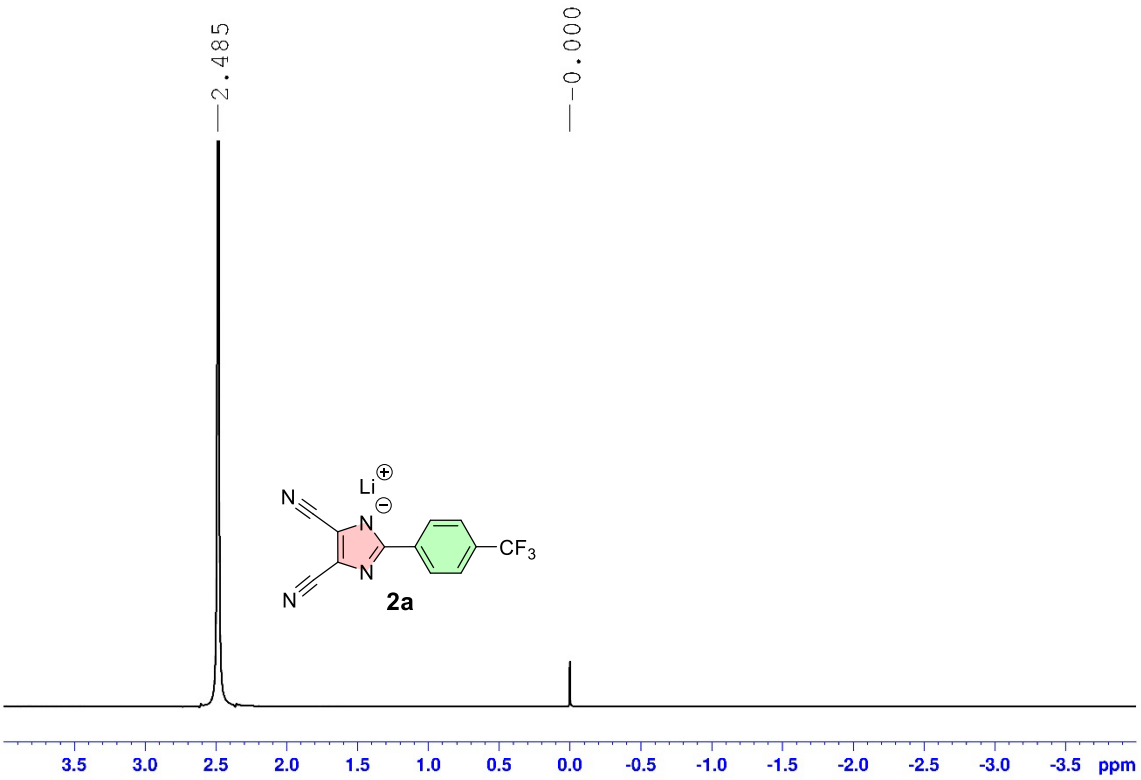

Figure S39. ^{7}Li-NMR (194 MHz, acetone-d_6, 25 °C) spectrum of compound **2a**.

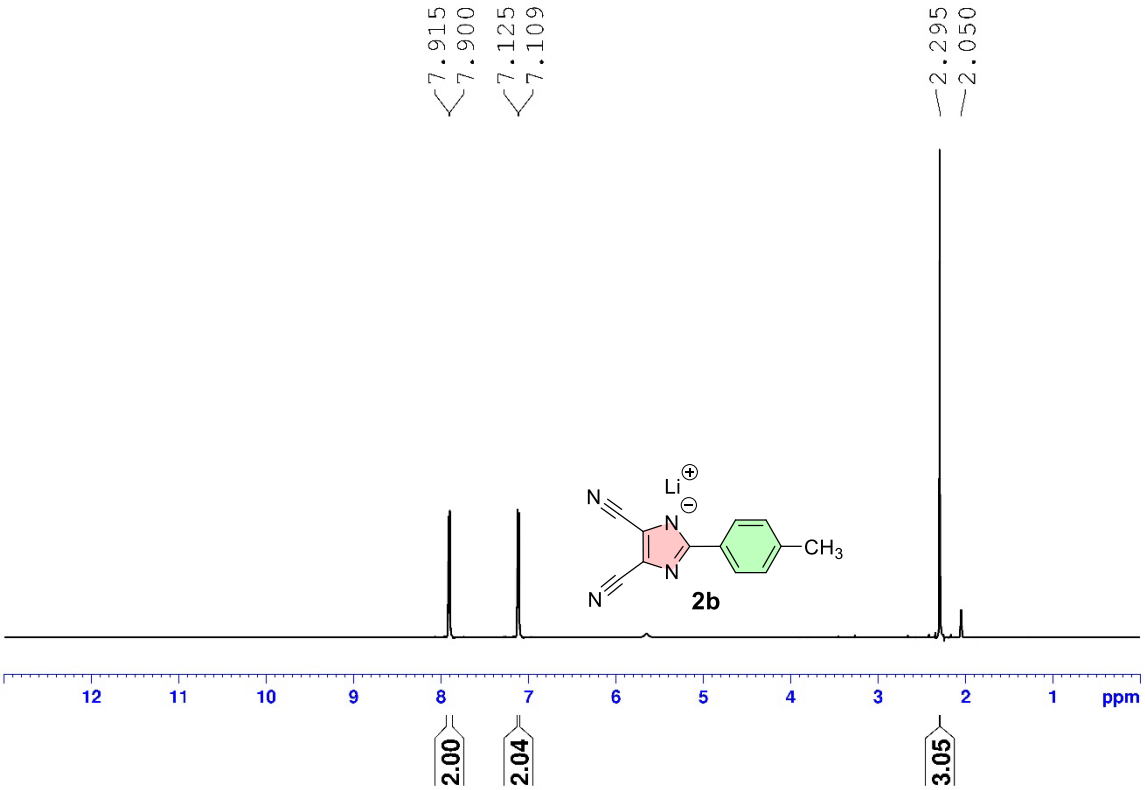

Figure S40. ^{1}H-NMR (500 MHz, acetone-d_6, 25 °C) spectrum of compound **2b**.

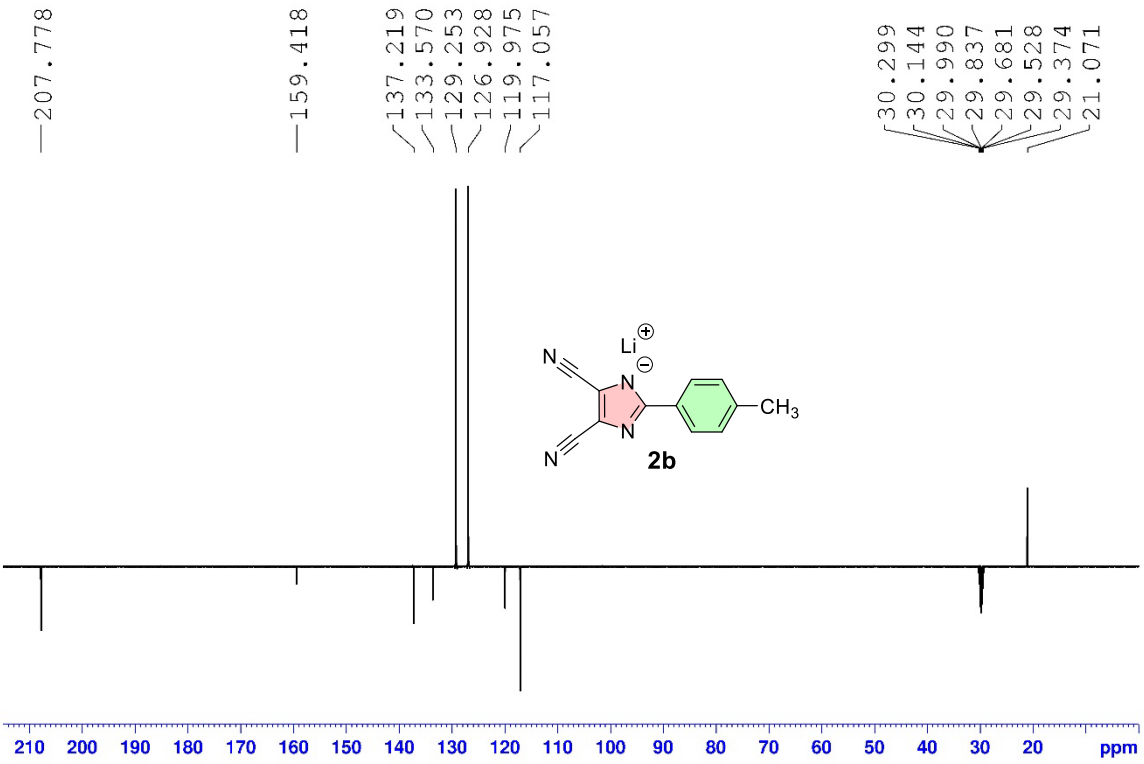

Figure S41. ^{13}C-NMR (125 MHz, acetone-d_6, 25 °C) spectrum of compound **2b**.

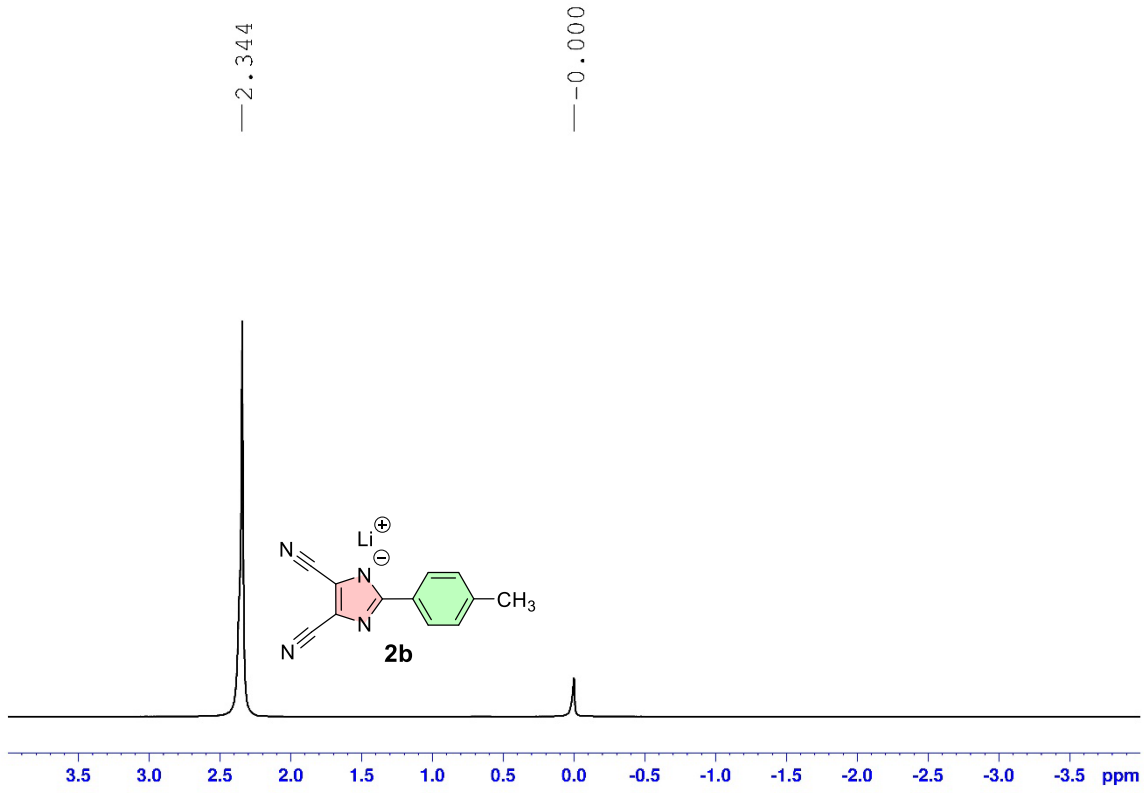

Figure S42. ^{7}Li-NMR (194 MHz, acetone-d_6, 25 °C) spectrum of compound **2b**.

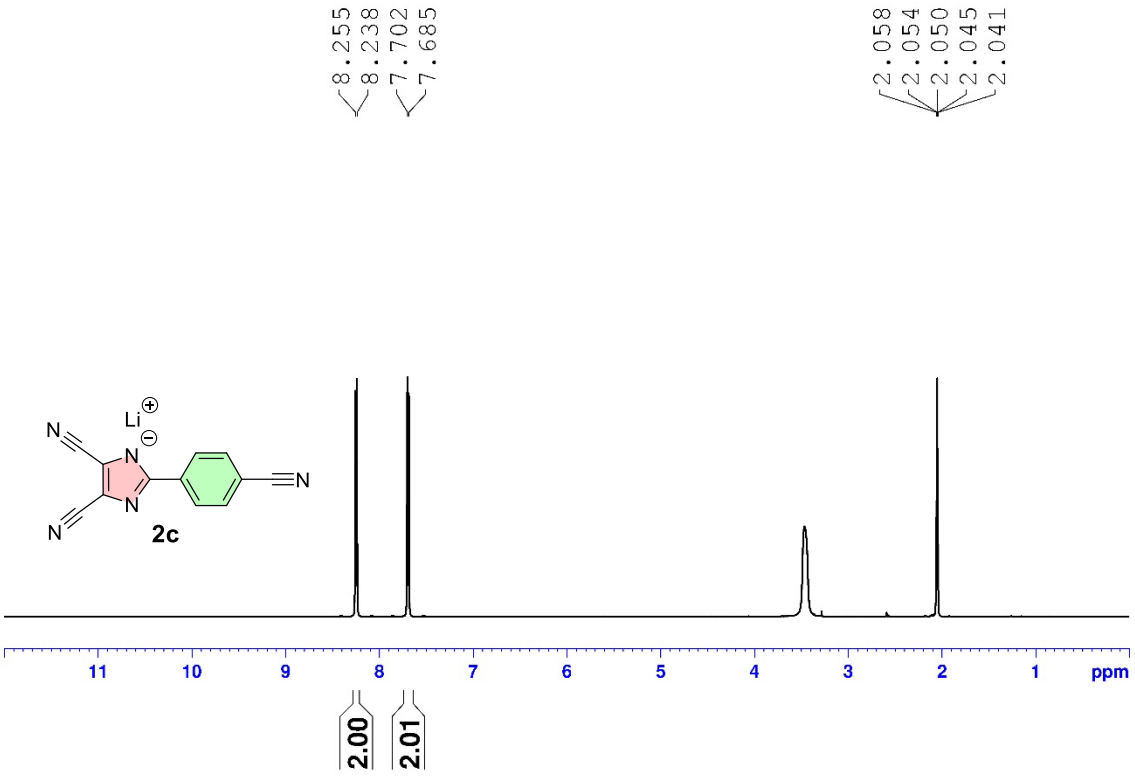

Figure S43. ^{1}H-NMR (500 MHz, acetone-d_6, 25 °C) spectrum of compound **2c**.

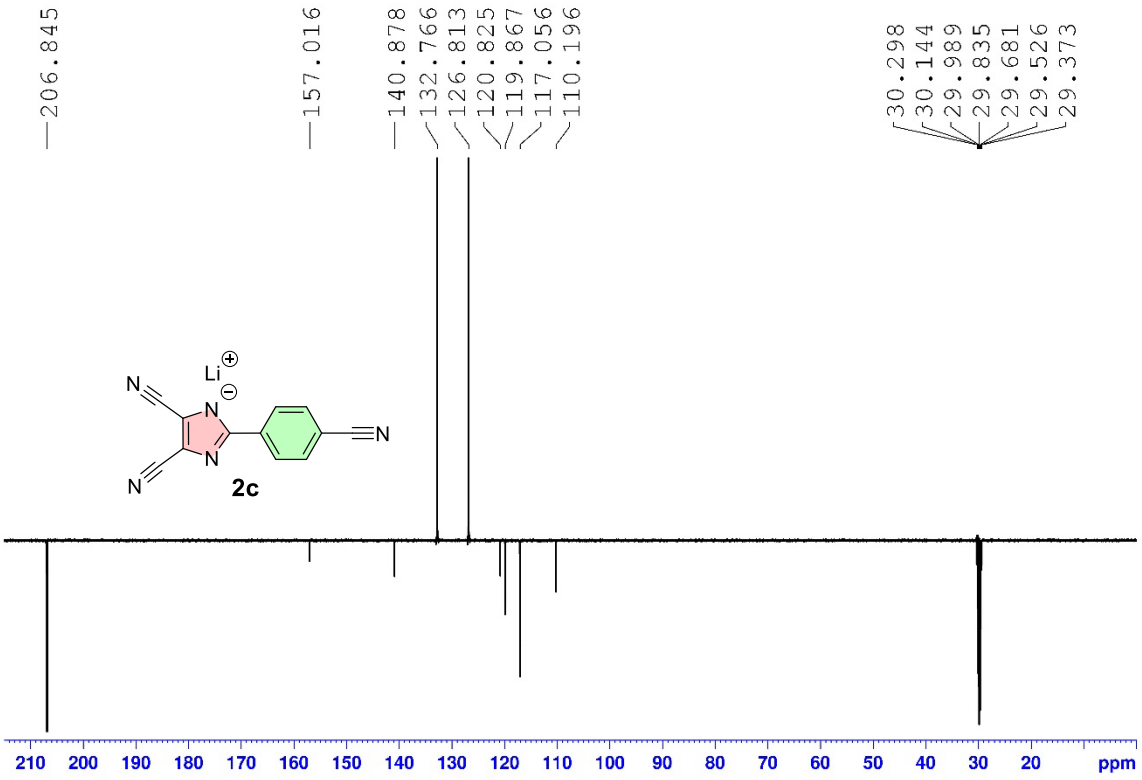

Figure S44. ^{13}C-NMR (125 MHz, acetone-d_6, 25 °C) spectrum of compound **2c**.

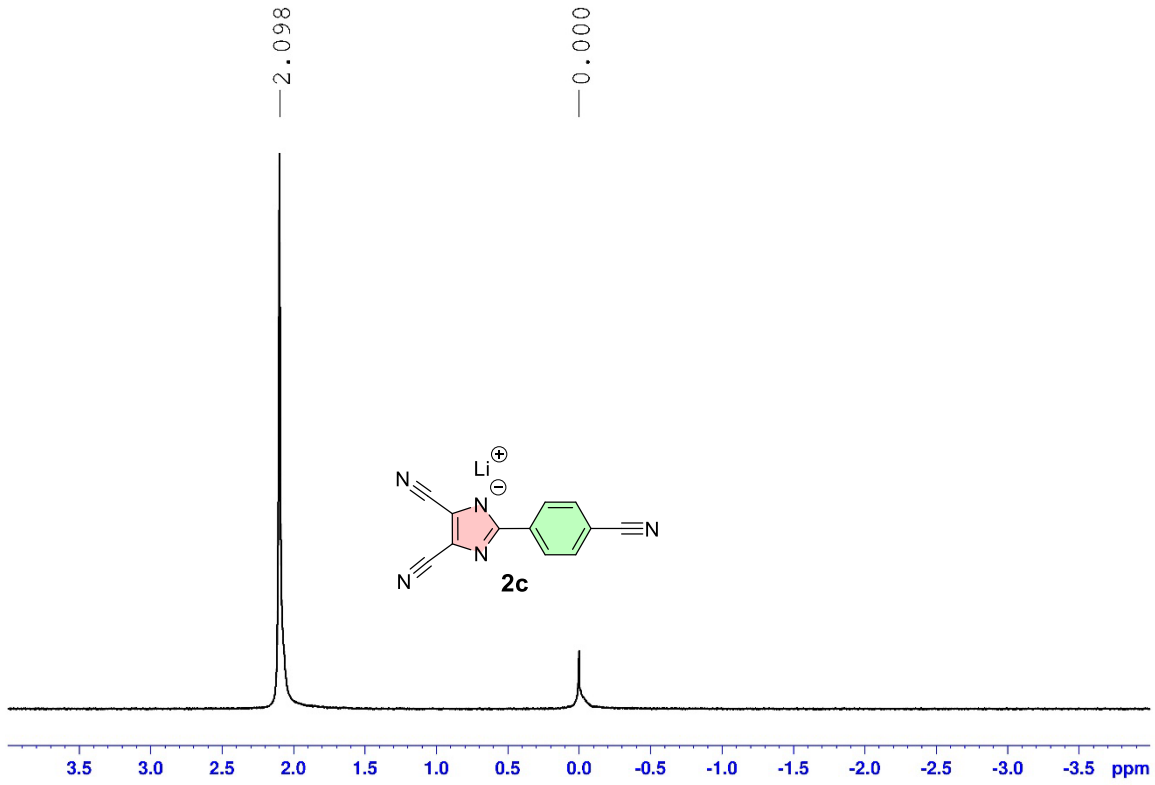

Figure S45. ^{7}Li-NMR (194 MHz, acetone-d_6, 25 °C) spectrum of compound **2c**.

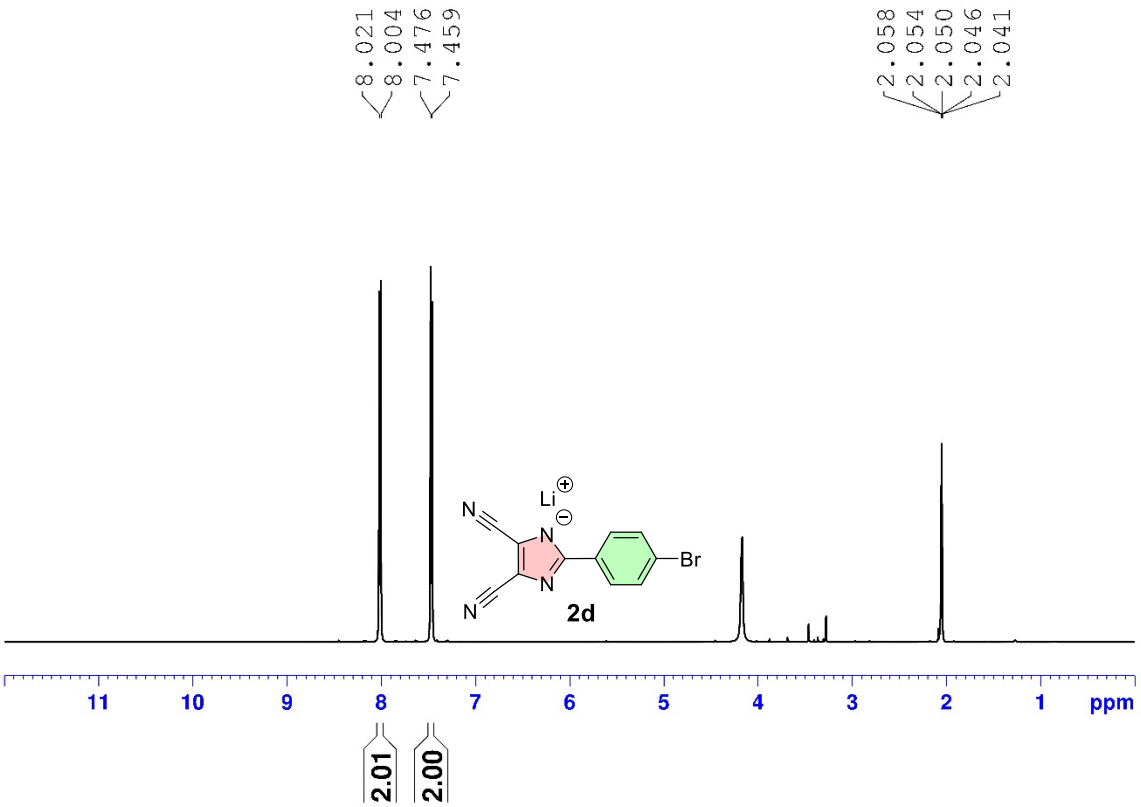

Figure S46. ^{1}H-NMR (500 MHz, acetone-d_6, 25 °C) spectrum of compound **2d**.

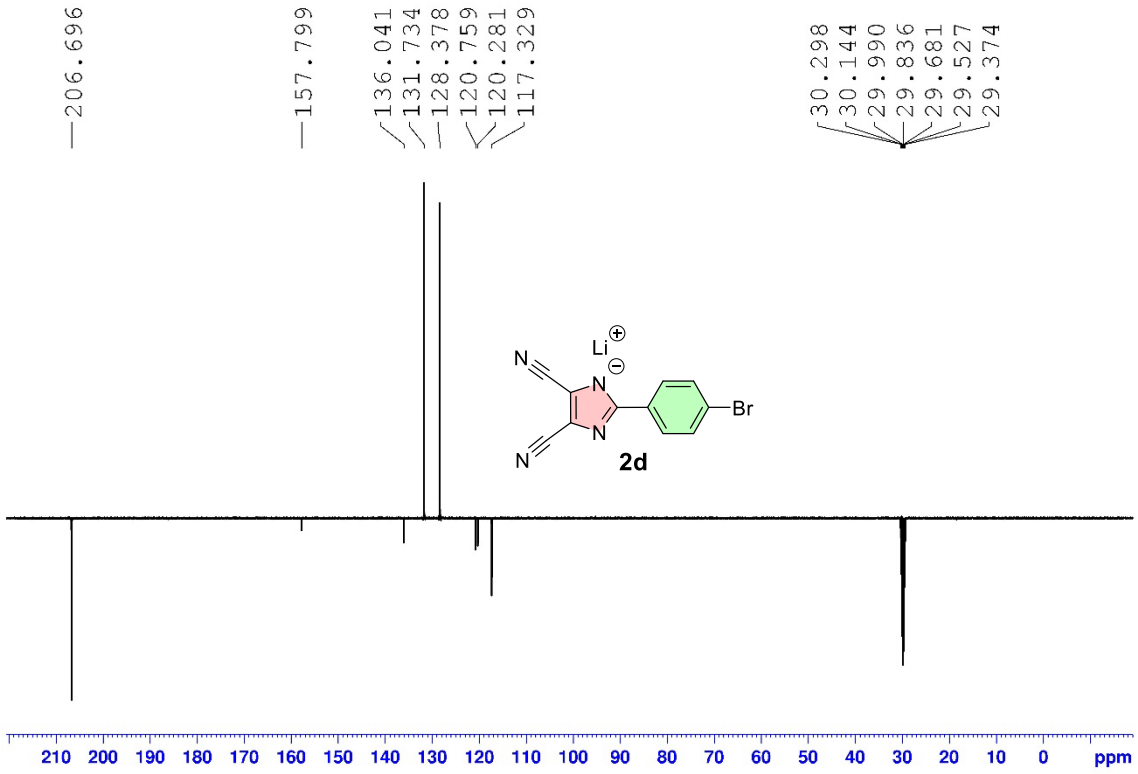

Figure S47. ^{13}C-NMR (125 MHz, acetone-d_6, 25 °C) spectrum of compound **2d**.

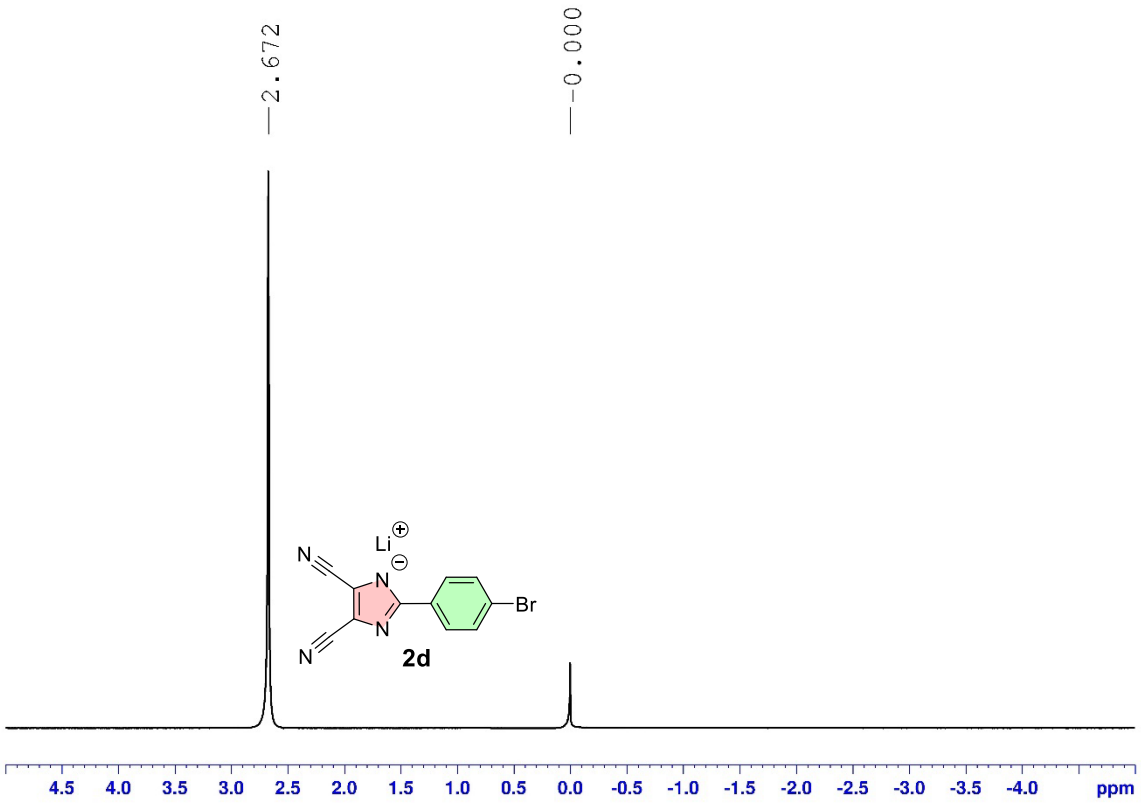

Figure S48. ^{7}Li-NMR (194 MHz, acetone-d_6, 25 °C) spectrum of compound **2d**.

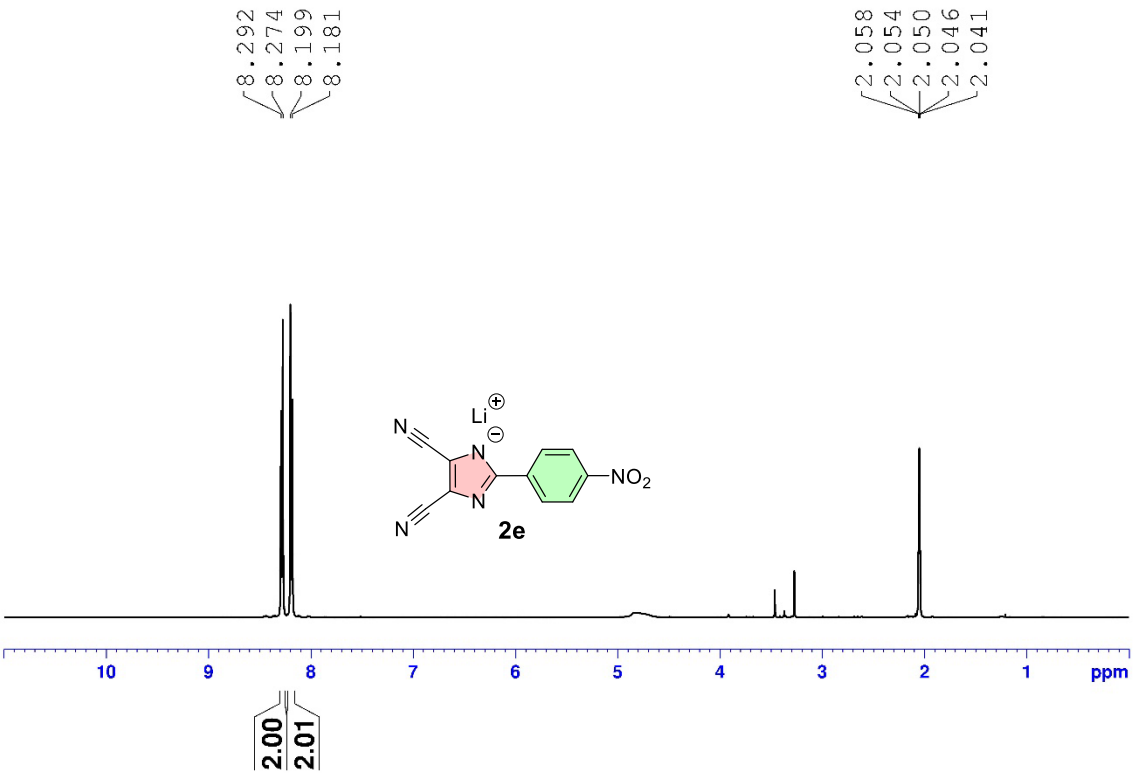

Figure S49. ^{1}H-NMR (500 MHz, acetone-d_6, 25 °C) spectrum of compound **2e**.

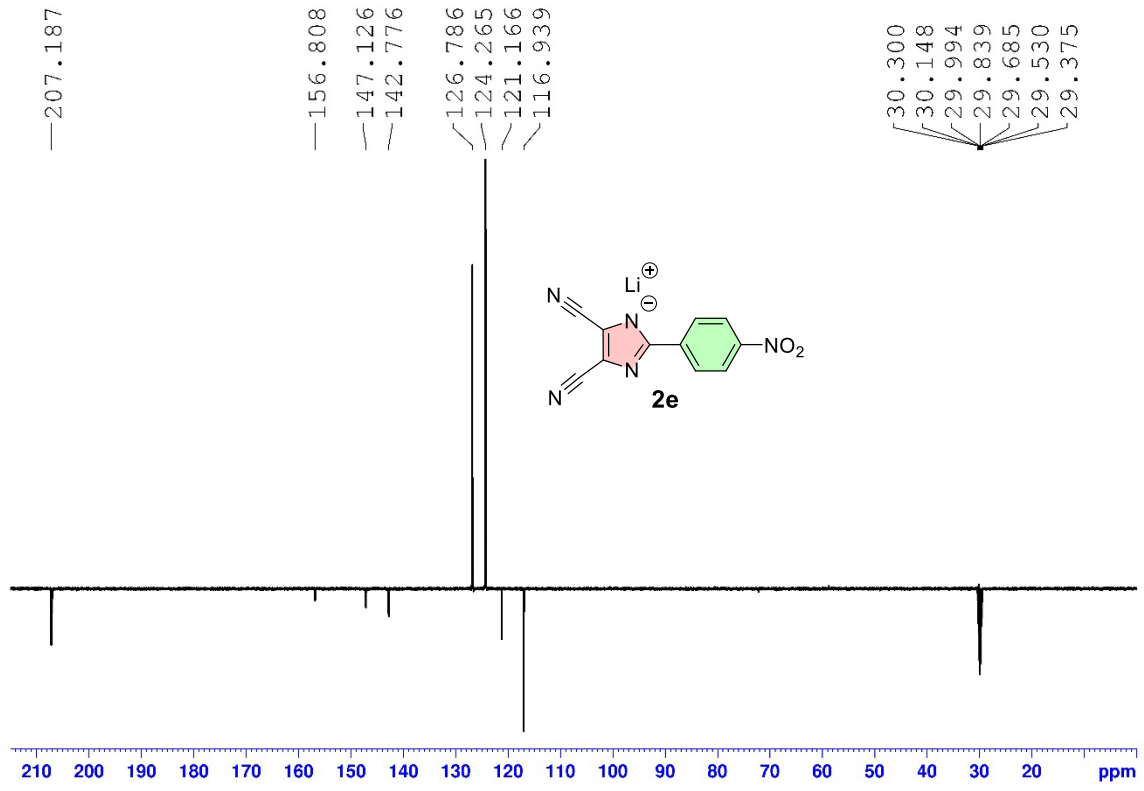

Figure S50. ^{13}C-NMR (125 MHz, acetone-d_6, 25 °C) spectrum of compound **2e**.

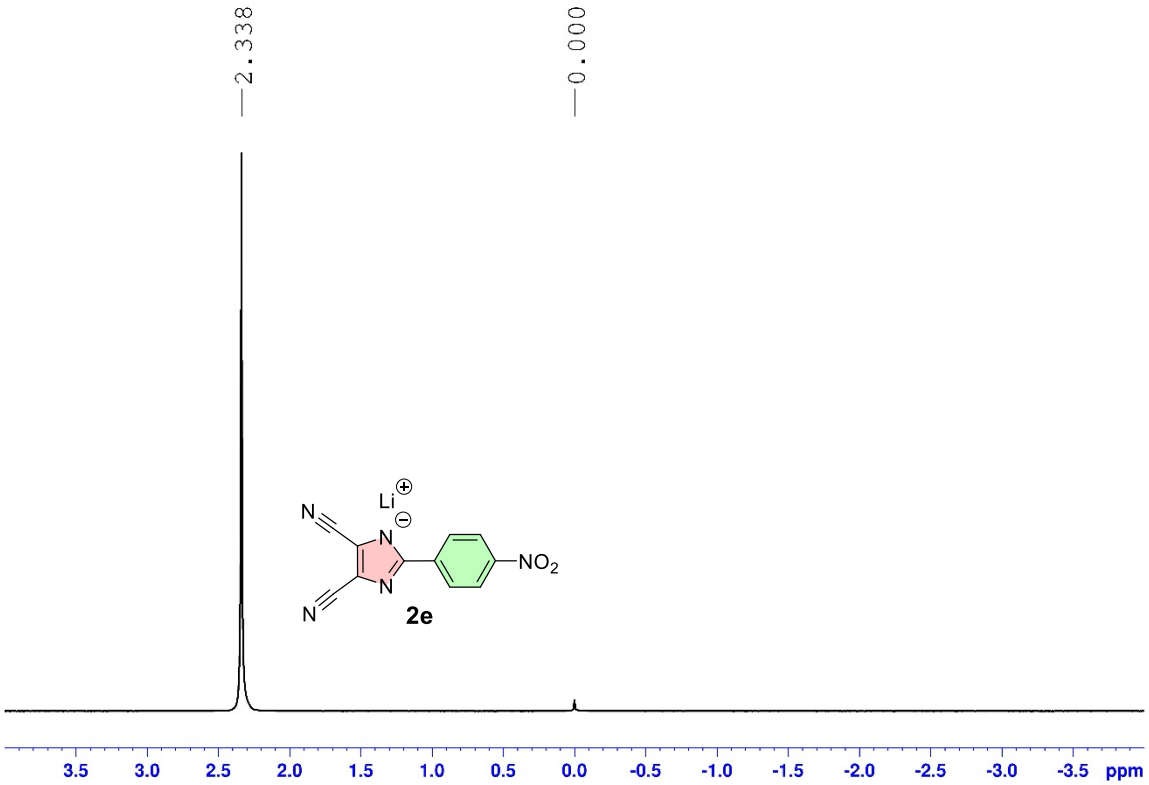

Figure S51. ^{7}Li-NMR (156 MHz, acetone-d_6, 25 °C) spectrum of compound **2e**.

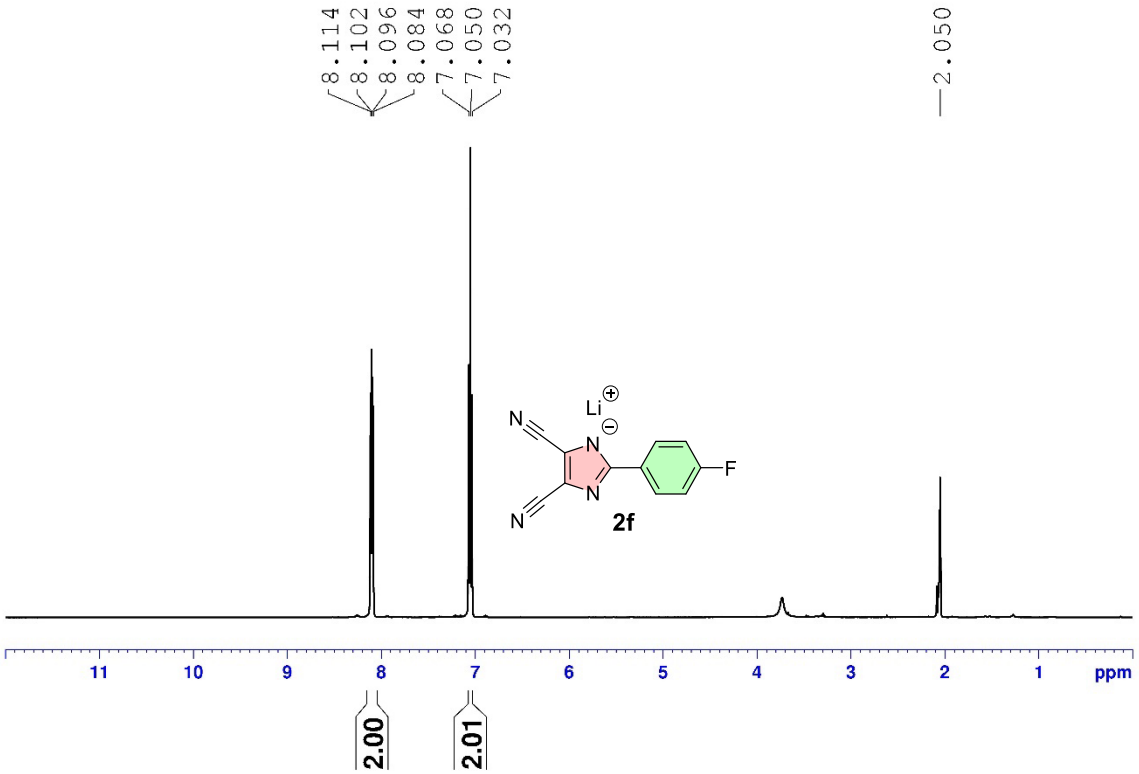

Figure S52. ^{1}H-NMR (500 MHz, acetone-d_6, 25 °C) spectrum of compound **2f**.

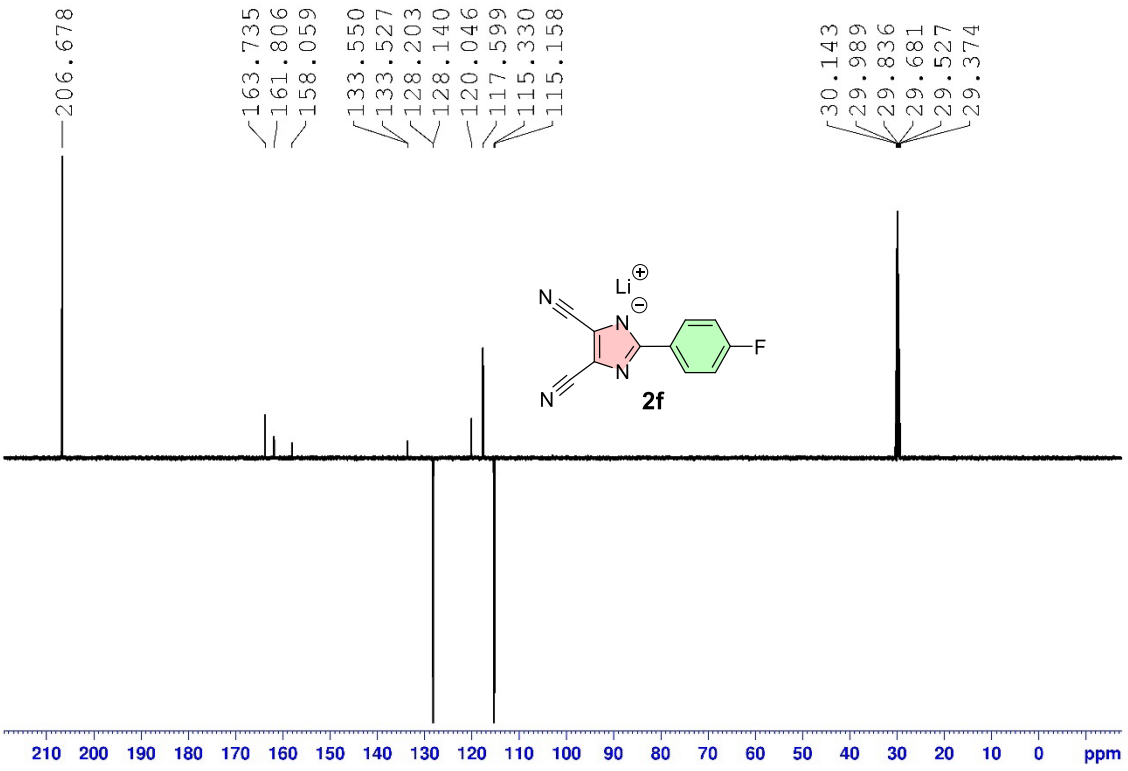

Figure S53. ^{13}C-NMR (125 MHz, acetone-d_6, 25 °C) spectrum of compound **2f**.

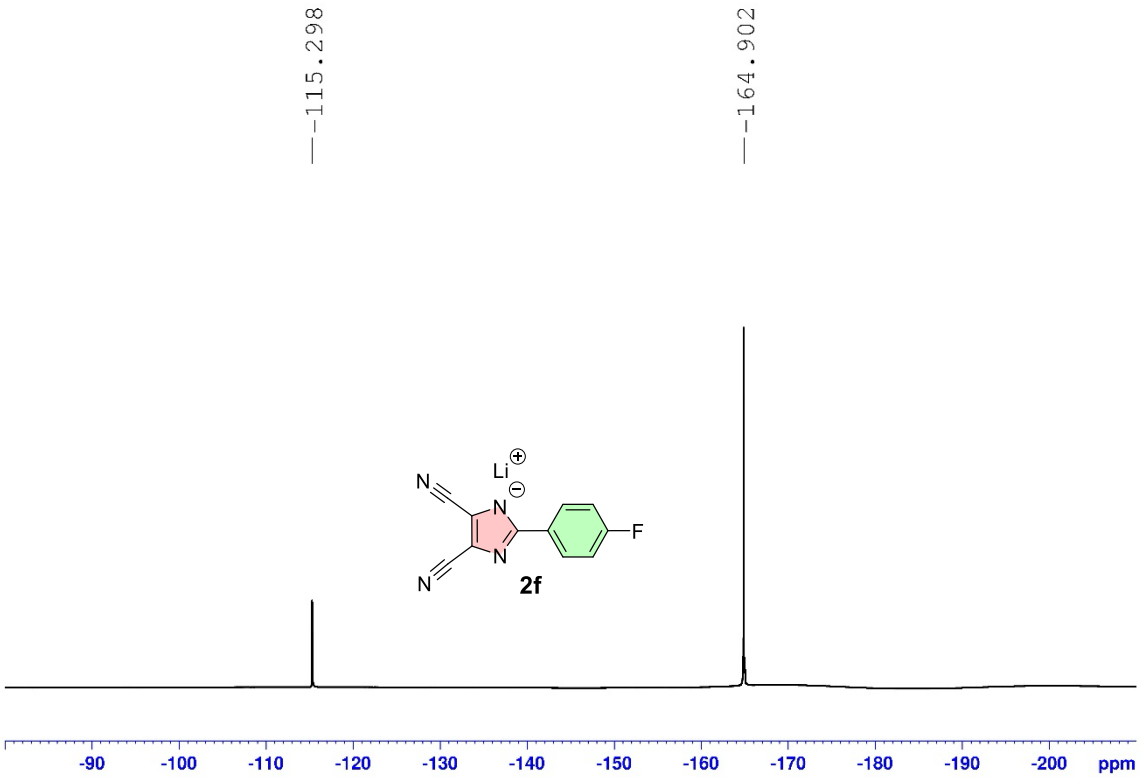

Figure S54. ^{19}F-NMR (470 MHz, acetone-d_6, 25 °C) spectrum of compound **2f**.

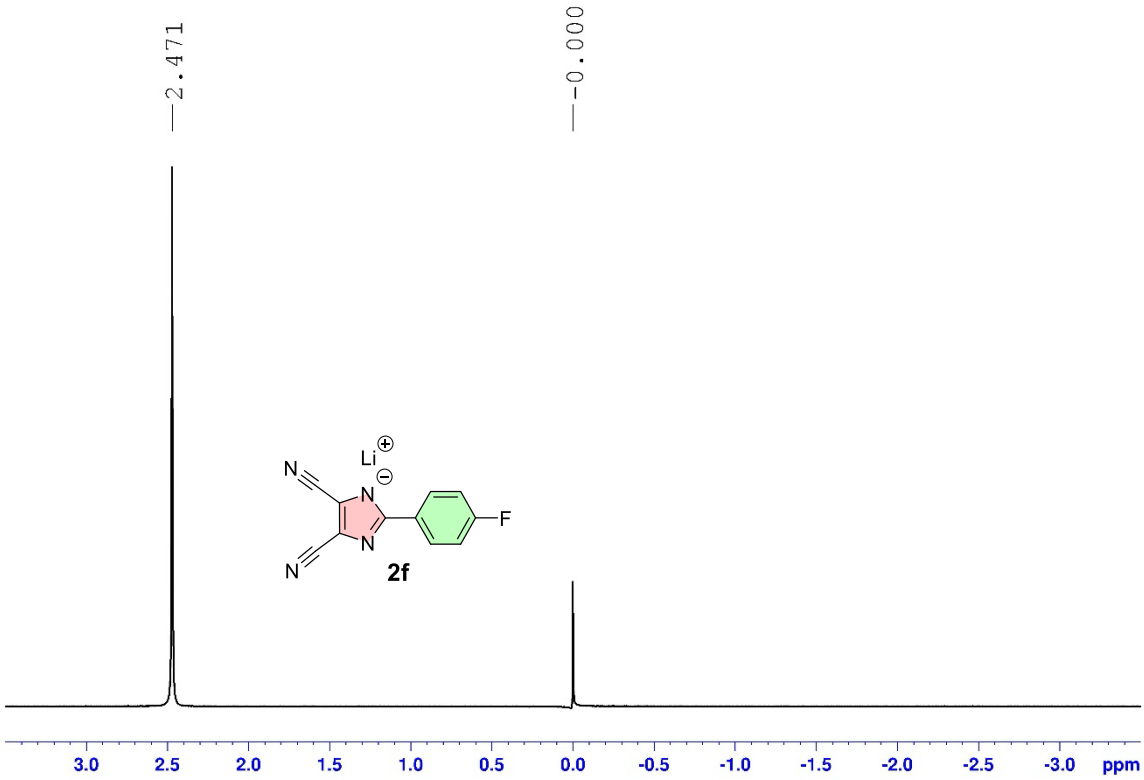

Figure S55. ^{7}Li-NMR (194 MHz, acetone-d_6, 25 °C) spectrum of compound **2f**.

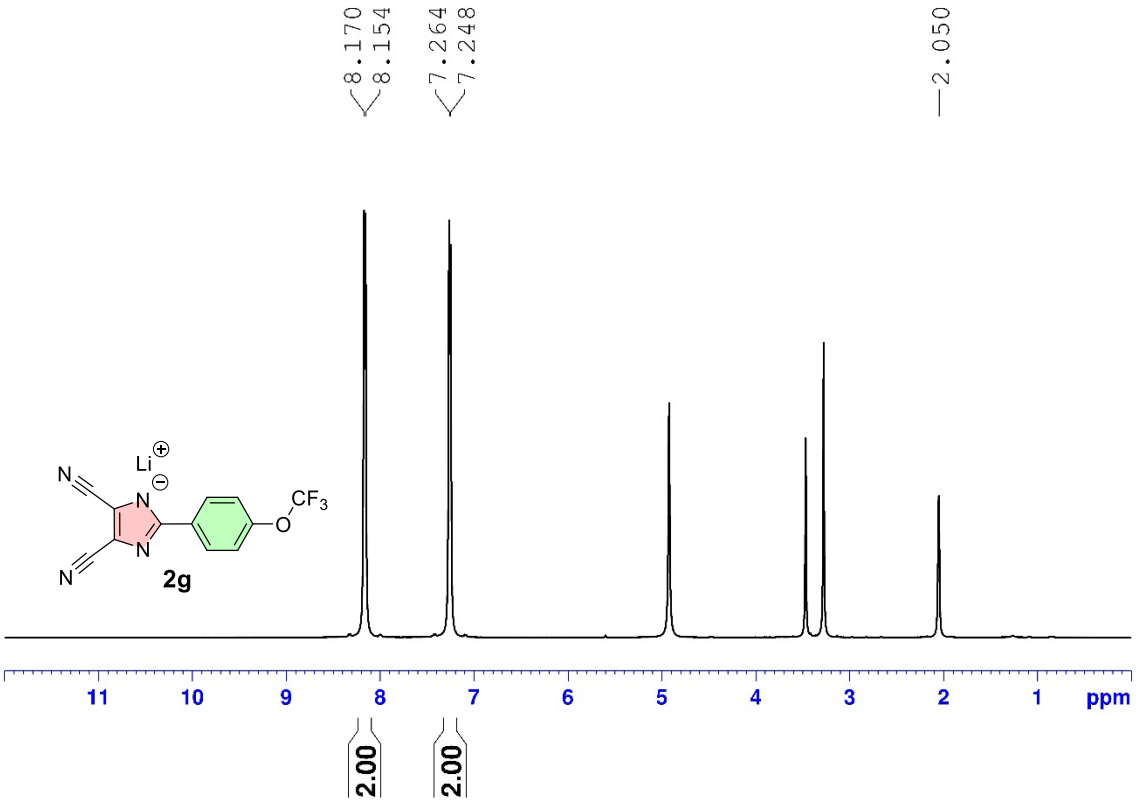

Figure S56. ^{1}H-NMR (500 MHz, acetone-d_6, 25 °C) spectrum of compound **2g**.

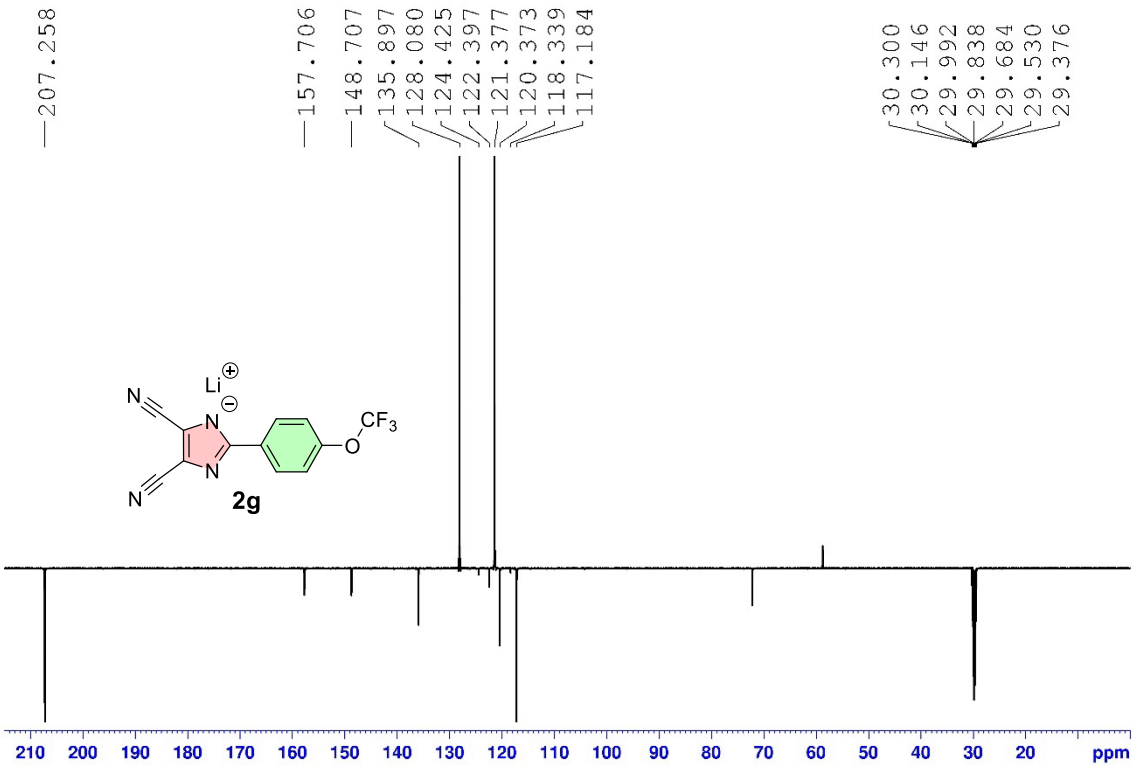

Figure S57. ^{13}C-NMR (125 MHz, acetone-d_6, 25 °C) spectrum of compound **2g**.

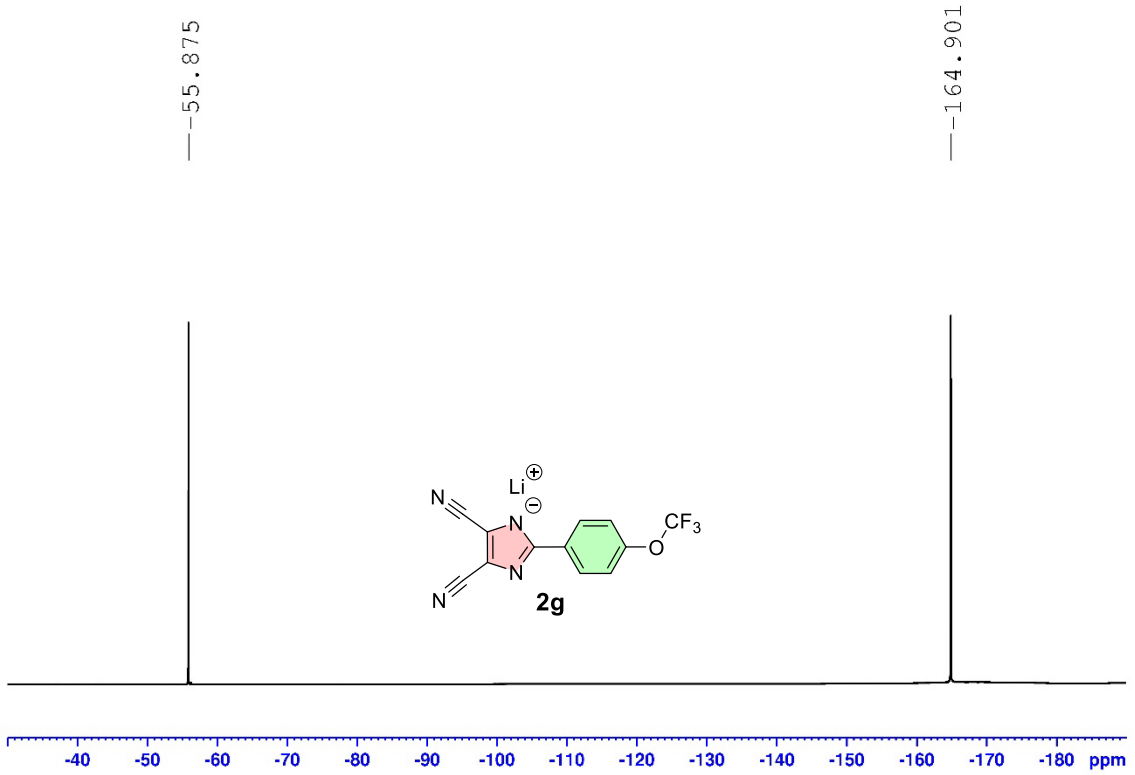

Figure S58. ^{19}F-NMR (470 MHz, acetone-d_6, 25 °C) spectrum of compound **2g**.

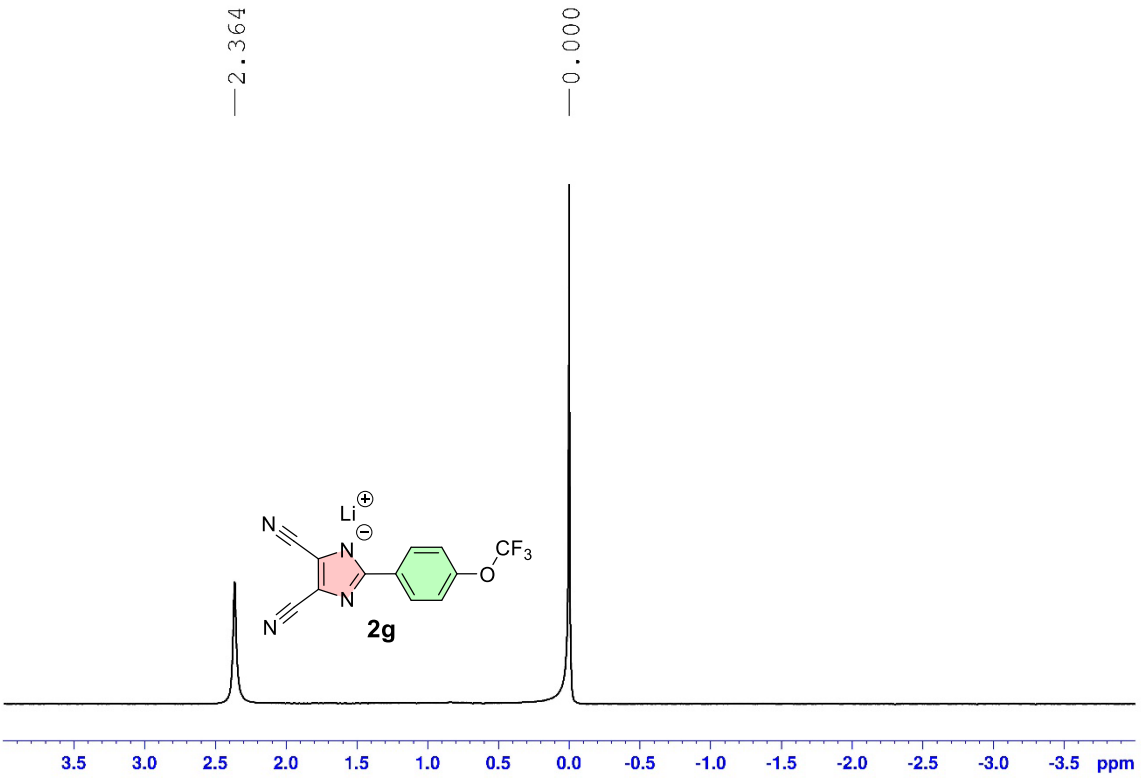

Figure S59. ^{7}Li-NMR (194 MHz, acetone-d_6, 25 °C) spectrum of compound **2g**.

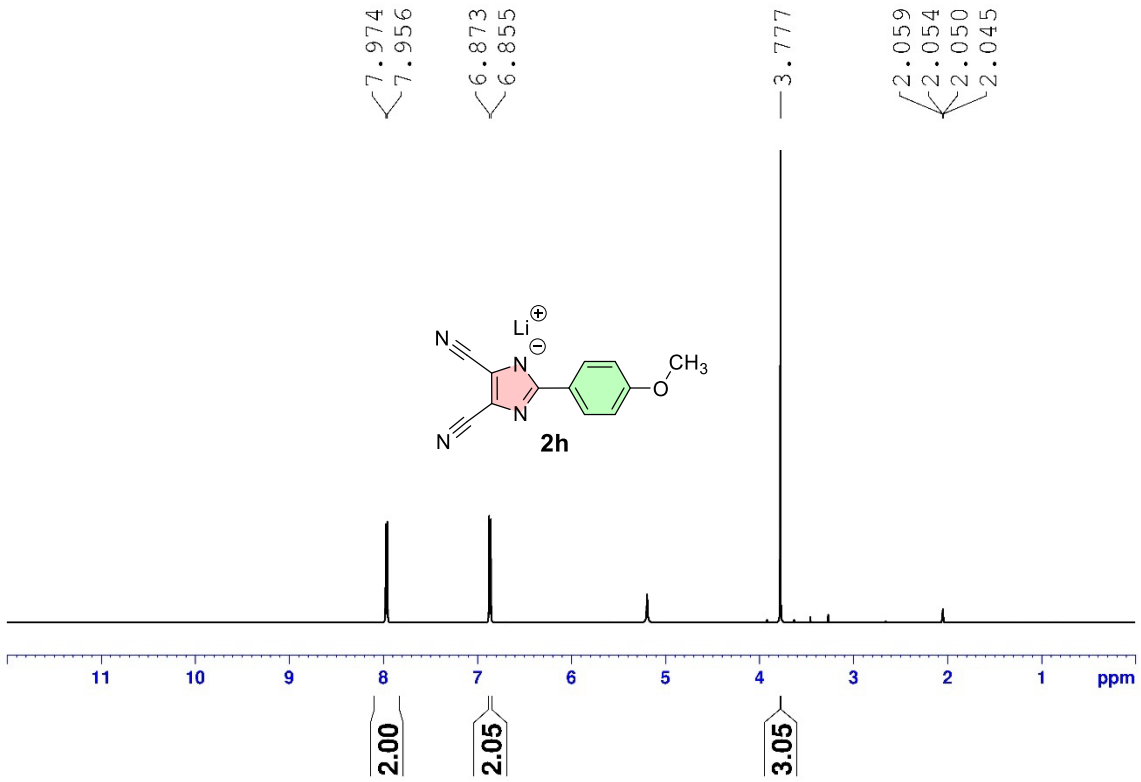

Figure S60. ^{1}H-NMR (500 MHz, acetone-d_6, 25 °C) spectrum of compound **2h**.

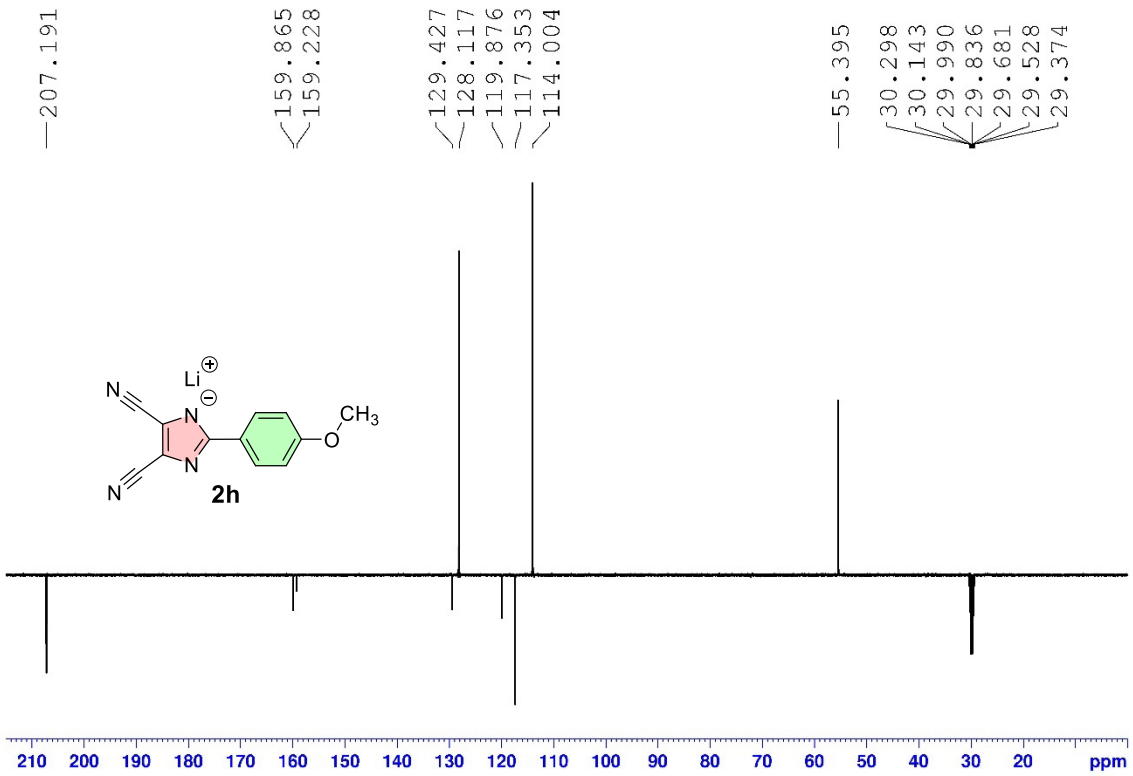

Figure S61. ^{13}C-NMR (125 MHz, acetone-d_6, 25 °C) spectrum of compound **2h**.

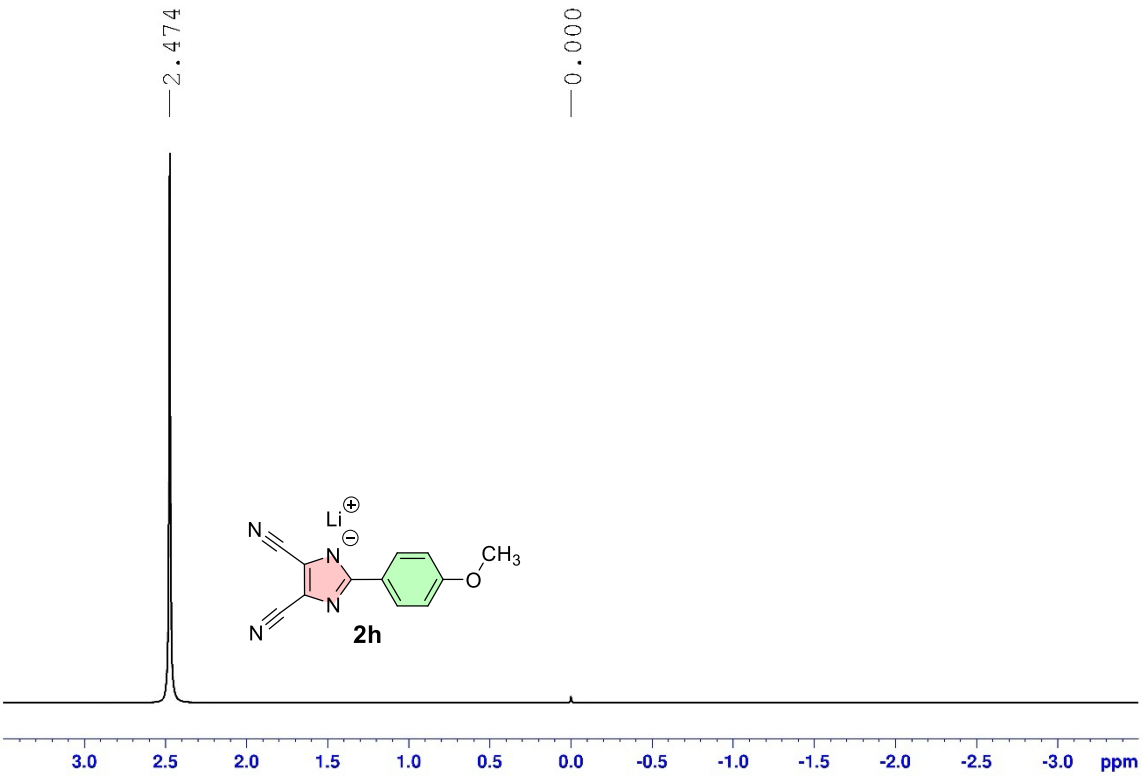

Figure S62. ^{7}Li-NMR (194 MHz, acetone-d_6, 25 °C) spectrum of compound **2h**.

8. High Resolution MALDI MS of imidazolides 1 and 2

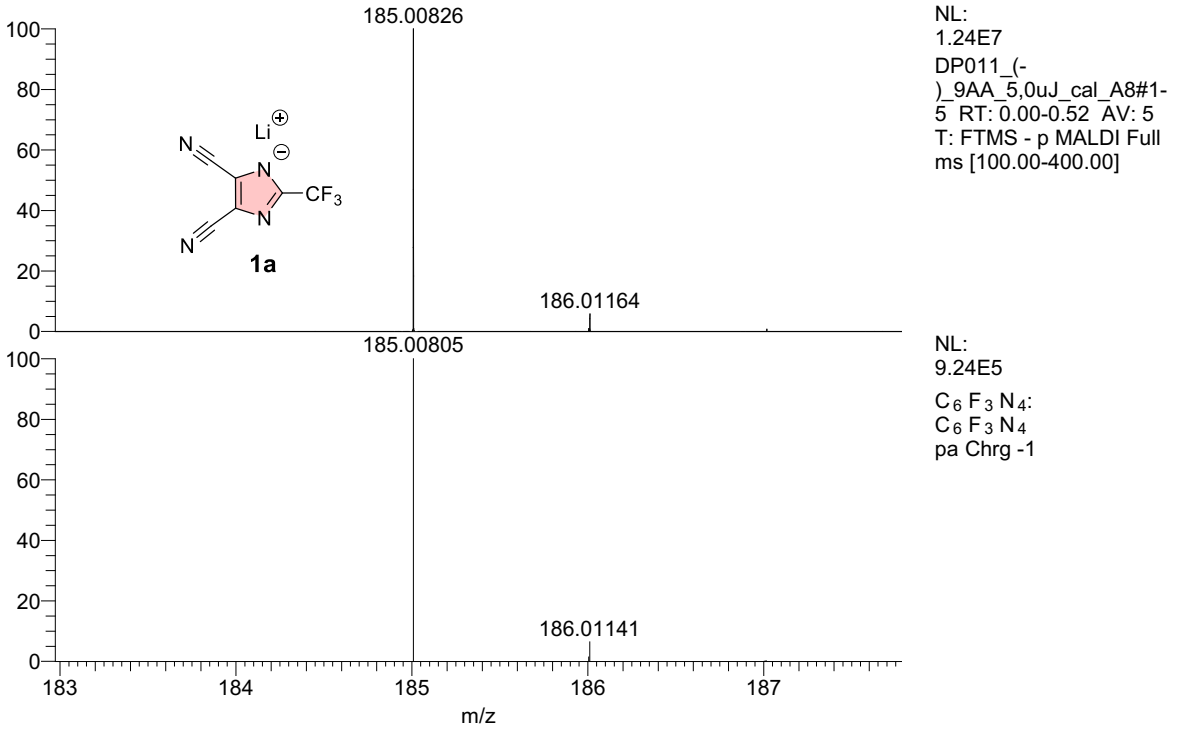

Figure S63. HR-FT-MALDI-MS spectrum of **1a** ($[M]^-$ = 185.00805 Da); top measured and bottom predicted spectrum.

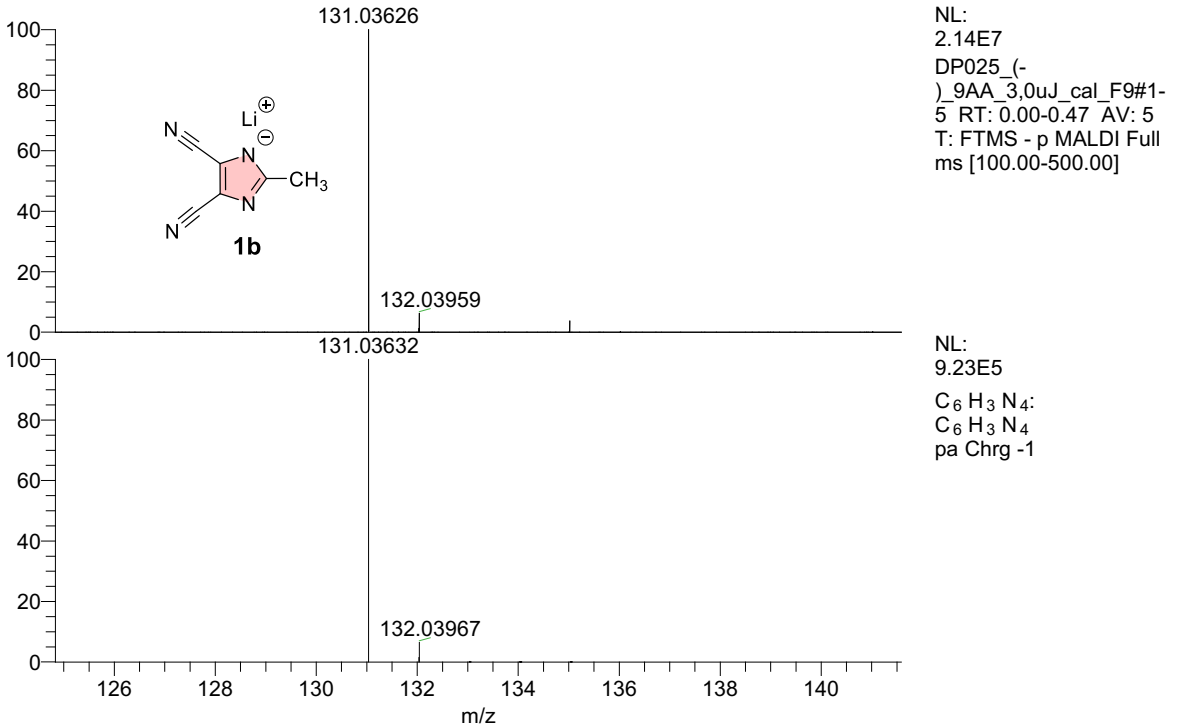

Figure S64. HR-FT-MALDI-MS spectrum of **1b** ($[M]^-$ = 131.03632 Da); top measured and bottom predicted spectrum.

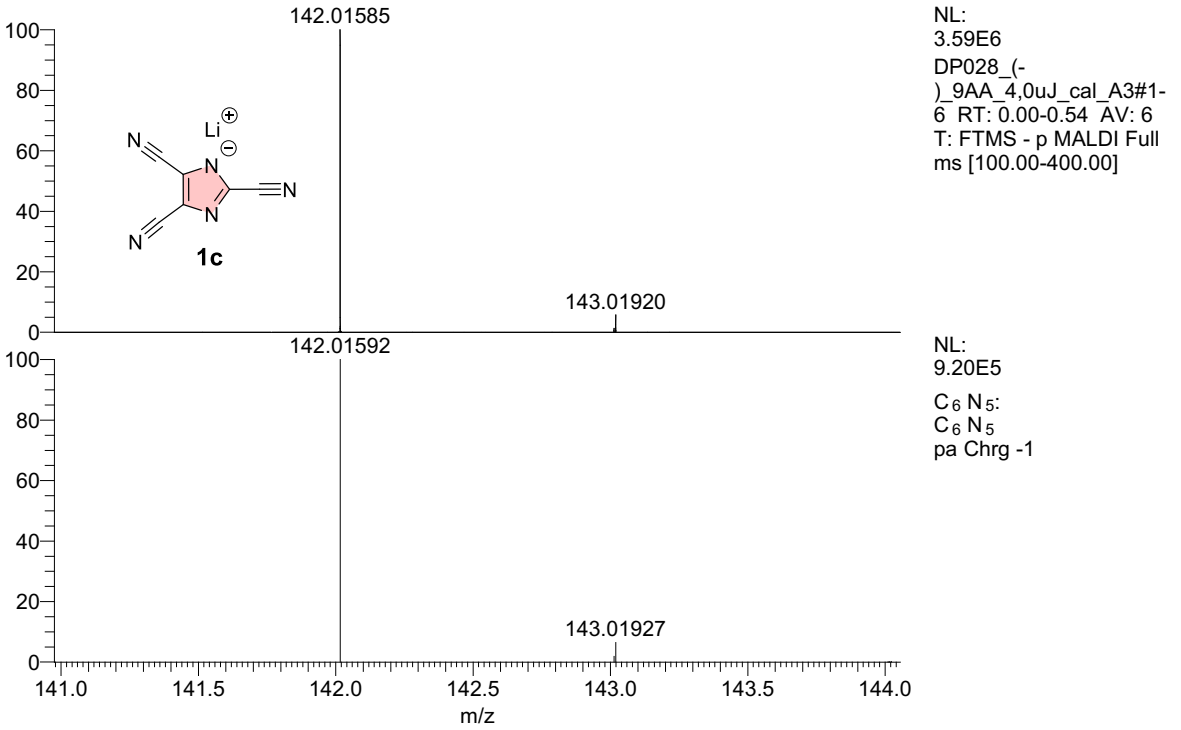

Figure S65. HR-FT-MALDI-MS spectrum of **1c** ($[M]^-$ = 142.01592 Da); top measured and bottom predicted spectrum.

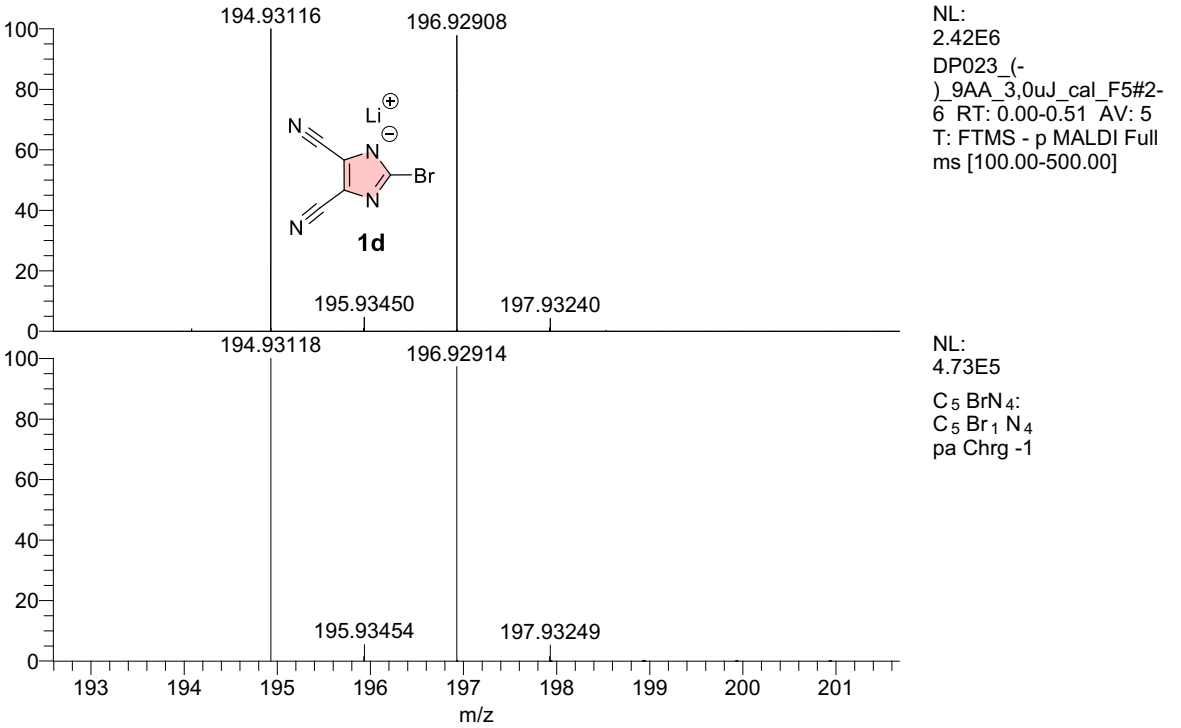

Figure S66. HR-FT-MALDI-MS spectrum of **1d** ($[M]^-$ = 194.93118 Da); top measured and bottom predicted spectrum.

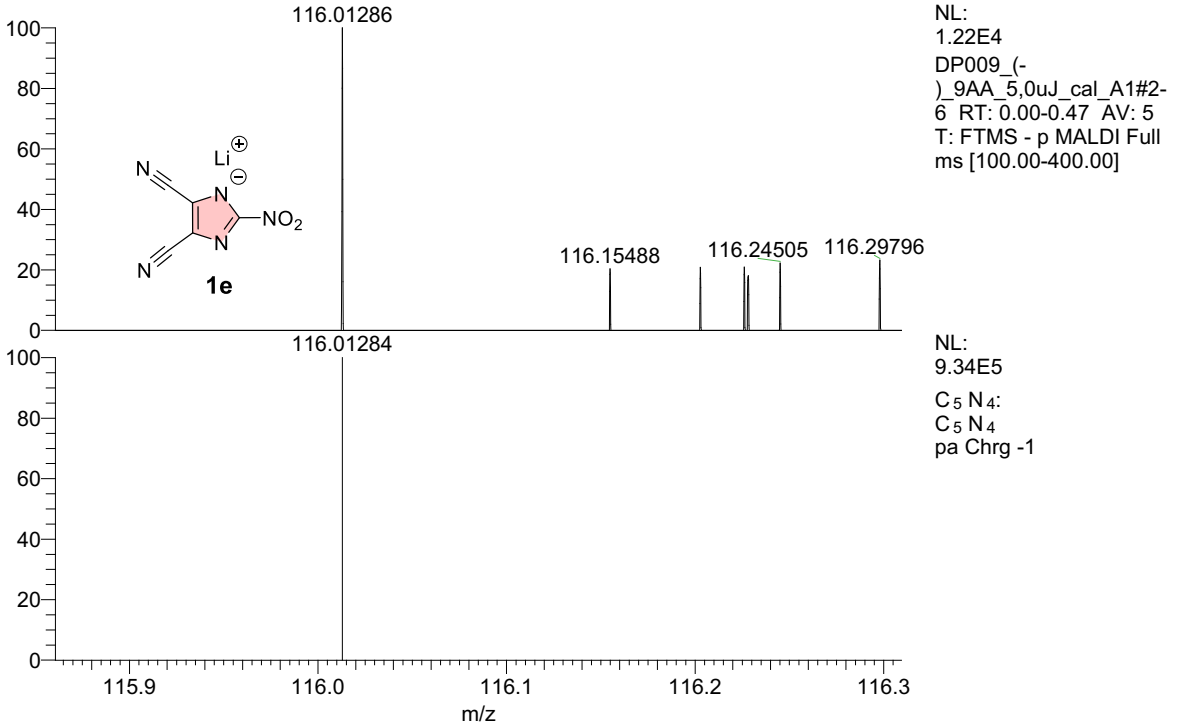

Figure S67. HR-FT-MALDI-MS spectrum of **1e** ($[M–NO_2]^-$ = 116.01284 Da); top measured and bottom predicted spectrum.

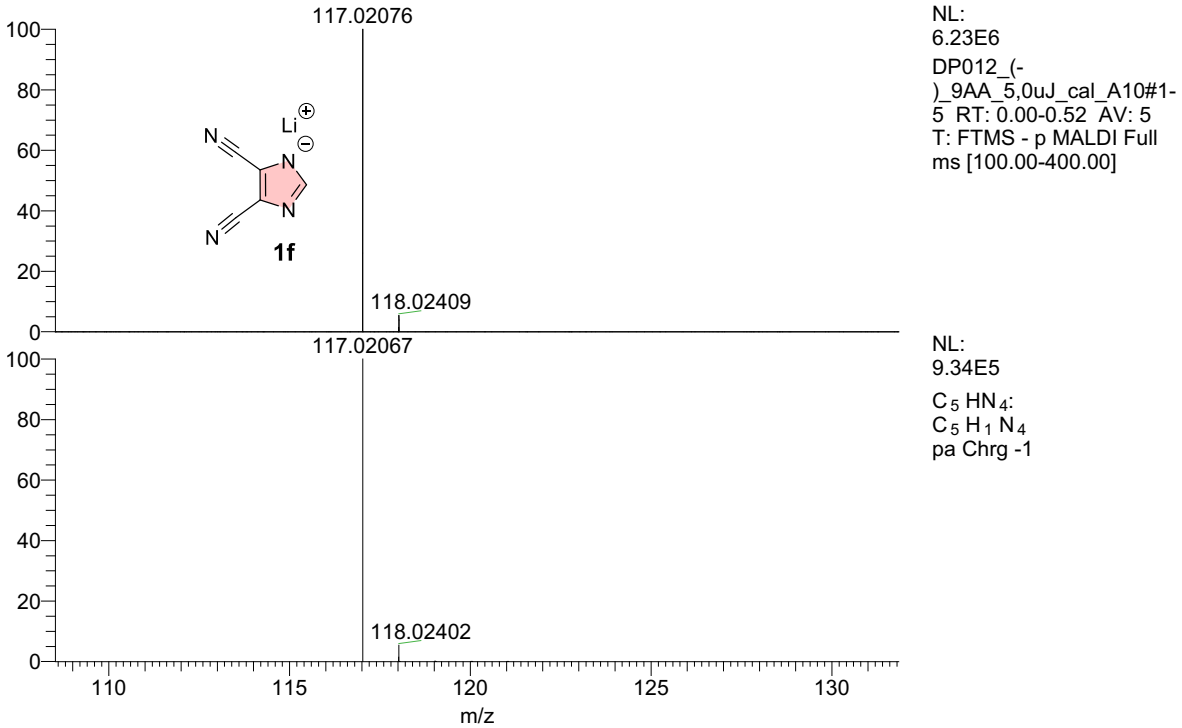

Figure S68. HR-FT-MALDI-MS spectrum of **1f** ($[M]^-$ = 117.02067 Da); top measured and bottom predicted spectrum.

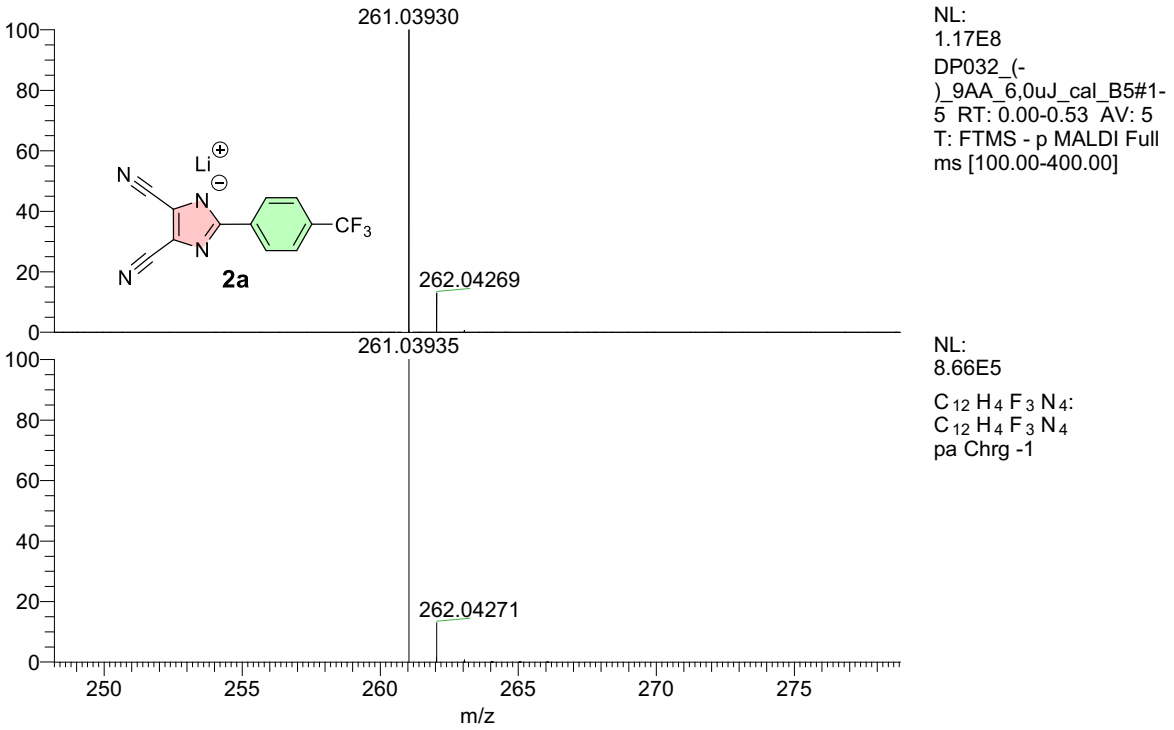

Figure S69. HR-FT-MALDI-MS spectrum of **2a** ($[M]^-$ = 261.03935 Da); top measured and bottom predicted spectrum.

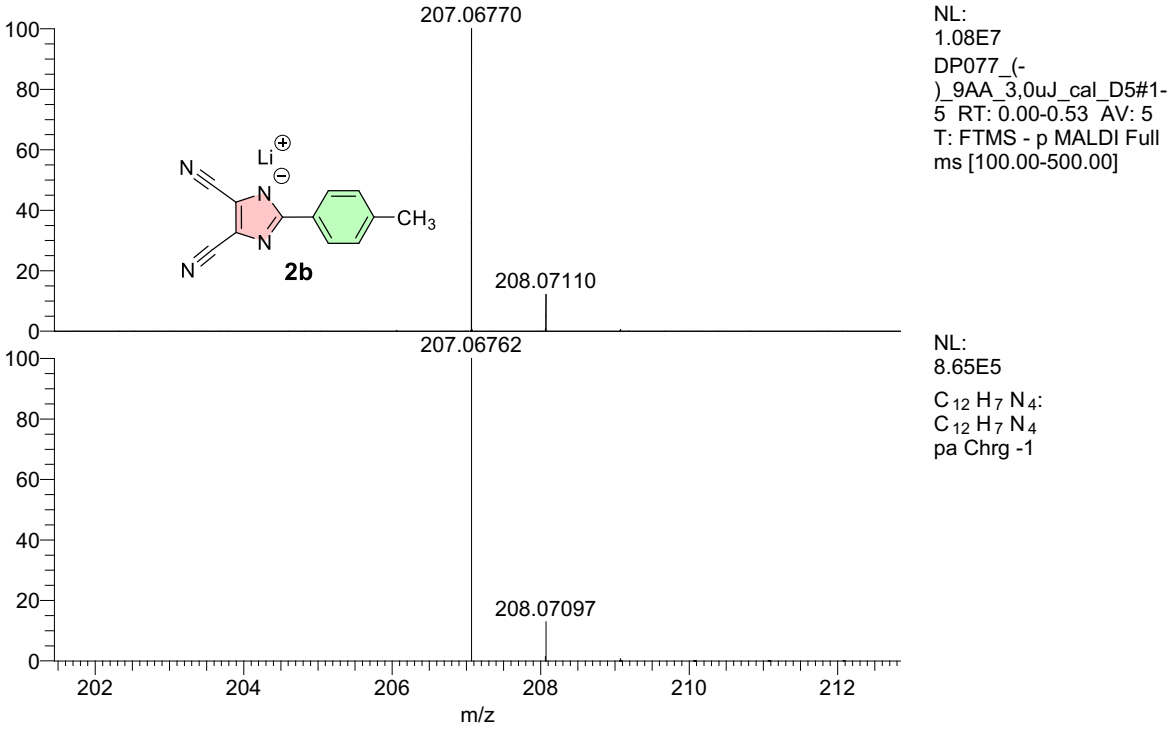

Figure S70. HR-FT-MALDI-MS spectrum of **2b** ($[M]^-$ = 207.06762 Da); top measured and bottom predicted spectrum.

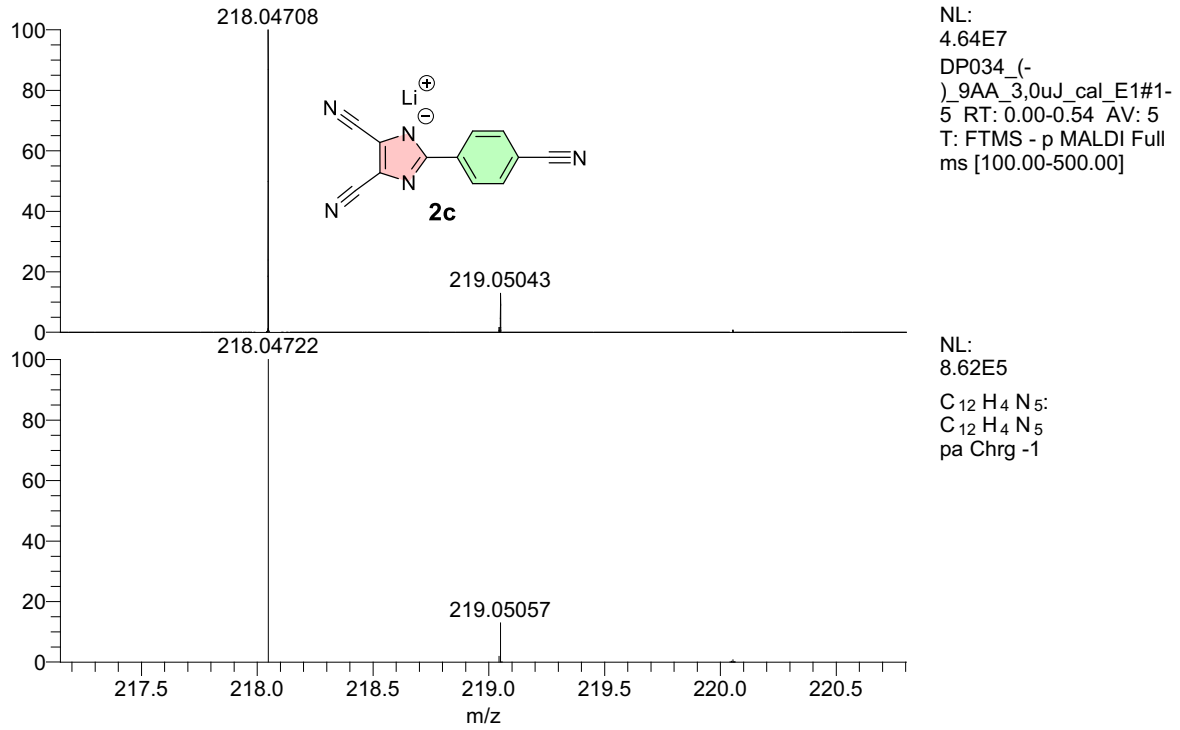

Figure S71. HR-FT-MALDI-MS spectrum of **2c** ($[M]^-$ = 218.04722 Da); top measured and bottom predicted spectrum.

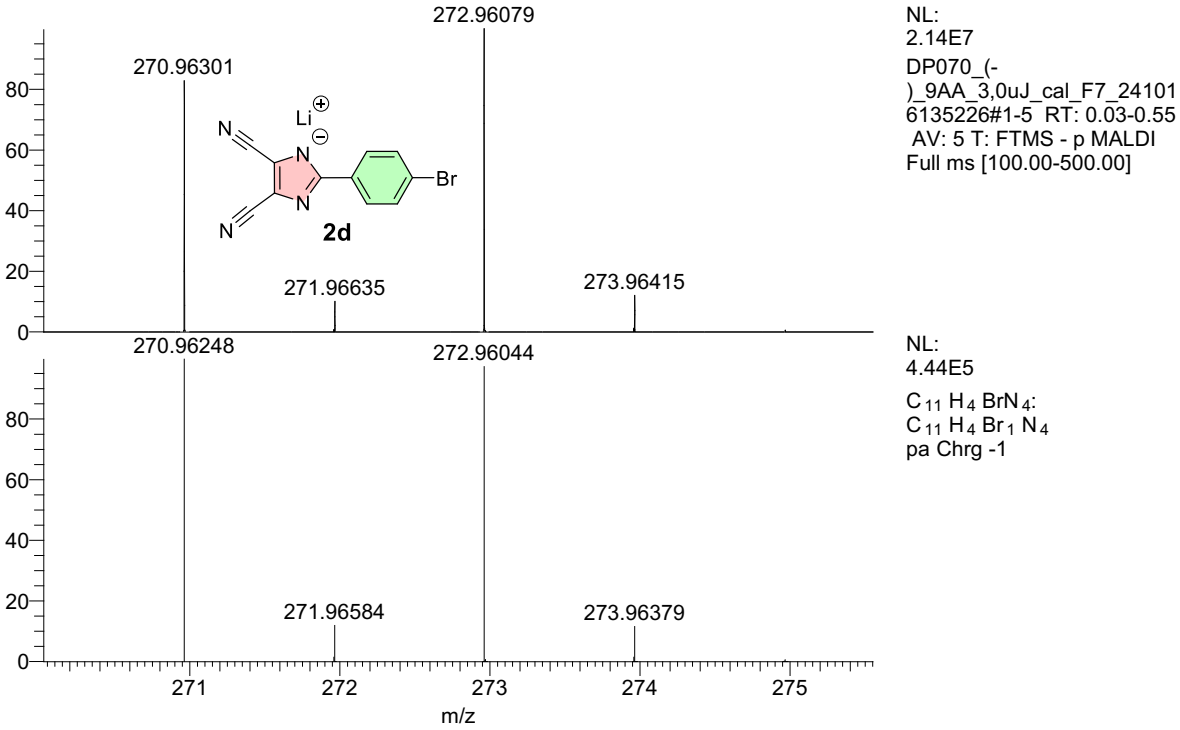

Figure S72. HR-FT-MALDI-MS spectrum of **2d** ($[M]^-$ = 270.96248 Da); top measured and bottom predicted spectrum.

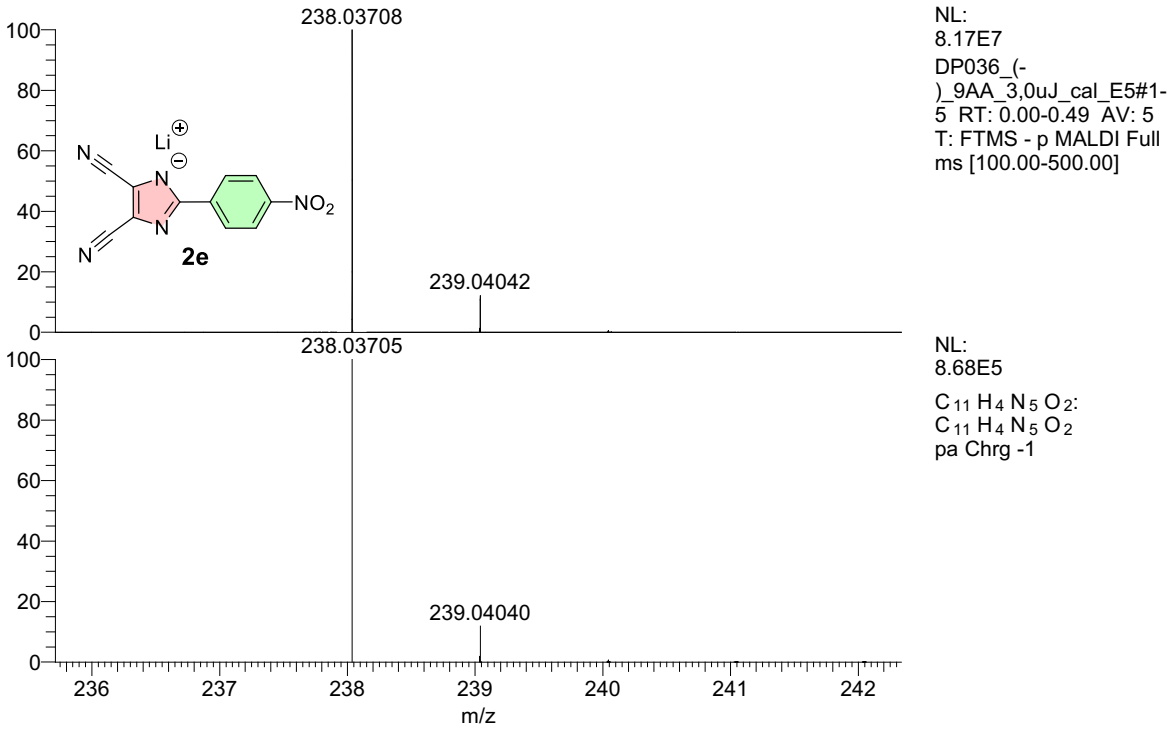

Figure S73. HR-FT-MALDI-MS spectrum of **2e** ($[M]^-$ = 238.03705 Da); top measured and bottom predicted spectrum.

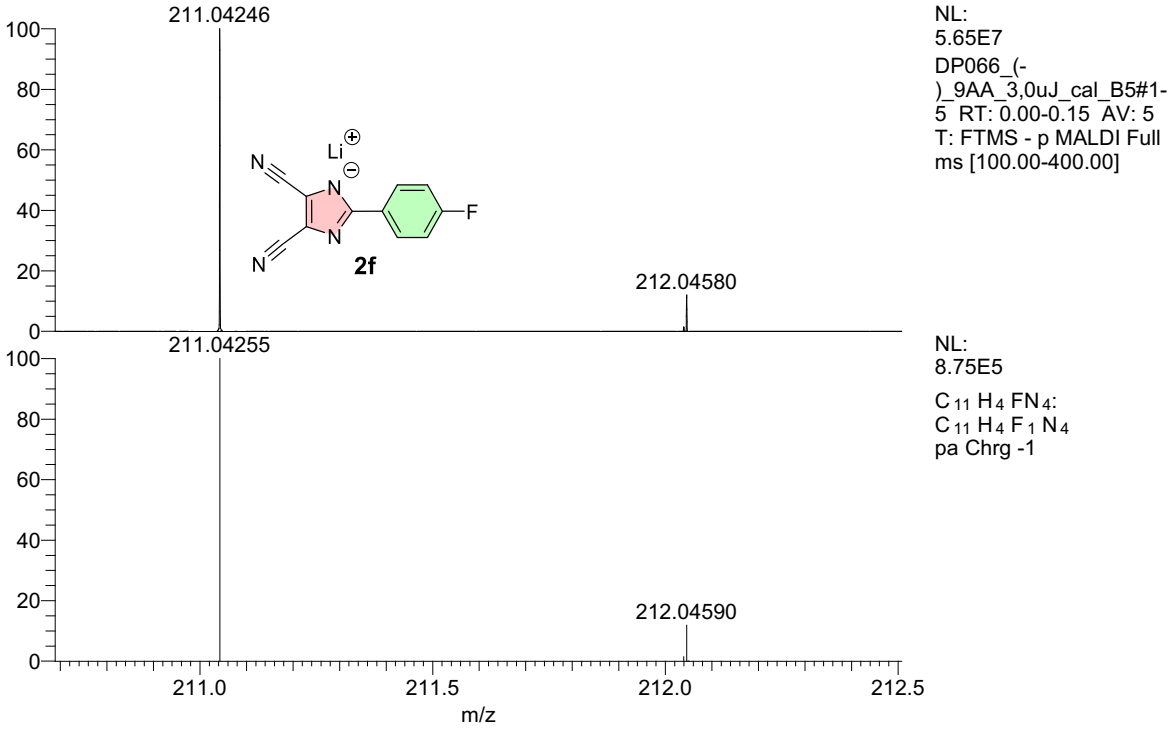

Figure S74. HR-FT-MALDI-MS spectrum of **2f** ($[M]^-$ = 211.04255 Da); top measured and bottom predicted spectrum.

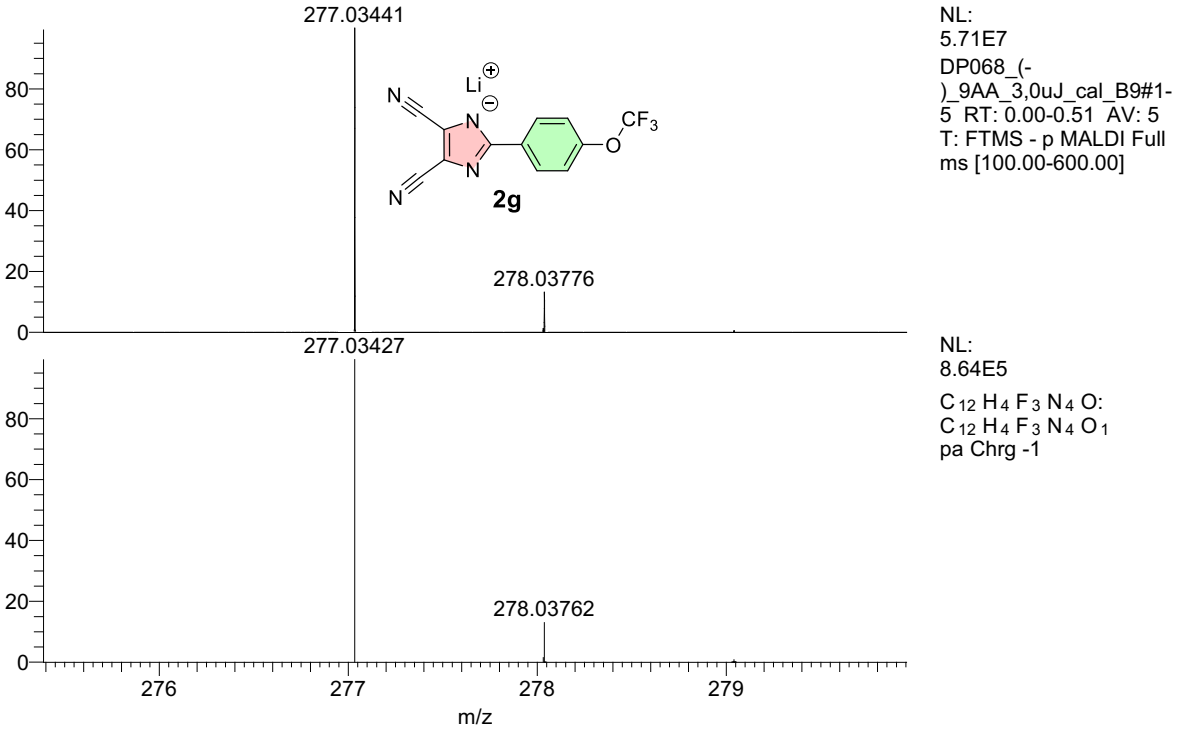

Figure S75. HR-FT-MALDI-MS spectrum of **2g** ([M]$^-$ = 277.03427 Da); top measured and bottom predicted spectrum.

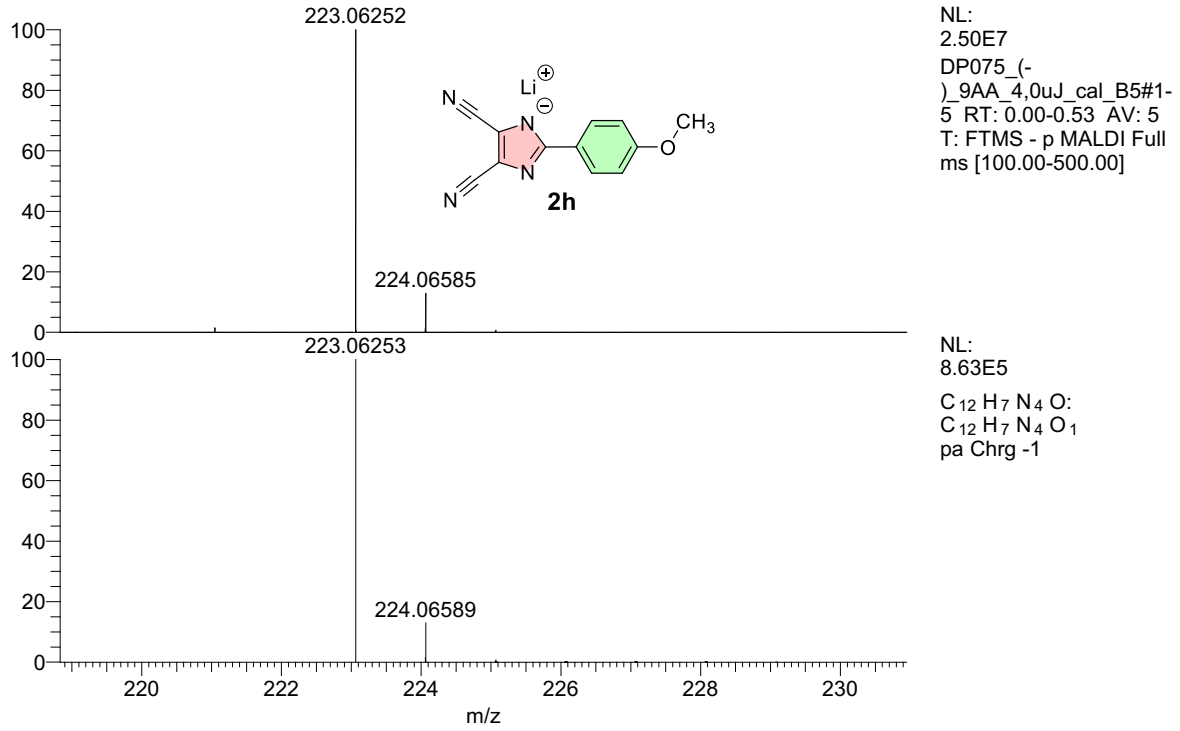

Figure S76. HR-FT-MALDI-MS spectrum of **2h** ([M]$^-$ = 223.06253 Da); top measured and bottom predicted spectrum.